


Review

A Technological Update on Heat Pumps for Industrial Applications

Sergio Bobbo ^{1,*}, Giulia Lombardo ^{1,2}, Davide Menegazzo ¹ , Laura Vallese ^{1,2}  and Laura Fedele ¹ 

¹ Construction Technologies Institute, National Research Council (CNR ITC), Corso Stati Uniti 4, 35127 Padova, Italy; lombardo@itc.cnr.it (G.L.); menegazzo@itc.cnr.it (D.M.); laura.vallese@phd.unipd.it (L.V.); laura.fedele@itc.cnr.it (L.F.)

² Dipartimento di Ingegneria Industriale, Università di Padova, Via Venezia 1, 35131 Padova, Italy

* Correspondence: sergio.bobbo@itc.cnr.it; Tel.: +39-340-1490148

Abstract: It is now widely confirmed by scientific evidence that greenhouse gas emissions must be reduced to counteract the effects of global warming. The production of heat for industrial purposes is responsible for 36.8% of world energy-related emissions due to the widespread use of fossil fuels. Heat pumps are a key technology in the transition towards more sustainable industrial processes. In this paper, a systematic review of the literature produced in the last 5 years in international journals regarding the integration of heat pumps in industrial processes is presented. Firstly, papers presenting innovative configurations for high temperature heat pumps (HTHP), i.e., heat pumps delivering temperatures in the range between 100 °C and 200 °C, suitable for many industrial processes but still under development, are reviewed. Then, papers reporting innovative solutions for the integration of heat pumps in specific industrial processes and sectors (e.g., distillation, drying, desalination, etc.) are analyzed. Finally, the literature about alternative low-GWP refrigerants for industrial heat pumps, both pure compounds and mixtures, is described. It is concluded that many progresses have been realized in the last 5 years (2020–2024) regarding the identification of innovative heat pumps for industrial applications, but further research is certainly required.

Keywords: heat pumps; cycle configurations; energy efficiency; industrial applications; review



Citation: Bobbo, S.; Lombardo, G.; Menegazzo, D.; Vallese, L.; Fedele, L. A Technological Update on Heat Pumps for Industrial Applications. *Energies* **2024**, *17*, 4942. <https://doi.org/10.3390/en17194942>

Academic Editor: Antonio Rosato

Received: 30 July 2024

Revised: 27 August 2024

Accepted: 24 September 2024

Published: 2 October 2024



Copyright: © 2024 by the authors. Licensee MDPI, Basel, Switzerland. This article is an open access article distributed under the terms and conditions of the Creative Commons Attribution (CC BY) license (<https://creativecommons.org/licenses/by/4.0/>).

1. Introduction

Historically, the impact of greenhouse gas emissions on global climate change has been recognized since the early 1990s, leading to international agreements such as the United Nations Framework Convention on Climate Change (UNFCCC) [1], the Kyoto Protocol [2], and the Paris Agreement [3], which aim to reduce atmospheric greenhouse gases and mitigate climate change. In recent years, many countries have committed to achieving carbon neutrality, with targets set as early as 2025 for Denmark and 2060 for China. These commitments highlight the global urgency of reducing greenhouse gas (GHG) emissions, particularly from industrial sources such as heating processes, which are responsible for significant emissions. The continued growth of industrial processes corresponds also to an increase in energy consumption and GHG emissions. In 2019, global primary energy consumption reached 178,899 terawatt hours (TWh), with fossil fuels accounting for 82.9% of this total [4]. Although the heat required by industrial processes constitutes only 19% of total energy demand, they are responsible for 36.8% of energy-related emissions, due to the predominance of fossil fuel boilers [5]. To meet the International Energy Agency (IEA) benchmarks for net-zero greenhouse gas emissions by 2050, industries must transition to sustainable and renewable energy sources, increasing the energy efficiency of industrial processes and reducing direct greenhouse gas emissions from fossil fuel combustion. Heat pumps, providing heat at temperatures up to 200 °C, emerge as a key technology in this transition. In particular, high temperature heat pumps (HTHP), delivering heat over 80 °C,

are attractive and suitable for various industrial applications. Heat pumps can recover low-quality waste heat by requalifying it at higher temperatures, significantly improving energy efficiency compared to traditional heat production methods (primarily fossil fuel boilers). Recent papers highlight the importance of heat pump technology in industrial applications to reduce energy consumption and CO₂ emissions, but also the technological challenges and barriers to their diffusion. Kosmadakis [6] maps the potential of industrial heat pumps across EU industries, focusing on waste heat recovery for decarbonization. Key findings include a total potential of 28.37 TWh/year, covering 1.5% of total heat consumption. Non-metallic minerals, food, paper, and non-ferrous metals show the highest potential. Results highlight the capability to cover 15% of heat consumption within the 100–200 °C range, mainly in nonferrous metals. The study underscores opportunities for heat pump applications in industry, emphasizing the need for site-specific assessments to fully realize this potential and address existing barriers effectively. Ononogbo et al. [7] highlight the use of heat pumps, including compression (CHP) and absorption (AHP) types, for upgrading waste heat (WH) for industrial processes and simultaneous heating and cooling applications. Hamid et al. [8] underscore the significant potential of HTHPs when integrated with various systems like thermal energy storage, waste heat recovery, and organic Rankine cycles. Challenges to widespread adoption include high costs, technological limitations, regulatory issues, and public acceptance. Golmohamadi [9] shows how industrial heat pumps play a significant role in enhancing the flexibility of industrial energy systems, aiding the integration of renewable energy by balancing power fluctuations. These systems are particularly effective in heavy industries like cement manufacturing, metal smelting, and oil refining, where energy-intensive processes can provide substantial power flexibility. Despite high potential, challenges include high costs and regulatory issues. Maruf et al. [10] address the complexity of modeling power-to-heat (P2H) and thermal energy storage (TES) technologies for large-scale energy systems in Europe. Electric heat pumps are identified among key P2H technologies and HTHPs are highlighted for their growing role in industrial sectors like food, paper, and chemicals. Studies show significant market potential for industrial heat pumps, though economic constraints limit their current use. The paper also discusses the importance of combined heat and power (CHP) systems and various TES technologies. Nandhini et al. [11] explore low-temperature waste heat (LTWH) recovery technologies, emphasizing the efficiency and environmental benefits of heat pumps. Hybrid absorption-compression heat pumps can recover up to 95% of waste heat, while air-source and CO₂ transcritical heat pumps reduce energy consumption by 60–75%. Nanofluids like silver/pentane enhance system efficiency and reduce carbon footprints. Experimental and theoretical analyses of various heat pump configurations demonstrate significant energy recovery and efficiency improvements. Integrating heat pumps with power cycles, such as the organic Rankine cycle, boosts performance and energy output. Economic analyses indicate heat pumps are cost-effective with a maximum payback period of 16 years. Leonzio et al. [12] highlight air-source heat pumps (ASHPs) for water heating as a key technology for decarbonization. ASHPs can achieve high temperatures, with transcritical cycles reaching up to 90 °C, and heat recuperative solutions potentially achieving up to 99 °C. Absorption cycles, though less studied, can reach up to 115 °C. Despite industrial ASHPs typically achieving lower temperatures, they offer significant energy, cost, and CO₂ savings compared to traditional boilers, especially with renewable electricity. Integrating ASHPs with direct air capture (DAC) technologies can enhance efficiency and reduce environmental impact. Wang et al. [13] propose heat pumps as a key solution for reducing carbon emissions by efficiently using low-carbon electricity. Their study highlights the potential of heat pumps to support both heat and power decarbonization by offering flexibility on a gigawatt scale, which can aid in integrating variable renewable energy sources. Major challenges include high costs, complex system designs, and space constraints. Carmona-Martínez et al. [14] outline renewable energy (RE) technologies as crucial for decarbonizing Energy Intensive Industries (EIIIs) by 2050. It classifies these technologies into those utilizing renewable electricity and those providing renewable heat,

essential for industrial processes that cannot be electrified. Heat pumps, which cover various temperature needs, are identified as key technologies for these purposes. Rajabloo et al. [15] address the significant fossil CO₂ emissions from the energy and industrial sectors, focusing on energy-intensive industries like metallurgy and chemicals. The role of heat pumps is highlighted in reducing fossil CO₂ emissions from the energy sector, especially within energy-intensive industries like metallurgy and chemicals. They conclude that heat pumps are crucial for decarbonizing industrial processes by enhancing efficiency, integrating renewable energy, and reducing energy consumption.

The aim of this review is to update and summarize the scientific knowledge on industrial heat pumps through an exhaustive analysis of the literature from the last 5 years (2020–2024). A first goal is analyzing the most recent developments in HTHPs, with special attention to innovative configurations of the cycle, aimed at optimizing the performance in relation to boundary conditions and applications. Vapor compression cycles have mostly been considered, but also hybrid solutions with absorption cycles are included. Unlike common HPs, which are a mature technology, HTHPs are particularly interesting from a research point of view because they are under development and lots of enhancements have been proposed in recent years. A systematic bibliographic analysis has been performed through Google Scholar by using the specific keywords “industrial high temperature heat pumps”. The search has been performed limiting the period year per year (e.g., 2020), because in this way the search was more effective. The second goal is to describe the most recent proposals for the application of heat pumps in the most significant industrial sectors and processes. A specific search, again with Google Scholar, has been conducted using the keywords “industrial heat pump + specific sector/process” (e.g., “petrochemical”). Objectives and results of each relevant paper have been synthesized in such a way to give the reader enough information to be able to evaluate his interest for further in-depth analysis of the papers.

2. High Temperature Heat Pumps (HTHP) for Industrial Applications

In the current literature, heat pumps are generally classified in three different groups, as shown in Figure 1: heat pumps (HP) for supply temperatures up to 80 °C; high temperature heat pumps (HTHP) from 80 °C to 100 °C; and very high temperature heat pumps (VHTHP) from 100 °C up to 160 °C (or even 200 °C) [16]. For convenience, in this paper, we will use the acronym HTHP for both HTHPs and VHTHPs.

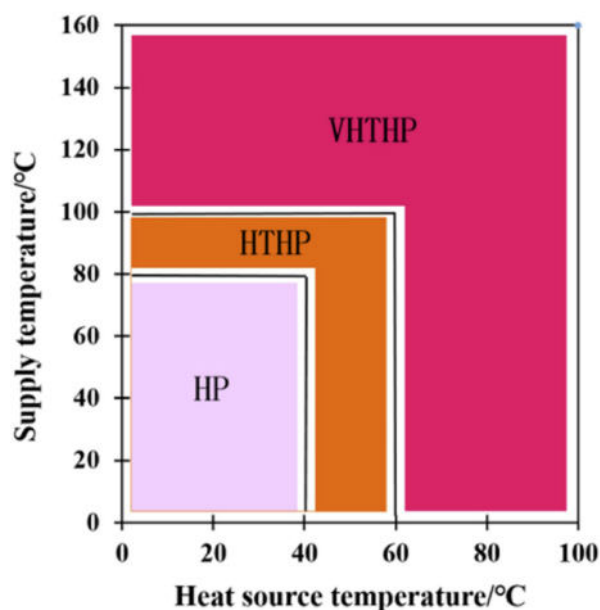


Figure 1. The classification of vapor compression heat pumps [16].

Current research on vapor compression HTHPs focuses on both subcritical and transcritical cycles, but absorption cycles also offer interesting opportunities that are being studied. In any case, to optimize the efficiency of the heat pump, a careful choice of its most appropriate configuration is needed (e.g., standard cycle, use of internal exchanger, economizer, intercooling, parallel compression, multistage compression, cascade cycle, etc.) in relation to the type of application and boundary conditions, with particular reference to the heat sink temperature and the temperature lift between source and sink. The integration of HTHPs with renewable energy sources and waste heat recovery systems can further improve their efficiency and sustainability. Furthermore, HTHPs can increase the flexibility of energy networks by acting as electricity demand response tools to support the integration of intermittent renewable energy sources.

In this paragraph, we concentrate on the recent literature on HTHPs, with particular attention to the proposal of new effective configurations to meet the requirements of the specific industrial processes where they must be integrated. Some recent papers report a general analysis of the possible configurations and applications of HTHPs. The review of Adamson et al. [18] compiles 49 high-temperature or transcritical heat pump cycle structures and identifies 10 performance-enhancing components. It addresses six technical challenges, proposing solutions including a new transcritical-transcritical cascade cycle. The review suggests that new transcritical cycles, with further research, can enhance COP, making them competitive with alternative fuels up to 200 °C and achieving mean temperature lifts around 100 °C. Tveit et al. [19] explore the growing adoption of high temperature heat pumps (HTHPs) in industries driven by environmental concerns and energy system electrification. These devices, including VHTHPs, address heat demands above 100 °C not met by conventional systems. Evaluating their environmental impact involves complexities like system efficiency, coefficient of performance (COP), and electricity source emissions. The paper employs thermodynamic tools like exergy and Pinch analysis with European energy data, alongside a life cycle impact assessment (LCA). Comparing a Stirling engine-type VHTHP with conventional heaters illustrates environmental benefits, though LCA demands extensive data and interpretation effort, while simpler analyses like Pinch or exergy offer clearer results at the cost of detail. Jiang et al. [20] review laboratory-scale HTHPs with heat sink temperatures over 80 °C, exploring single-stage, multi-stage, cascade, and hybrid systems. About 71% of prototypes use low-GWP refrigerants, some achieving temperature lifts above 100 °C. Industrial HTHPs range from 60 kW to 18 MW, mostly using high-GWP refrigerants like R245fa and R134a. The paper identifies some key perspectives for HTHPs, the most important of which are: low-GWP refrigerants, higher output temperatures (>100 °C), heating capacities over 1 MW, and COPs above 4 under a 40 °C lift; HTHPs need further development to handle higher temperature lifts, with research gaps above 100 °C output and COP > 4; the focus should shift from conventional cycles to new transcritical cycles for better performance at high temperatures; large-capacity HTHPs, proven effective in some applications, require further customization and cooling technology improvements for safe, high-temperature operations; future advancements should aim to achieve all four key prospects for HTHPs, creating an “Ultra Heat Pump.” The review of Hamida et al. [8] examines future HTHP improvements, addressing technical obstacles and integrating HTHPs into processes like thermal energy storage, waste heat recovery, and more. Challenges include technological limitations, high costs, regulatory uncertainties, policy issues, and public acceptance. The review consolidates data on HTHPs in industrial applications, emphasizing single-stage and multi-stage systems, vapor compression, absorption, hybrid systems, and novel combinations. It highlights issues such as compressor discharge temperature, lubrication, oil-free operation, and new developments, suggesting future research directions like refrigerant charge management and flash tank cycle control. Improving understanding among stakeholders and addressing integration costs and alternative heating technologies are essential for broader HTHP adoption. Mateu-Royo et al. [21] investigated high temperature heat pumps (HTHPs) for industrial waste heat recovery, evaluating eight advanced cycle configurations and nine

low GWP refrigerants. Configurations like TS Cascade excel at high temperature lifts (>60 K), while single-stage setups with economizers suit lower lifts (<50 K). Refrigerants HCFO-1233zd(E) and HCFO-1224yd(Z) balance COP and volumetric capacity, crucial for energy-efficient applications. Significant CO₂ reductions (up to 68%) compared to natural gas boilers highlight environmental benefits. Economically, advanced configurations show slight cost variations (~9%) from a reference TS Economizer cycle, proving viable for industrial adoption. Less recently, Arpagaus et al. [17] reviewed HTHPs with heat sink temperatures of 90–160 °C. Heat pump cycles and refrigerants were analyzed, identifying over 20 HTHPs from 13 manufacturers, suitable for industries like food, paper, metal, and chemicals, with capacities from 20 kW to 20 MW. Most HTHPs are single stage, using refrigerants like R245fa, R717, R744, R134a, and R1234ze(E). COPs range from 2.4 to 5.8 at a 95–40 K temperature lift. Research aims to improve COPs and temperatures, achieving up to 160 °C with refrigerant R1336mzz(Z). Key findings include potential for 113 PJ of process heat in Europe and barriers like insufficient integration knowledge, refrigerant availability, and electricity costs.

The next paragraphs are dedicated to the analysis of the literature reporting more specific cases of solutions for HTHPs, defined on the base of the numerosity of paper published in the last 5 years, i.e., cascade, transcritical, and hybrid absorption-compression heat pump systems. Single cases are grouped in the paragraph “other solutions”.

2.1. Cascade Heat Pump System

The most studied configurations for HTHPs cycles in the last 5 years are those based on cascade high-temperature heat pumps (CHTHPs), applying different refrigerants as working fluids. Figure 3 reports the scheme for a typical CHTHP system, with the corresponding T-s diagram of the cycle. Hu et al. [22] evaluated CHTHPs for recovering low-temperature industrial waste heat using conventional and advanced exergy and exergoeconomic analyses. Results highlight that 62.26% of the exergy destruction in CHTHP systems is avoidable, mainly attributed to component inefficiencies: thus, CHTHP systems still have significant potential for improvement. The exergoeconomic factor is notably low at 0.75%, emphasizing high exergy destruction costs. The high- and low-temperature compressors are identified as critical areas for improvement due to their significant exergy destruction.

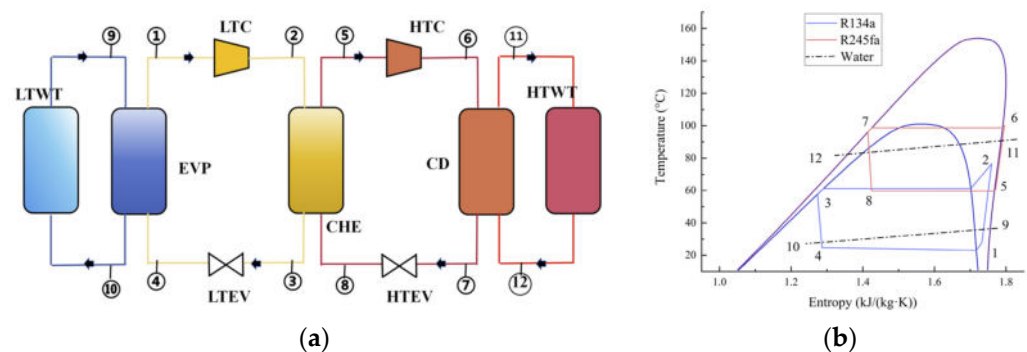


Figure 3. (a) Schematic diagram of a CHTHP system with (b) the corresponding T-s diagram [22].

Dong and Wang [23] analyze cascade high-temperature heat pump (CHTHP) configurations and fluid pairs across multiple criteria, emphasizing their suitability for utilizing ultra-low-grade waste heat efficiently. Key findings include the optimal $\Delta t_{\text{lift}} \geq 70$ °C for cascade configurations, shifting to two-stage, single-stage with injection, and single-stage setups as Δt_{lift} decreases. Preferred fluid pairs such as R1234ze(E), R1234ze(Z), R1224yd(Z), R1233zd(E), and R1336mzz(Z) demonstrate trade-offs in COP, cost, exergy efficiency, and TEWI. Schlemminger et al. [24] investigate a newly developed industrial propane-butane CHTHP designed for simultaneous cooling and heating in applications like dairy production. Featuring a semi-hermetic compressor for high-temperature operation, it achieves a temperature lift of 88 K to 108 K, with peaks at 125 K between evaporation and conden-

sation. The system, installed in a Norwegian dairy, supplies hot water at 112 °C from ice water at 0.5 °C, yielding a COP of 3.0 to 4.0. The HTHP reduces energy consumption by up to 64% and CO₂ emissions by up to 94%, suitable for both retrofit and new installations. Dai et al. [25] introduce CHTHP systems in comparison to conventional HTHPs and boilers. Five optimized layouts are proposed and evaluated using models for energy consumption, emissions, life cycle cost (LCC), and payback period (PBP). The cascade-heating water-cooled saturated system (CWSAS) (Figure 4) demonstrates significant advantages: 1.8–22.8% lower primary energy consumption (PEC) compared to HTHPs and boilers, 1.7–6.1% lower life cycle carbon emissions than HTHPs, and superior pollutant emission reductions. CWSAS emerges as the optimal choice for its comprehensive performance in energy efficiency, environmental impact, and economic feasibility in recovering waste heat from oil fields for hot water and steam production.

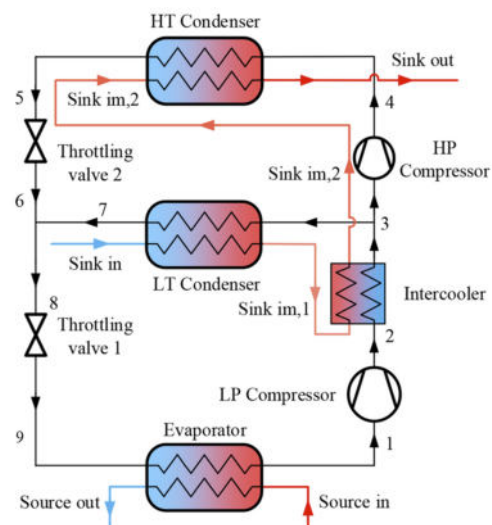


Figure 4. Cascade heating water cooled saturated suction system (CWSAS) [25].

Dong et al. [26] focus on optimizing CHTHP design parameters considering both thermodynamic and economic performance. Using a multi-objective optimization model with improved genetic algorithms, key parameters like evaporation and condensation temperatures were determined. Optimal values were found for certain conditions, showing slight variations with different operational scenarios. Results indicate that condensation temperature increases with output water temperature, while heat source temperature minimally affects optimal temperatures for constant output water conditions. Wu et al. [27] introduce a HTCHP system designed to recover waste heat from a chemical plant and replace steam, emphasizing economic and thermodynamic performance via a developed mathematical model. Simulation results with a multi-objective optimization method confirm system stability and feasibility under varying conditions. Optimal conditions at 71 °C heat source inlet and 145 °C condensing temperature yield a heating capacity of 498.9 kW and a 3.9-year payback period. Key conclusions highlight improved COP and exergy efficiency with higher inlet temperatures, ANP sensitivity to heating capacity variations, and favorable payback periods under specific economic conditions, validating HTCHP as a viable industrial solution. Ganesan et al. [28] explore a two-stage CHTHP using natural zeotropic refrigerants to produce hot water exceeding 100 °C, reaching up to 118 °C. MATLAB simulations were employed to design and analyze the HTHP model, highlighting its robust performance metrics including high heating capacity (up to 205 kW) and a total COP of 4.5. The system's use of CO₂ + butane and CO₂ + pentane mixtures (see Figure 5 for the temperature glide) in the Low-stage (LS) and High-stage (HS) cycles, respectively, demonstrated efficient heat transfer capabilities. Comparison with published results indicates a notable 36% COP improvement potential, emphasizing the system's advancement in achieving high-temperature heating efficiently.

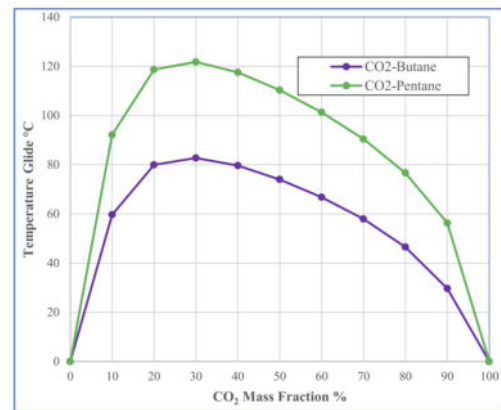


Figure 5. Temperature glide of the zeotropic mixtures employed by [28,29].

Ganesan et al. [29] present a modeling and optimization approach for a CHTHP using CO₂/butane and CO₂/pentane mixtures in the LS and HS cycles, respectively, for industrial high-temperature heating. The MATLAB-based model explored heating capacities up to 201.5 kW and COP improvements of 20% compared to pure fluids, showcasing the efficacy of the refrigerant mixtures. Analysis highlighted the influence of CO₂ composition on heat sink temperatures and system performance, with notable impacts on COP and efficiency metrics. Navarro-Esbrí et al. [30] evaluate a two-stage CHTHP system (Figure 6), aiming to produce hot water up to 150 °C from inlet temperatures of 35 °C and 25 °C. Using experimental data from single-stage prototypes (R-1234ze(E) and R-1336mzz(Z)), a semi-empirical model assesses energy performance with novel refrigerant mixtures like R-152a/600 and R-1233zd(E)/161 for the two stages, achieving up to 14% higher COP compared to baselines. Despite a 30% increase in volumetric heat capacity (VHC), negligible direct CO₂ emissions are observed due to low GWP refrigerants.

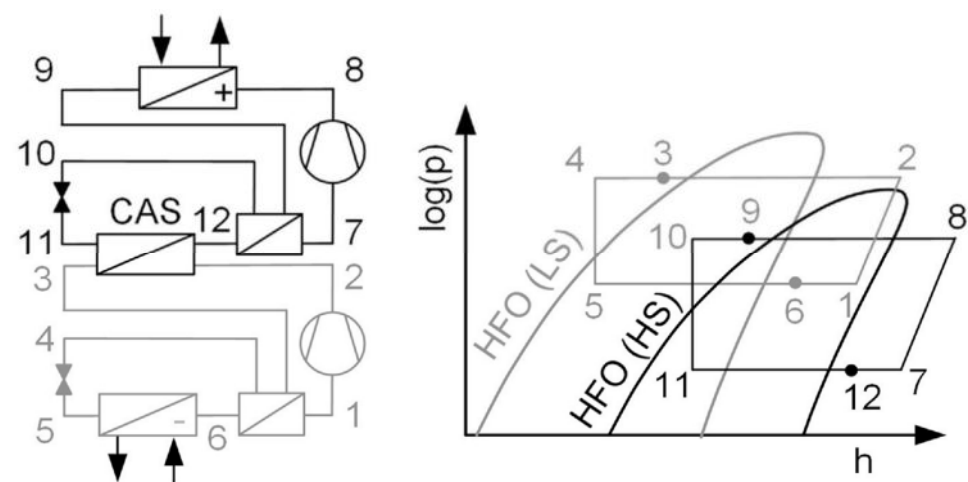


Figure 6. Schematic representation and P-h diagram of the two-stage cascade HTHP [30].

Chen et al. [31] introduce a novel vapor injection autocascade heat pump (VAHP) for high-temperature water heating. Through simulation-based investigations, it outperforms conventional autocascade systems with a 51.8% increase in COP and 104.3% in capacity at evaporating temperatures from 0 °C to 20 °C. Exergy analysis highlights reduced irreversible losses in throttling valves and cascade condensers, enhancing overall performance. The VAHP shows competitive energy costs and minimal pollutant emissions compared to conventional boilers. Kezier et al. [32] propose a novel semi-cascade heat pump system (Figure 7a) designed to enhance energy efficiency across varied temperature lifts. Operating in single-stage, conventional cascade, and semi-cascade modes, it adapts to $\Delta T_{\text{source-sink}}$ from 20 to 110 °C and ΔT_{sink} from 10 to 100 °C. A validated thermodynamic model evalu-

ates each mode's performance, revealing that the single-stage mode suits small $\Delta T_{\text{source-sink}}$ and ΔT_{sink} , while the conventional cascade is optimal for larger $\Delta T_{\text{source-sink}}$ and smaller ΔT_{sink} (see Figure 7b). Semi-cascade mode maintains high efficiency over a wide range. Compared to conventional cascade, the novel system achieves up to 22.3% energy efficiency improvement, making it promising for diverse temperature lift applications.

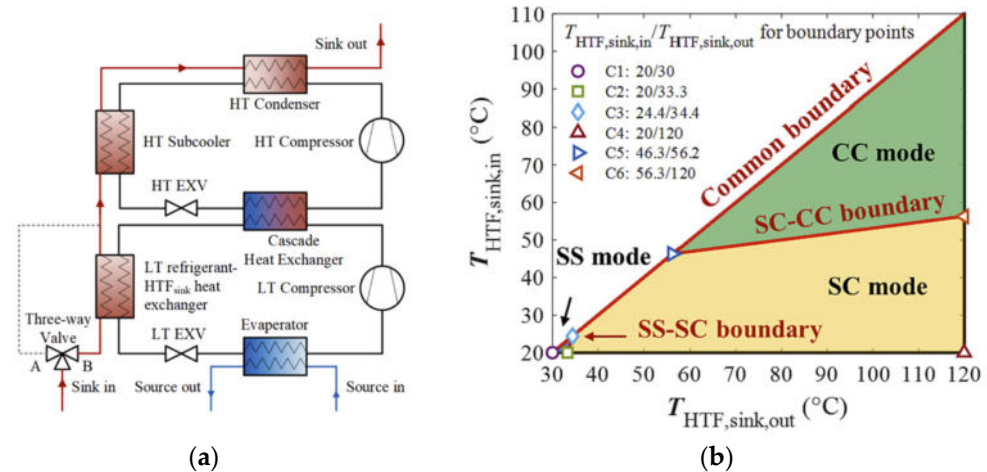


Figure 7. (a) Schematic of semi-cascade heat pump system and (b) operating range for each mode of the semi-cascade system [32].

Chen et al. [33] introduce a novel solar-assisted vapor injection autocascade high-temperature heat pump (SVAHP) designed to overcome insufficient heating performance limitations. It operates in two modes to efficiently utilize solar and air energy. Theoretical investigations highlight the SV mode's superiority over the simple vapor injection autocascade heat pump (VAHP) under solar radiation exceeding 200 W/m^2 . SVAHP shows average improvements of 16.5% in maximum heating COP and 18.1% in heating capacity compared to VAHP. It exhibits the lowest life cycle cost and air pollutant emissions, with payback periods of 2.06 years and 2.95 years relative to VAHP and the basic autocascade heat pump (ACHP), respectively.

2.2. Transcritical Heat Pump Systems

A significant interest has been found in the literature about heat pumps working with transcritical cycles. Zhao et al. [34] introduce high-temperature transcritical heat pump cycles using R1233zd(E), R1336mzz(Z), n-Butane, and ammonia for heating applications up to 200 °C in spray-drying processes. Emphasizing optimal COP through compressor pressure ratio optimization, R1233zd(E) emerges with a leading COP, balancing first- and second-law efficiencies with gas cooler sizing considerations. Despite ammonia's favorable pressure ratio, its complexity and size requirements highlight R1233zd(E) as the most promising option due to its safety, efficiency (COP of 3.6), and operational practicality at lower pressures. Yang et al. [35] compare high-temperature heat pumps with flash tank vapor injection (FTVC, Figure 8a) and sub-cooler vapor injection (SVIC, Figure 8b) configurations across various operational parameters. FTVC demonstrates superior COP, injection mass flow ratio, and volumetric heating capacity (VHC) compared to SVIC at 4 different injections and superheats (0 °C , 5 °C , 10 °C , 20 °C) under similar conditions. FTVC maintains discharge temperatures comparable to SVIC-0 but lower than SVIC-5, SVIC-10, and SVIC-20. However, caution is advised regarding potential wet compression at low compressor suction superheat, impacting system performance and safety. Key factors influencing COP include compressor isentropic efficiency, evaporation, and condensation temperatures, while suction superheat and subcooling have lesser effects. At 55 °C evaporation, 125 °C condensation, and 921.4 kPa injection pressure, FTVC achieves the highest COP of 4.49, outperforming SVIC configurations.

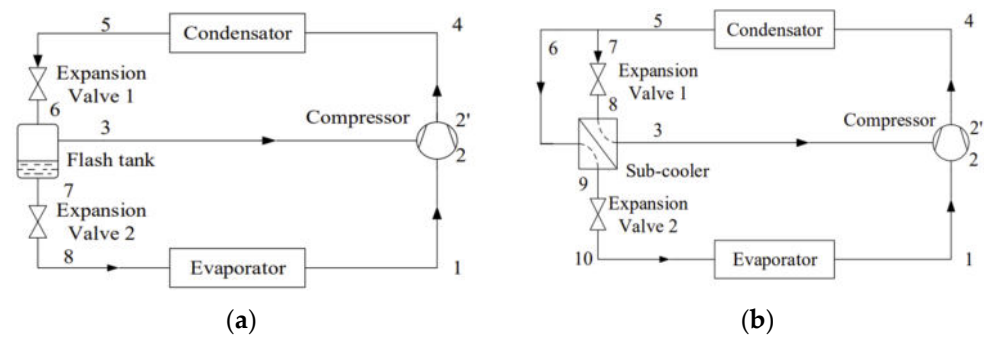


Figure 8. Principle diagram of the vapor injection heat pump with (a) flash tank and (b) sub-cooler [35].

Kong et al. [36] investigate HTHPs using transcritical-transcritical cascade CO₂ cycles with internal heat exchangers (IHX) to achieve 200 °C sink temperatures (in Figure 9a,b, an example of the P-h and the T-s diagrams, respectively). The evaluated cycles show that incorporating IHX in both top and bottom cycles lowers maximum discharge pressure by up to 1.27 MPa compared to single-stage configurations, enhancing COP to 2.22 for 200 °C air outlet temperatures. Despite increased exergy destruction with IHX, their strategic placement mitigates losses during expansion, optimizing performance.

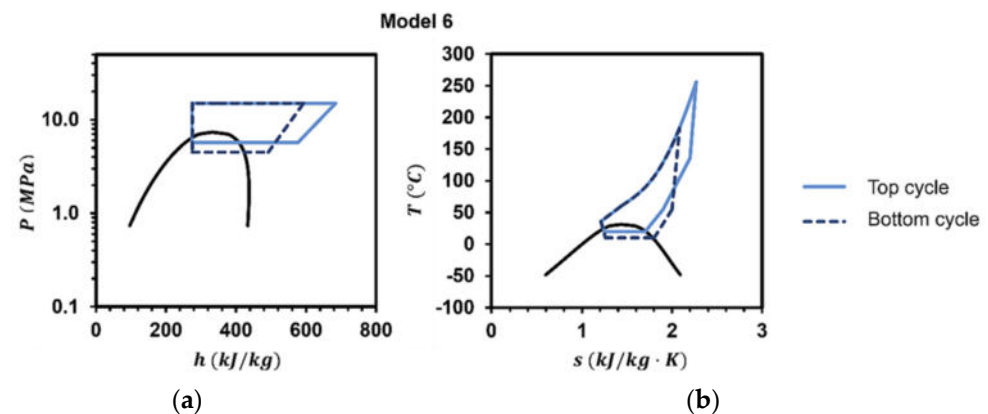


Figure 9. (a) P-h and (b) T-s diagram for one of the HTHP models analyzed by [36] for a sink temperature of 200 °C.

Udroiu et al. [37] propose a transcritical high-temperature heat pump (THTHP) utilizing R1336mzz(Z) to achieve temperatures up to 250 °C, feasible due to the refrigerant's thermal stability at this range. Computational models of the cycle, with and without internal heat exchangers, explore optimal parameters like evaporation, gas cooler temperatures, and superheating degrees. Results show COP enhancements from 2.5 to 5.9 by varying evaporation temperature (80 °C to 140 °C) and from 3.2 to 7 with superheating degree adjustments (20 °C to 100 °C). System efficiency peaks at COP 3.3 under a 150 °C temperature lift. Vieren et al. [38] proposes a thermodynamic model for optimizing transcritical cycles in industrial heat pumps up to 200 °C, focusing on three case studies: thermal oil heating, superheated steam drying, and spray drying with heat sink temperature glides of 60 K, 81 K, and 105 K, respectively. The T_s diagrams for the best performing subcritical and transcritical cycle are reported in Figure 10a and 10b, respectively. The model identifies that transcritical cycles outperform subcritical ones with temperature glides above 60 K, achieving up to 7.3% higher COP. The preferred working fluids, such as HFOs and HCFOs, offer superior performance in transcritical cycles, providing higher volumetric heating capacities and lower pressure ratios, despite requiring compressors capable of handling pressures up to 60 bar.

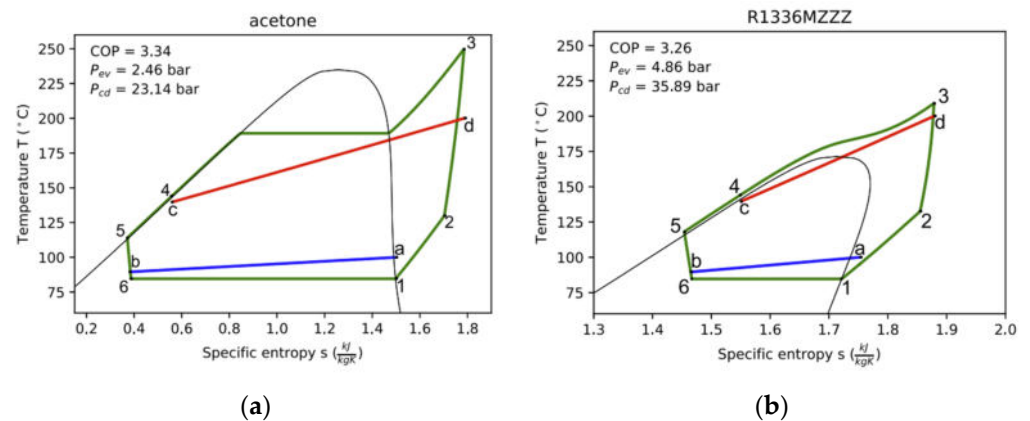


Figure 10. T,s-diagram, with scaled entropy for secondary fluid, for the best performing subcritical cycle (a) and transcritical cycle (b) [37,39].

Dai et al. [39] propose three novel transcritical CO₂ HTHP systems (Ej-Evap2-A, Ej-Evap2-B, and Ej-Evap2-C) featuring dual-temperature evaporation using an ejector for industrial waste heat recovery. Compared to traditional boilers, these systems are evaluated using comprehensive life cycle models focusing on energy, exergy, emissions, and economic aspects. Ej-Evap2-C achieves a maximum COP of 4.85, 14.40% higher than baseline systems, with exergy efficiency improvements of 7.86–15.19%. The scheme and the T-s diagram for the Ej-Evap2-C cycle are reported in Figure 11. It exhibits the lowest emissions and life cycle costs, with a payback period under 7 years, making it a promising alternative for high-temperature heating applications.

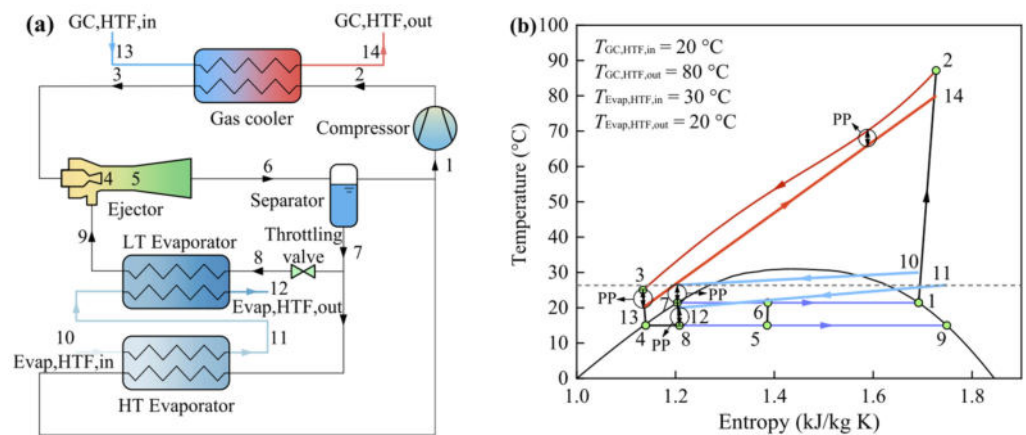


Figure 11. (a) Dual-temperature evaporation transcritical CO₂ heat pump system C with ejector (Ej-Evap2-C). (a) Schematic. (b) T,s diagram [39].

2.3. Hybrid Absorption-Compression Heat Pump System

Thermally coupled hybrid absorption-compression heat pump cycles raise some interest because they could achieve large temperature lift and high output temperature. You et al. [40] explore thermally coupled hybrid absorption-compression heat pump cycles for high-temperature industrial applications, highlighting their potential but also the challenges from multiple heat exchange processes causing performance degradation. Entransy dissipation analysis is introduced to evaluate irreversibilities and optimize heat exchange components, showing up to 3.92% COP improvement by reducing internal heat recovery irreversibilities. The optimal coupling temperature of 73.9 °C, aligns with enhanced COP and minimized exergy destruction, demonstrating the efficacy of entransy analysis in optimizing thermal system performance and guiding heat pump design improvements. Kosmadakis [6] explores three-stage hybrid absorption-compression heat pump (HACHP) cycles for enhancing temperature lift in air-source systems, crucial for industrial heat appli-

cations. Internal heat recovery configurations are investigated to boost output temperatures (100–190 °C) and COP (1.26–2.23) under 30 °C ambient. The proposed enhanced HACHP (EHACHP) overcomes HACHP limitations, achieving up to 190 °C output and 170 °C temperature lift, with 13% higher COP under 100 °C lift. Figure 12 reports the schematic diagram of the EHACP cycle. Despite higher refrigerant pressures, EHACHP offers a broader operational range and superior performance, laying the groundwork for advanced high-temperature heat pump applications in diverse industrial settings.

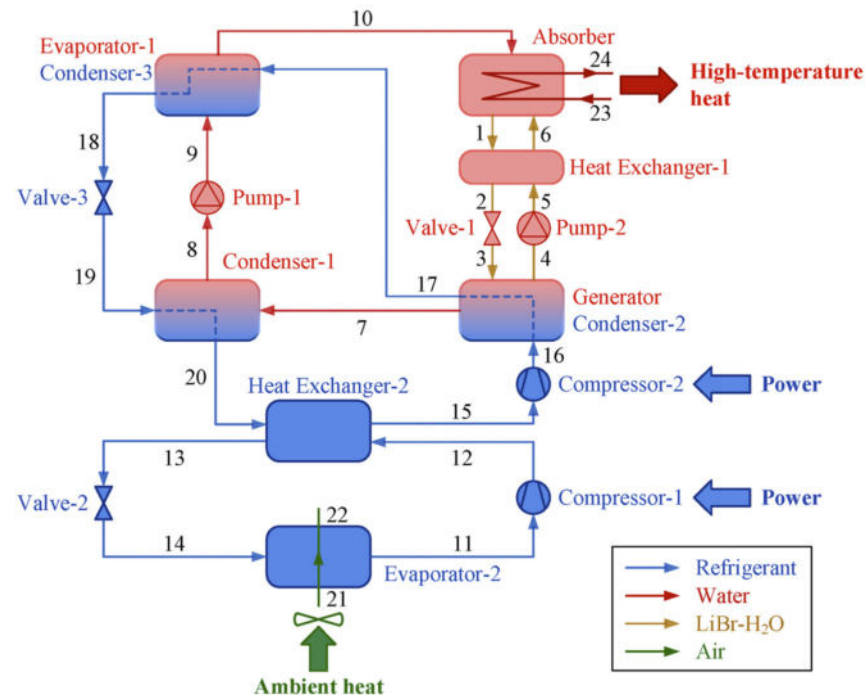


Figure 12. Schematic diagram of the EHACHP cycle, where the exhaust heat is recovered to medium-temperature stage. The blue blocks represent VCHP sub-cycle, the red blocks represent AHT sub-cycle, and the blocks with gradient color from blue to red are the coupling component [6].

2.4. Other Solutions

Several other configurations of HTHPs have been proposed in the literature in the search for innovative and efficient solutions to enhance their performance. Dai et al. [41] propose dual-temperature condensation and dual-temperature evaporation (Ej-DCDE) heat pump systems for high-temperature industrial heating, integrating ejector and two-stage compression technologies. Comparative analyses with five existing heat pumps and four boilers highlight Ej-DCDE-2 (see Figure 13) as optimal, achieving a COP of 4.25, which is 11.55% and 1.43% higher than dual-temperature condensation and single-temperature evaporation HP and Ej-DCDE-1, respectively. It reduces exergy destruction by 27.88% and primary energy consumption by 22.19% compared to baseline systems. Ej-DCDE-2 also exhibits the lowest CO₂ emissions and life cycle cost (LCC), surpassing traditional boilers by significant margins, making it highly recommended for industrial heating applications.

Huang et al. [42] introduce a novel vapor-injected high-temperature heat pump (LEHP) integrating a liquid-separation condenser (LSC) and an ejector for zeotropic mixture composition adjustment. The scheme and the T-z diagram for the LEHP cycle are reported in Figure 14. Compared to conventional heat pumps, LEHP achieves a 21.86% higher coefficient of performance (COP). Parametric studies show benefits from adjusting vapor quality and flash tank pressure to enhance system performance and temperature matching. Genetic Algorithm mappings reveal optimal zeotropic mixtures: Propane/Cyclobutene below 30 °C, Cyclopropane/Pentane or Cyclopropane/Hexane from 40 °C to 50 °C, and Butene/Cyclohexane above 50 °C. Butene/Cyclohexane exhibits the highest COP and exergy efficiency.

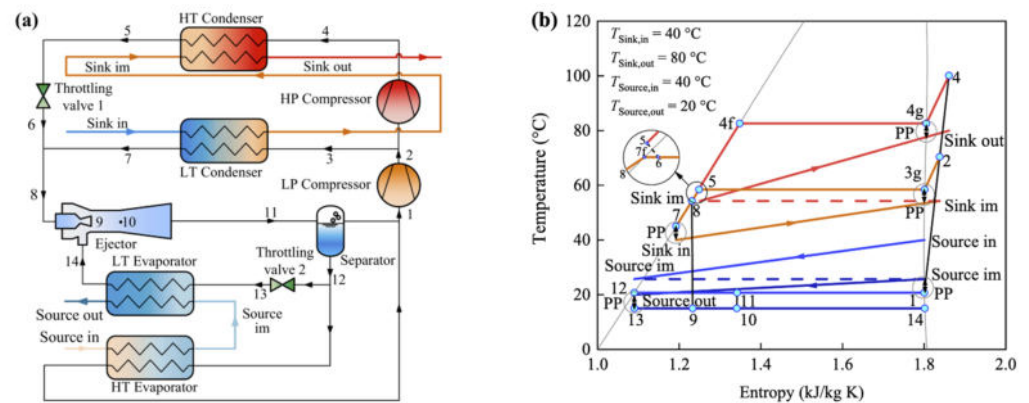


Figure 13. Dual-temperature condensation and dual-temperature evaporation HP 2 with an ejector (Ej-DCDE-2). (a) System diagram. (b) T-s diagram [41].

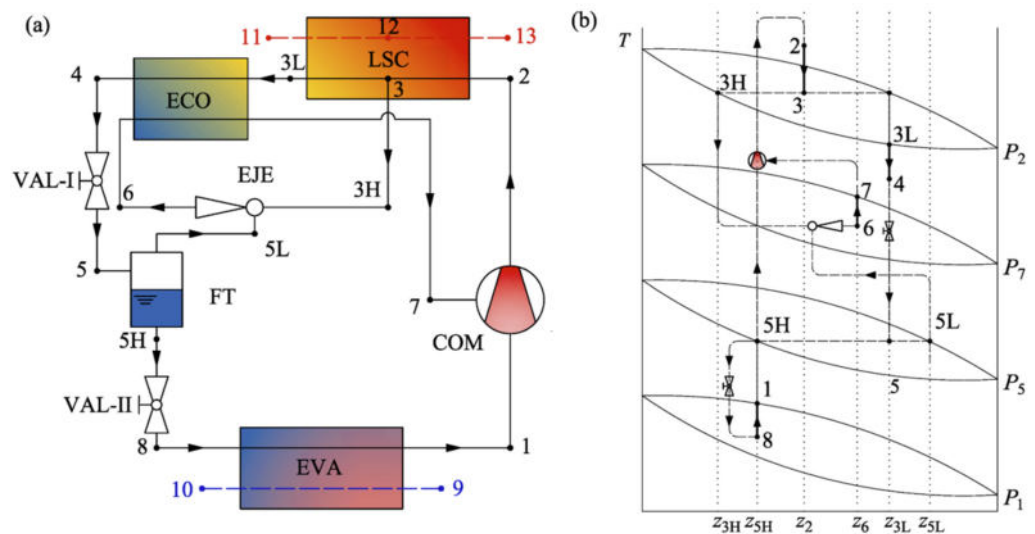


Figure 14. (a) Schematic view of LEHP and (b) its T-z diagram [42].

Wang et al. [43] explore the feasibility of using Advanced Nuclear Reactors to supply high-quality heat to Industrial Processes. While Advanced Reactors offer higher operating temperatures than Light Water Reactors, their steam characteristics generally do not align with industrial needs without additional modifications. Proposals include enhancing steam quality through heat pumps, analogous to refrigeration technology, to raise steam temperatures to 900 °C. The scheme of the Brayton heat pump and the T-s diagram for the cycle are reported in Figure 15. Numerical examples from a Pressurized Water Reactor demonstrate improved thermal efficiencies when integrating a compressor to boost steam heating values, compared to direct electric heating methods. Pettinari et al. [44] investigate Brayton heat pumps as a pivotal technology for integrating renewables into grids, focusing on their adaptability and performance in industrial and energy storage settings. Emphasizing high-temperature heat supply via renewable electricity, these systems undergo evaluation through demonstration plants. The research assesses transient capabilities using a prototype model, exploring thermal and volumetric dynamics.

Briola et al. [45] introduce a novel high-temperature heat pump (HTHP) utilizing low-temperature waste heat via two-phase compressors and expanders, operating without external electric power. The scheme of novel HTHP is reported in Figure 16. A sensitivity analysis of five variables identifies optimal conditions for a rubber manufacturer and a canning industry, achieving maximum COP values of 0.258 and 0.452, respectively. The system’s economic viability hinges on achieving isentropic efficiencies above 0.59 for compressors, above 0.55 for expanders in the rubber industry, and above 0.45 in the canning

industry. Key contributions include overcoming current HTHP limitations with efficient performance across high temperature differentials and no electric consumption, benefiting diverse industrial heating needs with significant energy and cost savings potential.

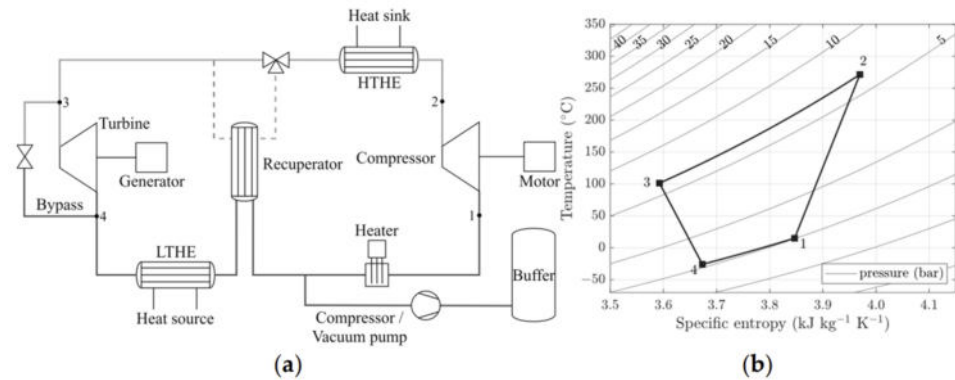


Figure 15. Brayton heat pump developed by DLR: (a) plant layout; (b) T-s diagram [44].

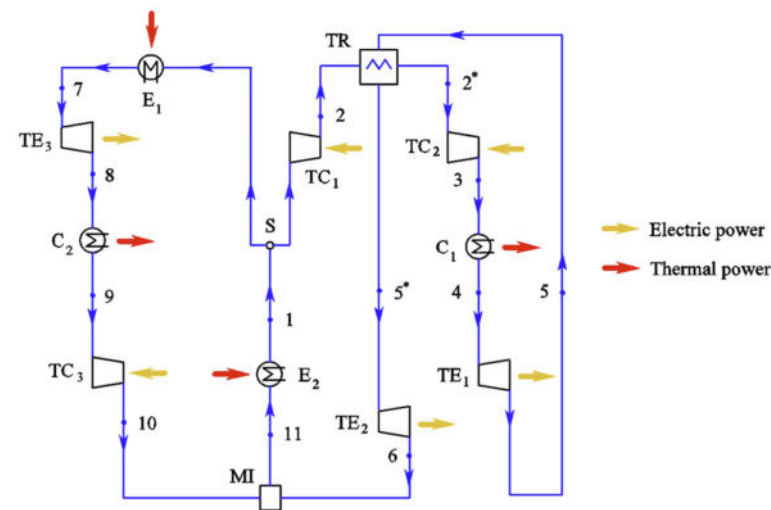


Figure 16. Novel HTHP system: circuitual scheme [45].

Xie et al. [46] introduce a novel ammonia-based hybrid chemisorption-compression high-temperature heat pump using $\text{SrCl}_2\text{-NH}_3$ to efficiently convert 50–80 °C waste heat into 90–120 °C high-temperature heat without requiring a costly high-pressure ammonia compressor. Figure 17 reports the scheme and the $\ln p\text{-}(1/T)$ diagram of the cycle. Key parameters like sorption pressure and reaction time are optimized, achieving a COP of 4.58 at 70 °C waste heat and 110 °C output, 14.5% higher than R245fa compression pumps.

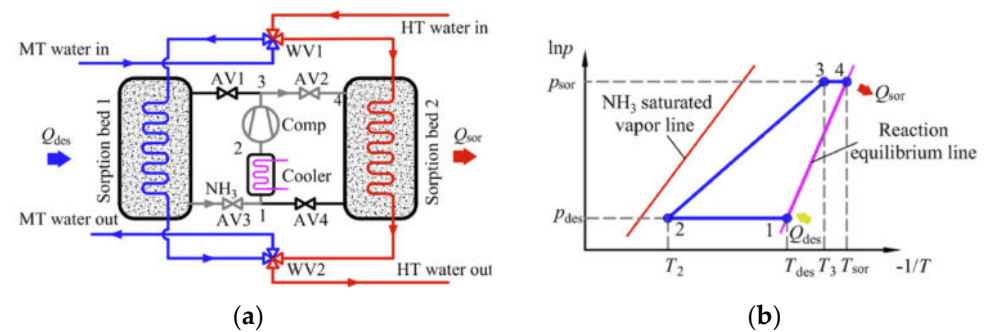


Figure 17. Hybrid chemisorption-compression high-temperature heat pump cycle: (a) schematic and (b) $\ln p\text{-}T$ diagram (HT: high temperature, MT: medium temperature) [46].

Kim et al. [47] explore HTHPs using water vapor (R-718) in three reversed Rankine cycles with varied intercooling strategies to deliver thermal energy above 200 °C. Thermodynamic analyses revealed optimal performance with equal pressure ratios (PR) across compressors, enhancing efficiency metrics such as φ and η_{exergy} . Among cycles tested, the cycle with intercooler (IC) between the first and second compression stages and with an inward flow direction of heat sink to the IC (IC-in cycle) showed superior COP and T_{sink} out values compared to spray-injection and IC-out cycles, achieving a COP of 5.86 and T_{sink} out over 200 °C at practical PR limits (PR < 2.5). Marinelli et al. [48] conduct a comprehensive life cycle assessment (LCA) of a dual-source heat pump (DSHP), utilizing air or ground as heat sources, with data provided by the manufacturer. Figure 18 reports the layout of the DSHP prototype. The study covers production, use, maintenance, and end-of-life phases, using dynamic simulations for energy performance evaluation. Results highlight the DSHP's environmental benefits in respect to conventional air and ground source heat pumps, especially in varied energy scenarios and climates.

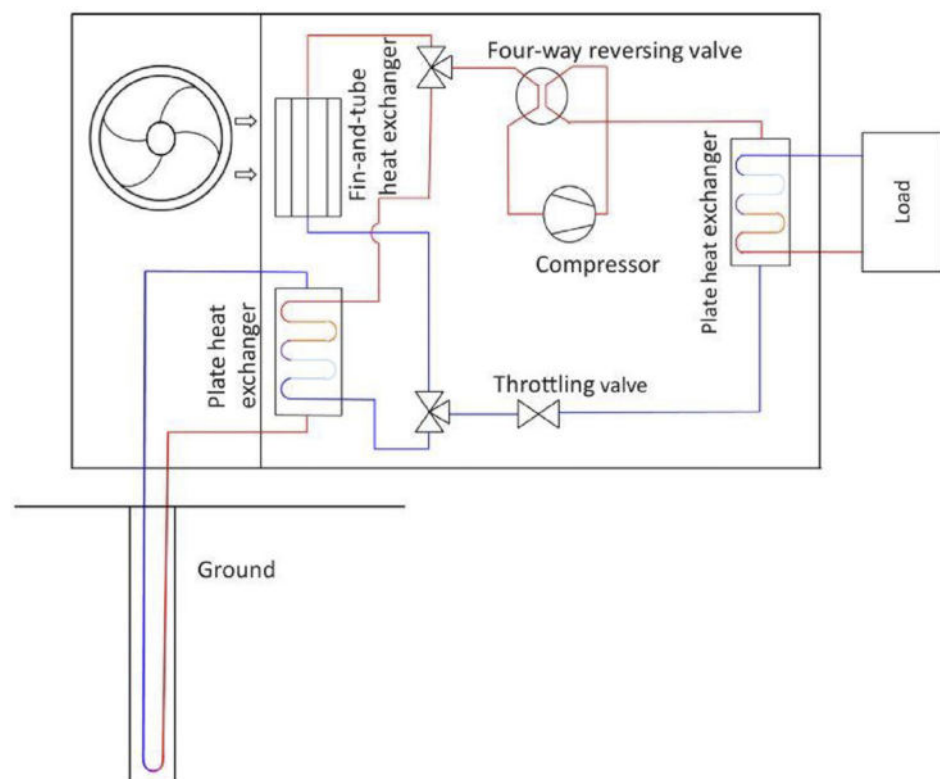


Figure 18. Layout of the DSHP prototype [48].

Zhang et al. [49] introduce a high temperature heat pump double effect evaporation concentration system to enhance energy efficiency in low vacuum, low temperature evaporation processes. An industrial experimental platform validates its performance, achieving a heat pump COP of 4.92 and 11.86 kg/(kW·h) unit power consumption evaporation. Key conclusions highlight system feasibility and stability, with insights into heat transfer performance under variable conditions and economic analysis supporting energy-efficient operations and future system advancements. Talaba et al. [50] focus on high-temperature water heating using CO₂ heat pumps, highlighting their efficiency compared to electric heating. One-stage and two-stage configurations are parametrically tested to optimize structure and operation, aiming to minimize exergy destruction. The flow chart of the cycles is reported in Figure 19. While two-stage systems show potential with external precooling, exergy coefficients in gas-coolers play a crucial role.

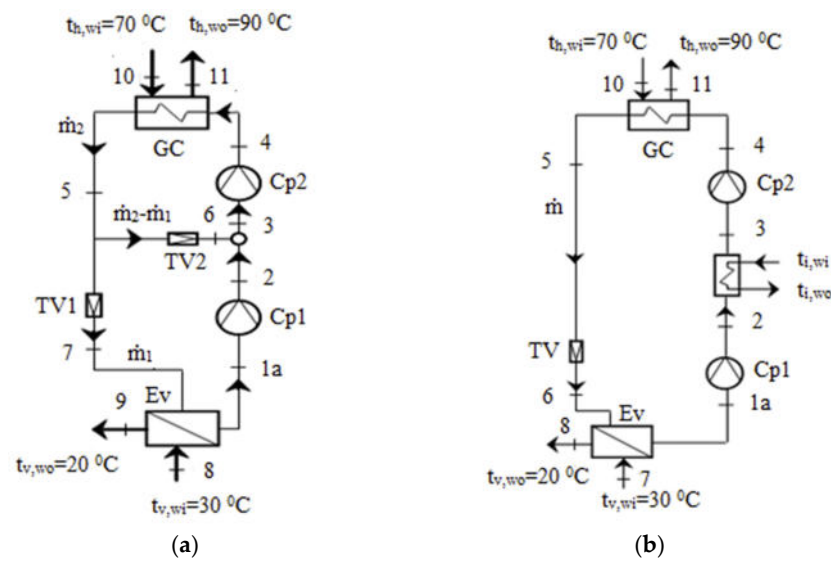


Figure 19. Flow chart of (a) two-stage system with the injection of a cold stream between the two compression stages and (b) two-stage cycle with intermediary external cooling by preheating a stream of water [50].

Stefanou [51] focuses on high-temperature heat pumps (HTHPs) as crucial for industrial heat decarbonization above $90\text{ }^{\circ}\text{C}$. Two prototypes were developed and tested: the first, integrated into a district heating loop, achieved temperatures limited by external factors, while the second, using environmentally friendly R1233zdE, operated under controlled conditions. The first prototype employed R245fa, achieving COP of 5.3–6 with heating capacity up to 43.7 kW and saving 1.44 tCO₂/yr. The second prototype achieved outlet temperatures up to $123.4\text{ }^{\circ}\text{C}$, with COP values ranging from 2.5 to 4.5 and efficiencies up to 85%. Economic analysis showed payback periods from 2.3 to 3.4 years, highlighting significant CO₂ emissions savings, up to 85%, compared to gas boilers. Gao et al. [52] proposed a novel air-source hybrid absorption-compression heat pump for stepped temperature lifts. The scheme is reported in Figure 20. It achieves a large temperature lift (over $90\text{ }^{\circ}\text{C}$) and thermodynamic perfectibility (0.34). The coefficient of performance (COP) changes from 1.7 to 1.2 as temperature lifts from $70\text{ }^{\circ}\text{C}$ to $110\text{ }^{\circ}\text{C}$. Internal heat recovery reduces heat exchanger area and cost. This system offers a feasible and efficient method for upgrading ambient heat for industrial uses.

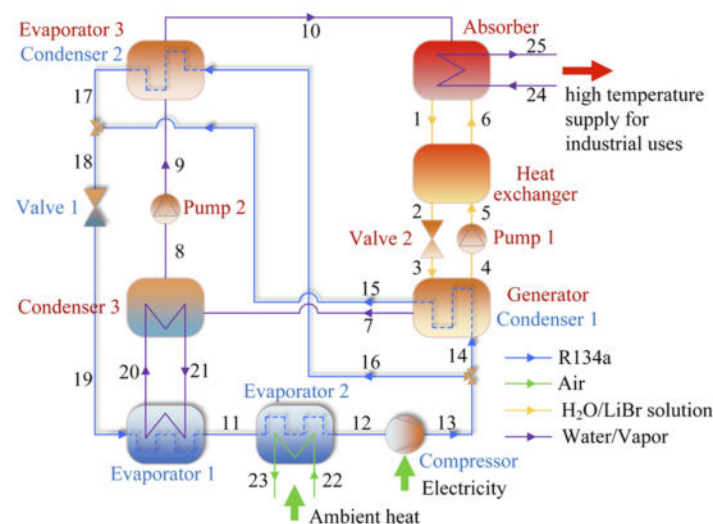


Figure 20. Schematic diagram of the air-source hybrid absorption-compression system [52].

3. Industrial Heat Pumps Applications by Sector

As already said, heat pumps, and particularly HTHPs, are a very promising solution to improve the energy efficiency of industrial processes and to reduce CO₂ emissions. However, every industrial process has its own necessities, and heat must be recovered at different source temperatures and released at different sink temperatures, thus requiring specific heat pump configurations to optimize the performance. In this paragraph, the objectives and the results of the most relevant papers published in the last 5 years dealing with innovative and specific solutions for the application of heat pumps in the main industrial sectors will be synthesized.

3.1. Chemical and Petrochemical Industries

The chemical and petrochemical sector is of vital economic importance. Global production amounted to 5.7 trillion United States dollars (USD) in 2017, including pharmaceuticals. Production is projected to quadruple by 2060 [53]. The supply of process heat in the chemical industry is dominated by fossil fuel combustion. The chemical and petrochemical sector is a major contributor to global industrial CO₂ emissions, ranking third behind iron- and steelmaking and cement production. These sectors produce 1.6 gigatonnes (Gt) of CO₂ per year total direct emissions and 0.6 Gt of CO₂ per year of indirect emissions [54]. However, it could be supplied by vapor compression heat pumps (VCHPs), allowing for efficient electrification. VCHPs could supply heat with temperatures up to 200 °C and, as shown by Marina et al. [55], they are able to cover 614 PJ/a (171 TWh/a) in the EU-28, with the chemical sector having the largest opportunity (283 PJ/a).

The most important process in the chemical industry is distillation. Many papers propose new solutions to introduce heat pumps in distillation plants to optimize energy performance. Kiss and Smith [56] observe that heat pumping in distillation processes is crucial for energy conservation, utilizing various heat pump concepts to upgrade and reuse energy. Besides traditional heat pumps, new hybrid and novel designs are emerging for higher temperature lifts and performance (see Figure 21). Heat pumps can significantly reduce utility consumption, especially when waste heat is available. Compression heat pumps, using either closed cycles or process fluids, are being optimized with new eco-efficient working fluids. Heat pump-assisted distillation technologies can cut energy use by up to 70%. A notable innovation is the heat-integrated distillation column (HIDiC), which internally integrates heat by operating the rectifying section at a higher pressure. The SuperHIDiC, developed by Toyo Engineering, exemplifies advanced commercial applications of this technology.

Separating ternary azeotropes with a high content of one component using extractive distillation is energy-intensive, but pre-concentration can enhance process economy. Wu et al. [57] optimize three processes for recovering ethyl acetate (EAc) and ethanol (EtOH) from wastewater: the conventional three-column extractive distillation (TCED), four-column extractive distillation (FCED) with pre-concentration, and three-column extractive distillation with integrated distillation column (TCED-IDC), focusing on minimizing total annual cost (TAC). The IDC integrates pre-concentration and solvent recovery. A vapor recompression heat pump (VRHP) is introduced to the TCED-IDC process to reduce energy consumption, leading to two VRHP-TCED-IDC process designs. These processes are evaluated on economy, energy consumption, environment, and exergy destruction (4E analysis). The VRHP-TCED-IDC processes excel in 4E analysis. The most efficient VRHP-TCED-IDC process (the scheme is shown in Figure 22) reduces TAC by over 32.0%, energy consumption by 53.4%, GWP by 62.0%, and exergy destruction by 49.7% compared to TCED, with significant improvements over FCED and TCED-IDC as well.

Wang et al. [58] analyze the thermo-economic benefits of vapor recompression in an ethane-ethylene distillation process. Initial simulations of the current process align closely with real plant data, showing high refrigerant consumption. The proposed vapor recompression method reduces the investment cost by 5.72% and cuts refrigerant use by 34.29%. Exergy analysis shows significant improvements, with reduced losses in the reboiler

and condenser. Li et al. [59] explore separating cyclohexane/tert-butanol from industrial effluent using heterogeneous pressure-swing azeotropic distillation. Optimal parameters for the conventional process are determined using the simulated annealing algorithm. Heat pump and heat integration strategies are incorporated to enhance energy efficiency. The heat pump-assisted process with auxiliary reboilers and heat integration (HADPSD-ARHI) achieves significant reductions: 41.98% in total annual cost (TAC), 55.32% in total energy consumption (TEC), 52.30% in gas emissions, and 55.26% in exergy destruction, compared to the conventional process. The flowsheet of HADPSD-ARHI is shown in Figure 23.

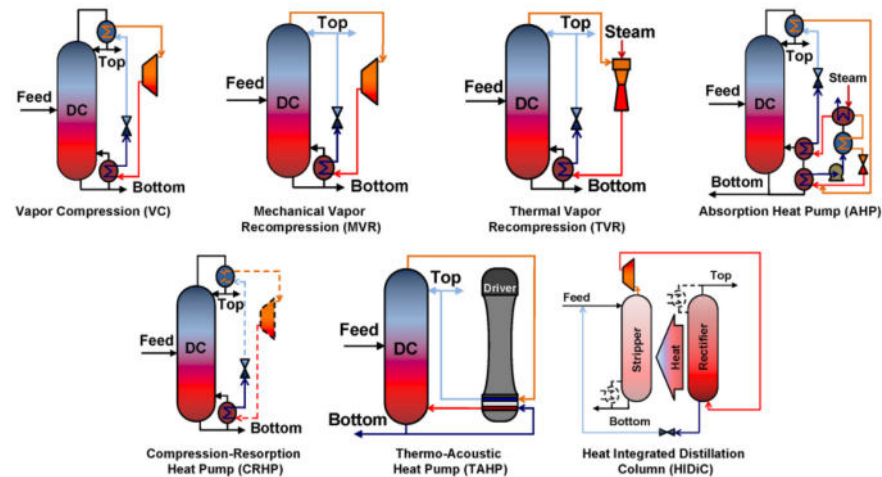


Figure 21. Main heat pump assisted distillation technologies [54,58].

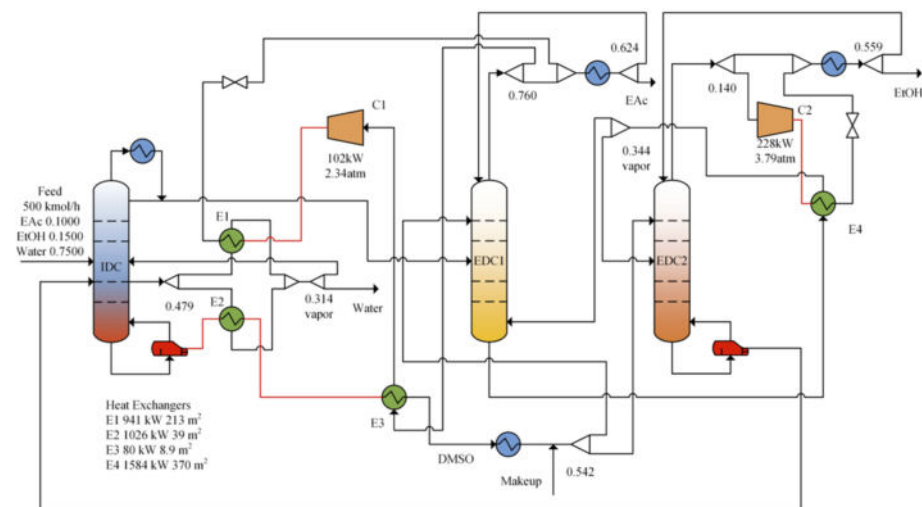


Figure 22. VRHP-TCED-IDC scheme (B) process [57].

Vieren et al. [60] discussed the potential application of heat pumps to deliver heat up to 200 °C in distillation, drying and steam production. Possible integration points and heat pump configurations are presented. Both the VCHP and a combination of a heat transformer with auxiliary natural gas boiler appeared as the most optimal solutions, depending on the energy prices. Steam production, however, may be of particular interest, since direct integration of heat pumps may be less favorable due to the potential reliability concerns. Li et al. [61] explore enhancing distillation energy efficiency through absorption heat pumps (AHP) and waste heat recovery in a petrochemical context. A novel AHP distillation system is proposed using intermediate heat exchange, optimizing parameters such as pressure and temperature to reduce steam consumption by 25%. The scheme of AHP distillation system is reported in Figure 24. The design includes a three-column

process yielding significant savings: 38.8% in steam, 42.5% in softened water, and an annual economic profit which ensures a quick payback period of 3 years.

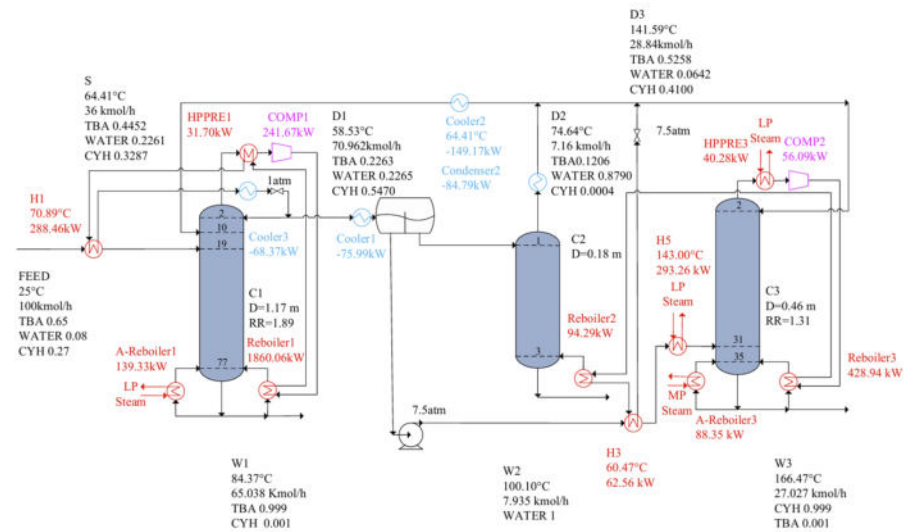


Figure 23. The flowsheet of HADPSD-ARHI [59].

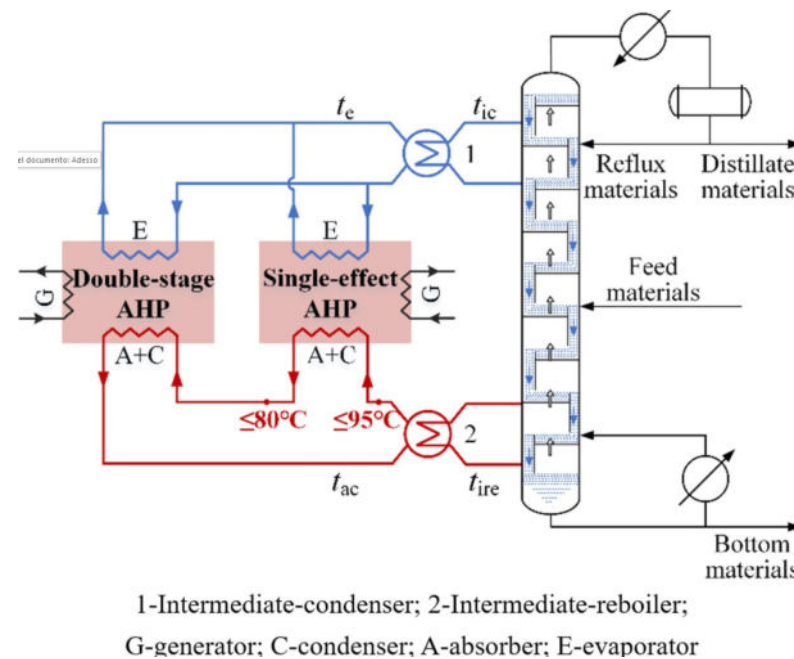


Figure 24. The form of AHPs for a new system [61].

Xu et al. [62] investigate the separation of isopropanol/tetrahydrofuran/water using extractive distillation methods, comparing indirect (IED) and direct (DED) approaches. Vapor recompressed heat pump technology and heat integration strategies are integrated to enhance energy efficiency. Evaluations encompass energetic, economic, environmental, and exergy considerations. DED proves superior to IED, with double-heat pump assisted direct approach (DED-DP) and heat integration achieving the highest energy savings (64.97%) and cost reduction (34.26%) compared to direct extractive distillation alone. Figure 25 shows the flowsheet of DED-DP process. The DED-DP process excels across all evaluated criteria, demonstrating substantial improvements in energy efficiency (64.97%), total annual cost (34.26%), and environmental impact (48.82%), with the highest exergy efficiency (11.34%) and lowest exergy destruction.

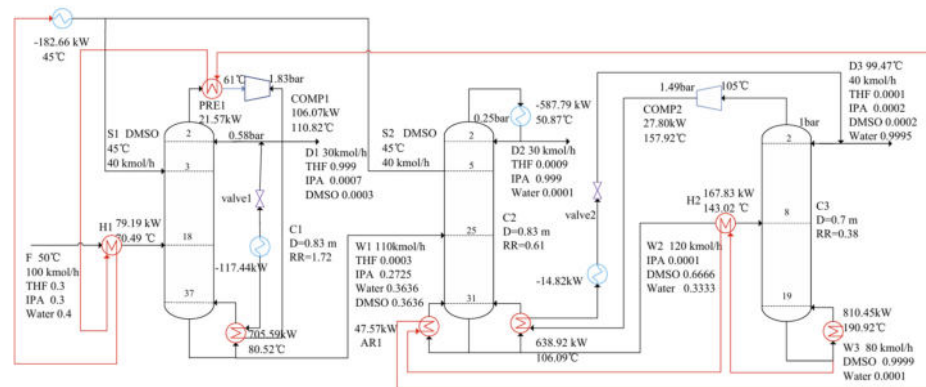


Figure 25. Double heat pump assisted DED process [62].

The same research group in [63] introduces two energy-efficient extractive distillation processes for separating acetonitrile/1,4-dioxane/water mixtures. Heat pumps and heat integration enhance energy conservation in both processes. The heat pump-assisted direct extractive distillation achieves a 53.58% energy reduction, and 53.56% CO₂ emission reduction compared to the indirect scheme, while direct distillation with heat integration reduces total annual cost by 40.38%. The direct extractive distillation with heat integration (DED-II) process excels in economic and exergetic aspects, while the heat pump-assisted DED process (DED-VR) demonstrates superior energetic and environmental benefits among the proposed designs. Zhu et al. [64] focus on the extractive distillation of the cyclohexane/sec-butyl alcohol/water azeotropic mixture, critical in environmental risk mitigation and solvent recycling. Using the COSMO-SAC model, solvents were screened based on relative volatility and solvent power, with ethylene glycol (EG) chosen for its lower boiling point. Optimizing the extractive distillation process with a sequential iterative algorithm and incorporating energy-saving methods like thermal coupling and heat pumps led to significant improvements. The best configuration (HPCWTCED, heat pump combined with thermal coupling extractive distillation), the scheme for which is shown in Figure 26, increased thermodynamic efficiency by 73.89%, reduced total annual cost by 25.62%, and decreased CO₂ emissions by 81.08%, supporting sustainable development in the chemical industry.

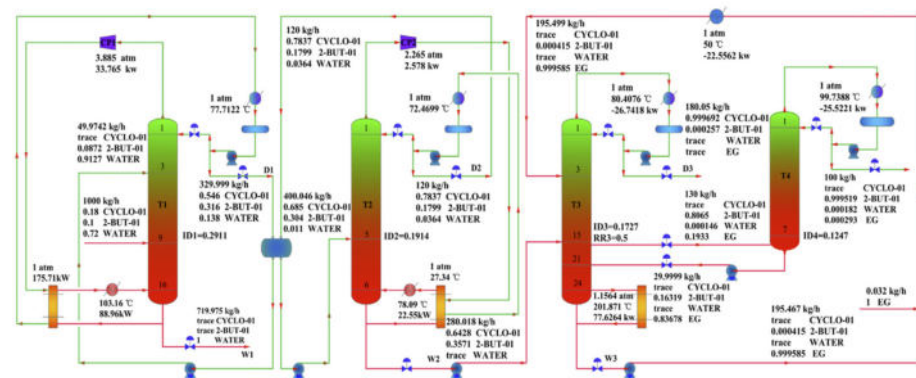


Figure 26. HPCWTCED process flow diagram [64].

Wang et al. [65] explore pressure-swing distillation (PSD) for separating water/acetonitrile/isopropanol, emphasizing two PSD processes with different separation sequences. The W-A-I sequence outperforms in economy, energy consumption, and environmental impact. Energy-saving techniques like heat integration, heat pumps, and heat exchanger networks utilize both sensible and latent heat effectively. T-S diagrams of overheads from heat-pump processes evaluate dry compression feasibility. PSD-THP-HEN (triple-heat-pump and heat exchanger network) exhibits the lowest cost, energy consumption, and emissions (CO₂, SO₂, NO_x), saving 71.4% TEC and 57.59% TAC compared to PSD-HEN. This study underscores PSD's efficiency without entrainers and validates energy-saving benefits via heat-pump

Trichlorobenzene, consisting of three isomers, requires significant energy for separation due to their close boiling points. Yang et al. [69] applied heat integration and mechanical vapor recompression (MVR) heat pump technologies to reduce energy consumption. Additionally, the Organic Rankine Cycle (ORC) is coupled with the MVR heat pump to convert waste heat into electricity for the compressor (the scheme of the process is shown in Figure 29). Compared to a four-column conventional distillation process, heat integration and MVR reduce energy consumption by 32.7% and 83.5%, respectively, and save total annual cost (TAC) by 12.4% and 22.9%, respectively. Coupling ORC with MVR further reduces energy consumption by 18.8% and TAC by 1.42%.

Wang et al. [70] explored improving the economic efficiency and environmental sustainability of the classic extractive distillation (CED) process using vapor recompression heat pump (VRHP) and an intermediate-boiling entrainer, benzene. The direct (DCED) and indirect (ICED) CED sequences for separating the acetone/n-heptane azeotrope were optimized to minimize total annual costs (TAC). Six VRHP-DCED and six VRHP-ICED sequences were designed to reduce steam and electricity consumption. Results show ICED outperforms DCED in economic and environmental aspects. VRHP-DCED (V) sequences reduced steam use by 83.38%, while VRHP-ICED (IV') sequences decreased TAC and gas emissions by 8.24% and 26.87%. Despite their benefits, VRHP-CED sequences face challenges in operability and controllability, warranting further optimization. Zhai et al. [71] addressed energy consumption in isopropanol recovery from wastewater using pressure-swing distillation (PSD) with heat pump (HP) techniques. Three energy-efficient PSD processes were proposed and optimized: HIPSD, PSD-HP, and HIPSD-HP. Compared to conventional PSD (CPSD), these alternatives achieved significant cost and energy savings. PSD-HP showed the highest efficiency, reducing total annual cost (TAC) by 51.30% and CO₂ emissions by 84.73%. The heat pump application proved most effective, despite a 54.51% higher capital cost. The combined heat integration and HP approach (HIPSD-HP) also improved economic, environmental, and thermodynamic efficiency. These methods promise significant improvements in sustainable industrial alcohol dehydration. Ulyev et al. [72] focus on the thermal integration of an existing ethylbenzene (EB) production facility. Four variants for modifying the heat exchange network (HEN) were investigated by applying a Hysys simulation model. The first variant, using classical Pinch analysis, reduced hot utility consumption by 10.7%. Two variants proposed integrating a recompression heat pump, each reducing hot utilities by 34% but differing in compressor power requirements. The first option was more economical despite both reducing utility consumption by 1691 kW. Combining Pinch analysis with the preferred heat pump integration reduced steam consumption by 37% and CO₂ emissions by 1.0 t/h, making it the most effective modernization project for the HEN of the EB production unit. This approach achieved greater reductions in steam consumption compared to previous methods and had a favorable payback period.

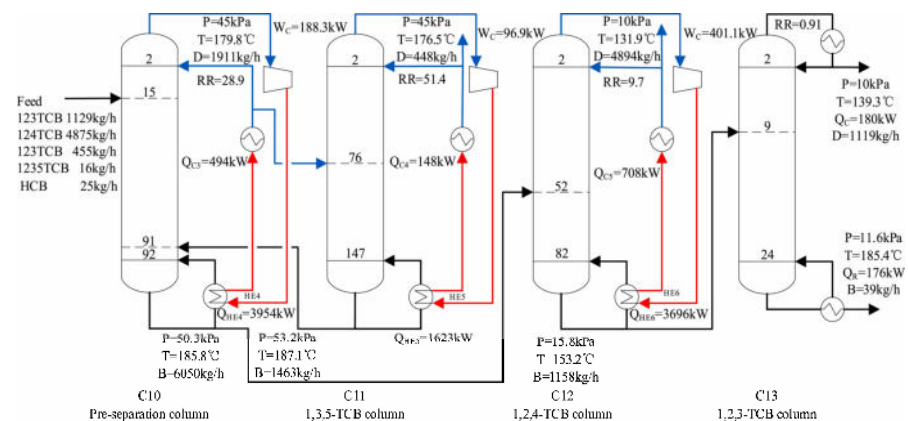


Figure 29. MVR heat pump distillation process with main parameters [67,71].

However, heat pumps can be applied also in other chemical processes. Boldyryev et al. [73] explore heat pump integration in natural gas–liquid processing within a petrochemical plant. They studied the simulation of 3 different types of heat pump equipment and evaluated the economic trade-offs for different pressures in evaporators and condensers. The total annual costs for the two best heat pumps were reduced by 6% and 50%, respectively, compared to configurations targeted by grand composite curves, despite increased electricity consumption and cooling requirements. This reduction translates to savings of 21.5 million EUR annually, highlighting significant investment potential. The study emphasizes optimizing heat exchanger networks (HEN) and addressing cost assessments for effective industrial application. Wu et al. [74] present a novel methanol steam reforming (MSR) system integrated with a CO₂ heat pump (HP) and cryogenic separation system to optimize performance. The diagram of the integrated system is shown in Figure 30. The cryogenic system separates CO₂ in liquid phase, while the CO₂ HP system connects the MSR and cryogenic systems, utilizing waste energy and providing necessary heat. This integration fully utilizes waste heat and CO energy, producing liquid CO₂ as a byproduct. Energy and exergy efficiencies improved by 5.57% and 5.15%, respectively.

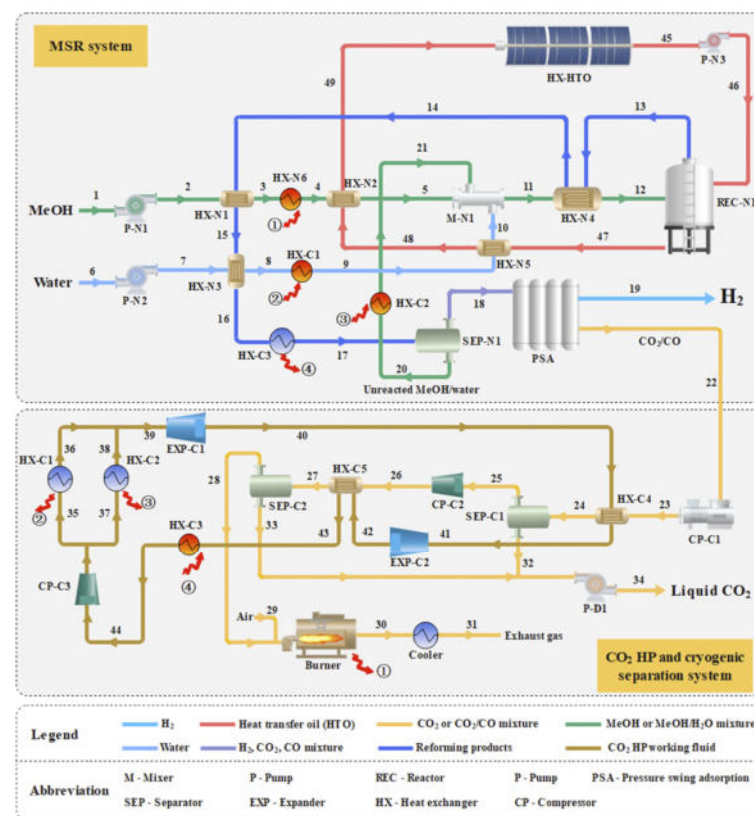


Figure 30. Schematic diagram of the integrated system [74].

De Raad et al. [75] used Process Change Analysis (PCA) with exergy to identify improvements, demonstrated in biodiesel and vinyl chloride monomer plants. In biodiesel production, a heat pump with a COP of 4.2 faced a 40 kW penalty for transferring heat above the Pinch temperature, which was mitigated by replacing the wet water washer with a membrane separation unit, reducing energy needs from 0.9 MW to 0.3 MW. In the vinyl chloride monomer process, strategic heat extraction increased the heat pump's performance by 6.5%.

3.2. Desalination

Desalination, the process of converting saltwater into freshwater, offers a viable approach to address challenges presented by water scarcity related to depletion of freshwater

sources and population growth [76,77]. Amongst the various techniques developed to make the desalination process consume minimum energy [78], humidification-dehumidification-based desalination (HDH) can benefit from the use of heat pumps, which could be employed as a heat source, or by the use of absorption heat pumps to exploit the exhaust heat of the desalination process. Heat pumps can also be integrated with the membrane method to improve thermal efficiency [79]. Several papers have been published in the last 5 years regarding new solutions to apply heat pumps to desalination. Tareemi et al. [80] address water shortage and energy utilization by enhancing production capacity and thermo-economic performance in solar still desalination. Passive modifications included a V-corrugated basin and black cotton wick material. Active enhancements used a 250 W heat pump, a 200 L evacuated tube water heater and glass cover cooling to improve evaporation and condensation. A scheme of the two systems is shown in Figure 31. The combined system achieved a daily yield of 19.75 L/m², thermal efficiency of 64.49%, and exergy efficiency of 6.31%, surpassing the basic design by 439.6%, 59.7%, and 81.84%, respectively. Economic analysis showed a distilled water cost of 0.0164 \$/L, a 9.4% reduction, and CO₂ mitigation increased from 1.35 to 9.31 tons/year, demonstrating environmental benefits and applicability in remote and arid regions.

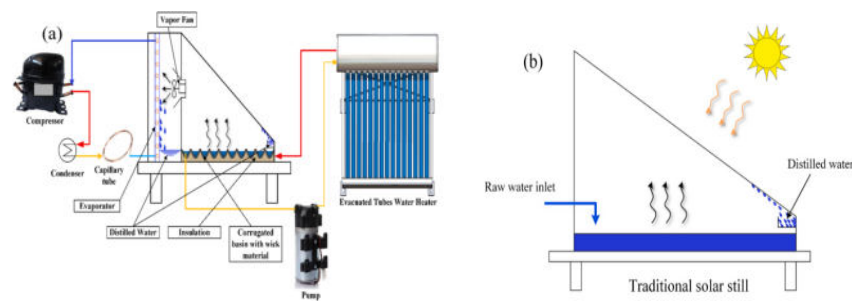


Figure 31. Test-rig real illustration of (a) proposed design with heat pump and (b) traditional design [80].

Hai et al. [81] explore eco-friendly organic mixtures in heat pump-driven humidification-dehumidification desalination systems, comparing organic blends with structural modifications. Two scenarios are analyzed: a basic heat pump and a vapor injection heat pump. Exergoeconomic analysis and optimization reveal significant efficiency improvements with organic blends. R142b, R22/R142b, and R142b/R22/R236fa have the lowest electricity consumption and highest GOR. Organic blends, especially ternary ones, significantly enhance cycle performance without high costs. R134a in humidification-dehumidification vapor injection head pump (HDH-VIHP) improves GOR by 14.25%, while R22/R142b in HDH simple heat pumps (HDH-SHP) boosts GOR by 41.26%. R142b/R22/R236fa increases GOR by 45.85% in HDH-SHP and 33.19% in HDH-VIHP. Figure 32 shows the scheme of HDH-SHP and HDH-VIHP. Optimizing scenarios improves exergetic efficiency by up to 12.55% and unit cost of distilled water by up to 16.21%.

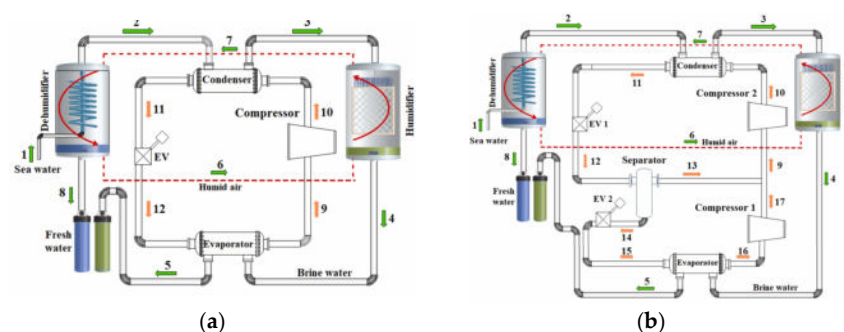


Figure 32. Layout of distilled water production systems coupled with different types of heat pumps: (a) first scenario (HDH-SHP); (b) second scenario (HDH-VIHP) [81].

Petersen et al. [82] explore integrating a transcritical CO₂ heat pump into thermal desalination, operating up to 180 °C with an eco-friendly fluid. Six configurations show energy demands comparable to reverse osmosis (RO), with the integrated system outperforming RO when considering cooling energy. A 19 MW_{el} CO₂ heat pump can produce 64,000 m³/d of potable water and 75 MW of cooling energy, highlighting its potential for water scarcity and cooling solutions. This integration could significantly reduce carbon emissions, potentially saving up to 19 kg CO_{2eq}/m³. Shahzad et al. [83] present a novel system combining an open cycle absorption heat pump (OAHP) and FlashME desalination to utilize waste heat from industrial flue gasses. The system, modeled in Aspen Plus, recovers 89.42% of waste heat at a thermal COP of 2.21, using it to heat seawater to 70 °C for the FlashME process, achieving a performance ratio of 3.05. The system's performance varies with inlet flue gas parameters and regeneration pressure, recovering 9.19% to 37.17% of water. The study concludes that the integrated OAHP-FlashME system is effective for waste heat recovery and seawater desalination, suitable for industries like coal-fired power plants and textiles. The same research group in [84] proposed a novel system combining the open absorption multifunctional heat pump, FlashME desalination, coupled to a compressed air dryer to recover latent heat from flue gas for seawater desalination and compressed air drying. The system, modeled in Aspen Plus, achieves 83.02% heat recovery efficiency, a thermal COP of 1.95, and 23.14% freshwater recovery. The system's performance is influenced by spray solution parameters and flue gas humidity, with water recovery dependent on heat capacity and regeneration pressure. The coupled system can reduce regeneration load by up to 37.78% and enhance distillate productivity by 54.24%. Chen et al. [85] propose a novel system combining a heat pump, multi-effect desalination (MED), and ice storage, providing both thermal and cold energy for desalination and ice generation. Compared to conventional mechanical vapor compression (MVC) and air conditioning systems, the proposed system shows significant improvements in thermodynamic, economic, and environmental performance. The specific energy consumption (SEC) is reduced from 8.94 kWh/t to 4.71 kWh/t, and the payback period decreases from 5.90 to 3.85 years. The environmental impact is also lower, with CO₂ emissions reduced by 7.68%. Zhou et al. [86] propose a heat pump coupled two-stage (HPTS) humidification and dehumidification (HDH) desalination system utilizing waste heat for heating feed seawater and brine (see Figure 33). Performance evaluations with different working fluids were conducted, focusing on freshwater production (mpw), gained output ratio (GOR), recovery ratio (RR), specific entropy generation (stot), and unit cost of fresh water (Zpw). Results indicate that R22 yields the highest mpw, while R600 achieves the lowest Zpw and stot and the highest GOR. Higher spraying temperatures improve mpw and Zpw and increase stot. Optimal performance occurs at specific mass flow rate ratios and compression ratios. The system shows promising thermodynamic and economic performance compared to existing systems.

Ghiasi et al. [87] address the high electricity consumption of integrated desalination and heat pump cycles by modifying a double-effect absorption heat pump cycle combined with a humidification-dehumidification desalination system. Innovations include preheating seawater with waste heat from the absorption chiller and designing a hybrid thermal-mechanical heat pump. A scheme of the system is shown in Figure 34. The proposed system increased freshwater and cooling production by 23.23% and 47.7%, respectively, and achieved a 17.89% higher energy utilization factor (EUF) of 6.96. Optimal steam extraction improved exergy efficiency by 27.23%, and freshwater cost was reduced to \$2.051/m³. The humidifier was the main source of exergy destruction, constituting 16.5% of the total rate.

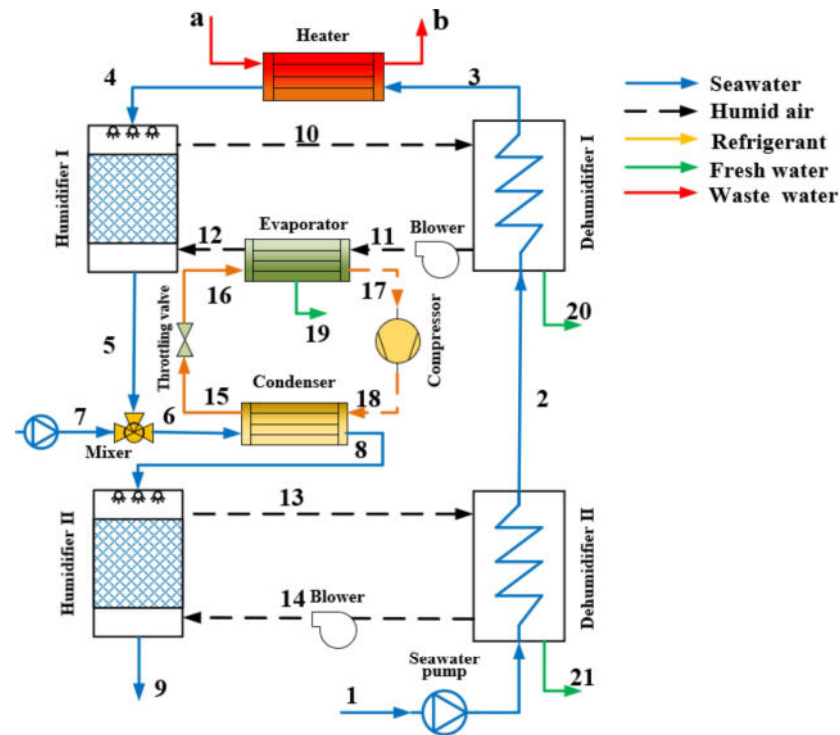


Figure 33. Schematic diagram of the HPTS-HDH system [86].

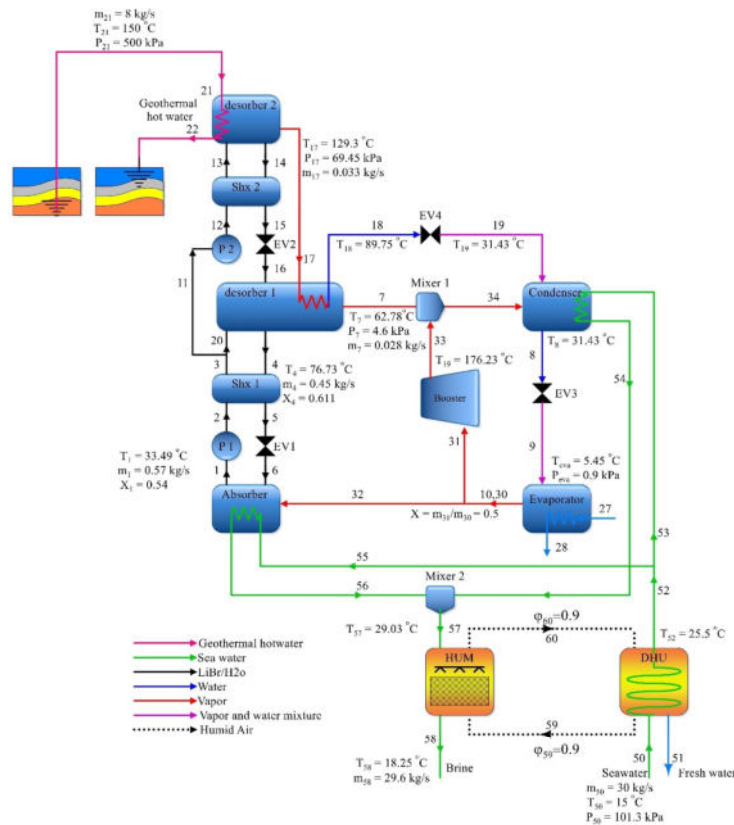


Figure 34. Sketch of the proposed new low thermal driven cooling/desalination system assisted with a booster (also called an integrated DEARC-HDH system) [87].

Khalifa et al. [88] present a theoretical analysis of integrated direct contact membrane distillation (DCMD) and heat pump (HP) systems for water desalination, focusing on performance, energy efficiency, and production cost. Various integration scenarios with open

and closed water cycles and refrigerants R134a and R22 were examined. Results indicated that heat pump specifications set the performance limits of condenser and evaporator heat exchangers. The DCMD-HP system showed lower energy consumption and production costs compared to electrically driven systems. Customizing a heat pump for DCMD in closed cycles achieved GOR values between 1.8 and 2.1, SEC values between 330 and 400 kWh/m³, and production costs from 0.5 to 4 \$/m³. Integrating a multistage parallel DCMD further reduced production costs to 0.5–2 \$/m³ while maintaining high efficiency.

3.3. Food and Beverage Industry

The food and beverage industry, focusing on energy use, water consumption, climate change, and other subsystems, has profound environmental impacts [89]. Increasing energy efficiency and reducing the use of fossil fuels are key strategies for achieving climate neutrality in the food supply chain. To this purpose, high-temperature heat pumps are a promising technology for both heat recovery and energy efficiency in this sector [90]. As an example, Zuberi et al. [91] explore the potential of electrifying industrial process heat in major U.S. food manufacturing sectors using high-temperature and steam-generating heat pumps. By 2050, it identifies substantial annual energy savings of 325 PJ and CO₂ reductions of 31 MtCO₂, equivalent to emissions from 6 million cars annually. Several papers in the last 5 years have analyzed the application of heat pumps in food and beverage sector. Loemba et al. [92] investigate a novel solar-assisted heat pump dryer with soapstone thermal energy storage, examining three operational modes: daytime storage (mode 1), nighttime without storage (mode 2), and daytime without storage (mode 3). Using 500 g of Cavendish banana, experiments showed moisture reduction from 74.4% to 9.6% in 270, 390, and 360 min for modes 1, 2, and 3, respectively. Mode 1 exhibited the highest efficiency at 23.23% and COP values of 3.69, 2.57, and 2.54 for modes 1, 2, and 3, respectively. Economic analysis indicated a 1.5-year payback period and 65% return on investment for mode 1.

Bhadbhade et al. [93] focus on decarbonizing industrial processes like Swiss chocolate production through heat pump (HP) electrification. It introduces a methodology to create exemplar, representative, and sector-wide energy demand profiles, using Pinch Analyses (Figure 35) for accurate data. Results identify five HP integration opportunities based on company size and operational parameters, showing HPs with COPs above 2.6 are generally cost-effective. Potential reductions include up to 56% in CO₂ emissions and 28% in energy efficiency.

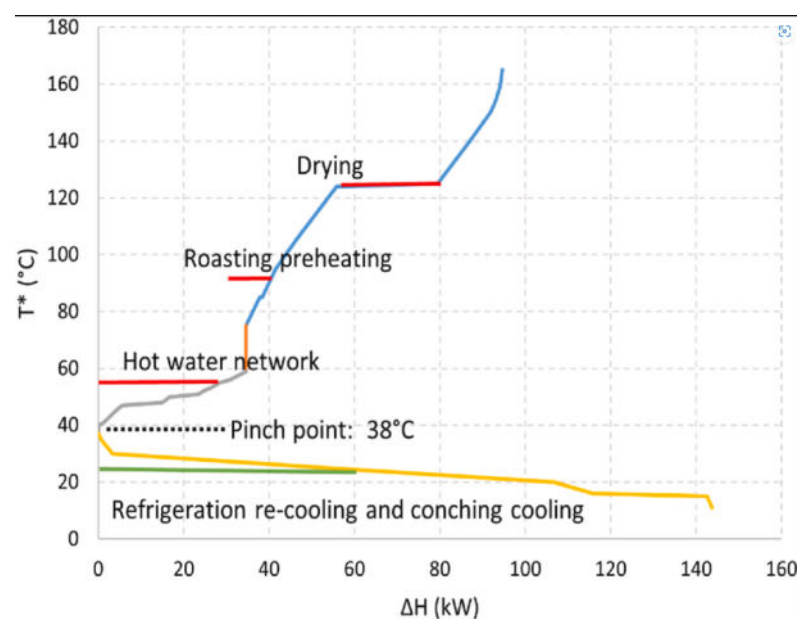


Figure 35. Representative grand composite curves (profile) for chocolate production in Switzerland [93].

Moritani et al. [94] propose a subirrigation system using heat pumps to control substrate temperature, enhancing greenhouse farming sustainability. Heat pumps sourced from air or geothermal systems maintained optimal growth conditions (18.4 °C) for strawberries, with geothermal heat pumps showing 1.8 times higher COP during heating and reducing electricity by 14.9%. Yields increased by 21% (geothermal) and 36% (air-source) compared to controls due to improved growth conditions. Knorr et al. [95] explore integrating renewable energy and enhancing energy efficiency in industrial heat generation, emphasizing electrification to reduce energy consumption and emissions. When comparing electric boilers and heat pumps using Pinch analysis and optimization, electrification can increase costs by 26% to 176% while reducing emissions by up to 39%. For sterilizing pet food pouches at 120 °C, electrification proves economically viable at average European prices in 2021, with electric boilers being the most cost-effective among electrified solutions. A hybrid approach combining a heat pump's efficiency with a boiler's flexibility offers the lowest costs and competitive performance with natural gas systems at specific electricity-to-gas price ratios. Klinac et al. [96] apply a novel Pinch-based Total Site Heat Integration (TSHI) method, tailored for industrial heat pump applications, at a meat processing site in New Zealand, leveraging renewable electricity to cut carbon emissions significantly. Figure 36 shows the total site integration plots of the heat exchange flows. The method enhances traditional approaches by pinpointing overlooked heat pump opportunities, like Mechanical Vapour Recompression (MVR) in the Rendering plant and a centralized air-source heat pump for the hot water ring main, potentially reducing site emissions by over 50%.

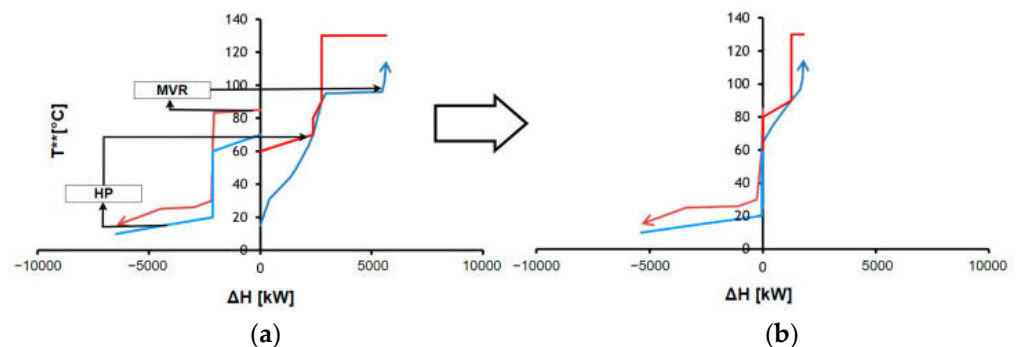


Figure 36. Total site integration plots showing potential heat pump installations (a), leading to final expected total site plot (b). The red lines on the Gross cold utility use side of the plot represent process streams that require cooling, and the blue lines represent the cold utility streams that would be required to carry out this cooling. The blue lines on the Gross hot utility use side of the plot represent process streams that require heating, and the red lines represent the hot utility streams that would be required to carry out this heating. Total site integration plots showing potential heat pump installations (a), leading to final expected total site plot (b). The red lines on the Gross cold utility use side of the plot represent process streams that require cooling, and the blue lines represent the cold utility streams that would be required to carry out this cooling. The blue lines on the Gross hot utility use side of the plot represent process streams that require heating, and the red lines represent the hot utility streams that would be required to carry out this heating [96].

Foslie et al. [97] emphasize the significance of electrifying low temperature heat in industries by applying heat pumps to cut emissions, using a model to optimize energy system investments at a dairy. Integrating thermal and electrical systems reduces costs by 24% and emissions by 96% compared to traditional methods, with thermal energy storage proving crucial for cost-effective flexibility. Martyanov et al. [98] highlight key principles for designing furnaces and thermal chambers for the heat treatment of meat products: efficient energy use, enhanced productivity via compact product arrangement, precise airflow direction, temperature and humidity control, reliability, and compliance with emission regulations. Heat pumps offer advantages in high-power enterprises where water as a

coolant is impractical, promoting uniform product quality and bacterial control in meat processing. Integrating heat pumps in industrial food equipment circuits, such as rotary kilns, optimizes energy use by harnessing waste heat, reducing fuel and electricity costs. Hermanucz et al. [99] investigate an experimental dual-source heat pump (DSHP) system designed to meet simultaneous cooling and heating needs in brewing processes, achieving a 60% reduction in CO₂ emissions and a 10% decrease in energy costs compared to traditional methods. The DSHP system operates with two evaporators at different temperatures and times, replacing natural gas for heating with energy from the heat pump's condenser. With an average COP of 2.5, the DSHP significantly lowers energy consumption, notably by reducing CO₂ emissions formerly attributed to natural gas combustion. Energy cost comparisons between the DSHP and boiler + chiller system (BCS) show a 10% cost reduction favoring the DSHP. Ahrens et al. [100] examined the energy consumption and performance of a green-field dairy's integrated heat pump system in Bergen, Norway. The dairy employs high-temperature heat pumps with natural refrigerants for all heating and cooling demands. A scheme of the integrated energy supply system is shown in Figure 37. An energy analysis based on a high-demand week in February showed the system meets demands with a specific energy consumption of 0.22 kWh/L, outperforming the replaced dairy. Energy consumption was reduced by 37.9% and GHG emissions by up to 91.7% through extensive waste heat recovery, which accounts for 32.7% of energy used and achieves a recovery rate over 95%. The system's COP is 4.1, with potential for further improvements.

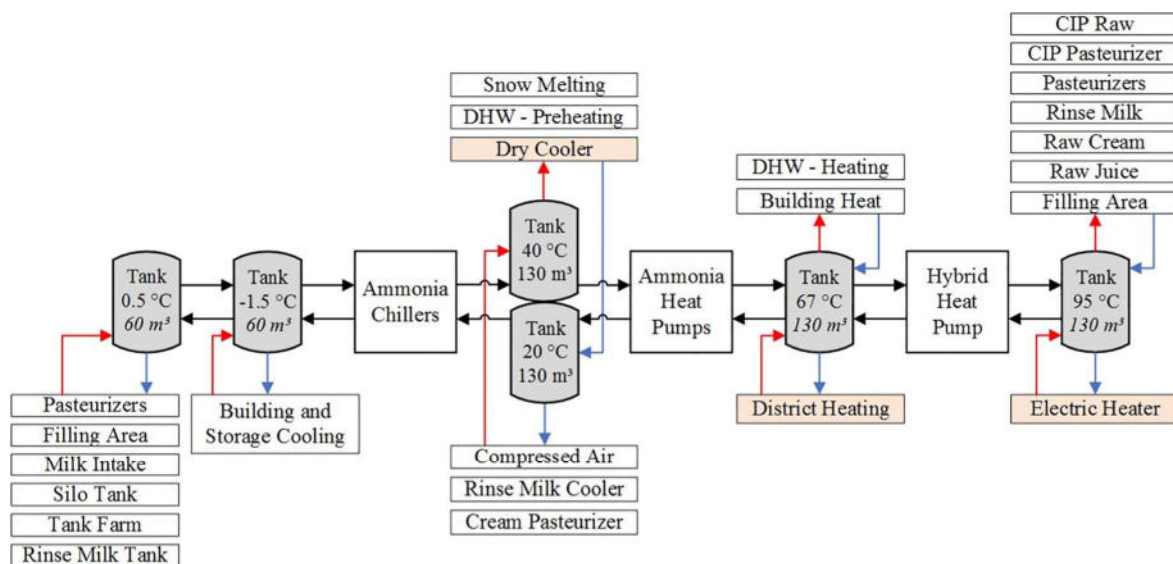


Figure 37. Integrated energy supply system including heat pump systems and thermal storage tanks [100].

3.4. Industrial Steam Generation

Several sectors, such as pulp, paper, or chemical industries, consume wide amounts of industrial steam to feed their processes that often require steam at temperatures from 100 °C to 200 °C. This temperature range involves 26% of total process heat demand, and the heat is generally produced with fossil fuel burners.

Payà et al. [101] evaluate replacing industrial gas boilers for steam production with Solar Heat for Industrial Processes (SHIP), Electric Boilers (EBs), High-Temperature Heat Pumps (HTHPs), and Absorption Heat Transformers (AHTs) across Europe. EBs are not cost-effective except in Sweden due to high electricity prices, while HTHPs achieve PBs < 4 years at 120 °C and are optimal with electricity-to-gas ratios < 3.5. Ma et al. [102] evaluate a High-Temperature Heat Pump Steam System (HTHPSS) generating steam at 170 °C from industrial waste heat, aiming to replace coal-fired boilers. Key findings include a maximum COP of 2.73, peak exergy efficiency at 43.26%, and a payback period (PBP)

ranging from 0.03 to 4.40 years, depending on waste heat and condenser temperatures. Feng et al. [103] focus on enhancing High-Temperature Heat Pumps (HTHPs) for steam generation using industrial waste heat. By employing two-stage separation and dual-pressure evaporation technology with low-GWP refrigerant mixtures, significant improvements were achieved. The schemes of the two systems are reported in Figure 38. The optimal R1234ze(E)/R1233zd(E) mixture outperformed others, showing 0.85%–1.86% higher thermodynamic effectiveness than benchmark mixtures. The improved cycle exhibited a 45.17% increase in heat source utilization efficiency and a 24.48% higher coefficient of performance (COP) compared to the basic cycle.

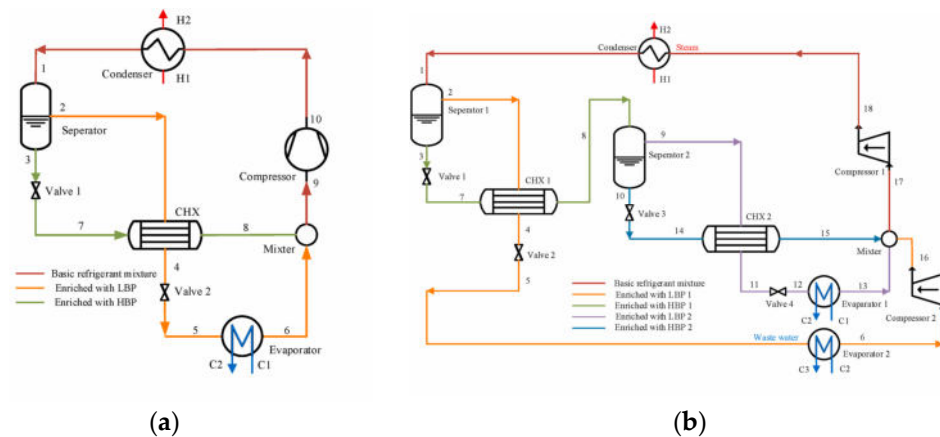


Figure 38. System schematic diagram of heat pump: (a) the basic auto-cascade cycle (basic cycle); (b) the dual-pressure evaporation auto-cascade cycle (improved cycle) [103].

Klute et al. [104] review Steam Generating Heat Pumps (SGHPs) as a crucial technology for decarbonizing industrial heat supply up to 250 °C. Various configurations (SGHP-A to SGHP-E) are highlighted utilizing advanced HP technologies, including closed-loop compression and absorption heat pumps achieving up to 250 °C and open-loop systems like MVR and TVR reaching 350 °C. Over 40 SGHP designs were analyzed and categorized, emphasizing flexibility in responding to diverse conditions while noting the challenge of complexity in system planning. Simplified modeling and cost estimation models are proposed to enhance accessibility and applicability of SGHPs in industrial settings. Kosmadakis et al. [105] explore integrating High-Temperature Heat Pumps (HTHP) for waste heat recovery in marine applications, focusing on two configurations: direct steam generation and preheating for auxiliary boilers. An electric-driven cycle with R1233zd(E) refrigerant is utilized. Performance assessments using validated models show COP values of 5.11 for preheating and 2.07 for steam generation, with significant fuel savings up to 2.5% in oil tankers and cruise ships. Despite longer payback periods (over 20–30 years) for steam generation due to lower COP, the preheating option achieves quicker returns (2–6 years), supported by substantial emissions reductions, particularly CO₂. Koundinya et al. [106] explore a Steam-Generating Heat Pump (SGHP) system utilizing a high-temperature scroll compressor to replace diesel boilers in industrial kitchens, aiming to reduce CO₂ emissions. The SGHP achieves steam generation at 1.5 bar, 81.43 kg/h, and 108.52 °C, simulated via DWSIM under steady-state conditions without pressure drop. Field deployment in a canteen showed a COP of 2.2. Despite emitting 20.3% more carbon than diesel in India, it could potentially reduce emissions by 57.8% under EU emission factors. Zeilerbauer et al. [107] evaluate large-scale high-temperature heat pumps (HTHPs) (see Figure 39) for industrial steam provision through a comprehensive life cycle assessment (LCA). A new scaling approach was developed and applied using data from commercial HTHP trials at 2 and 5 bar steam pressures. Results showed up to a 98% reduction in greenhouse gas emissions, with mixed impacts across other environmental categories compared to fossil fuel steam boilers.

trial applications using heat-pump technology. Fossil fuel, electric, and heat-pump methods are analyzed, highlighting heat-pump heating as the most efficient and adaptable. A system using a heat pump for preheating low-temperature evaporation, followed by steam compression, is proposed. Key parameters and optimization opportunities are identified. The second steam-generation path, involving evaporation under sub-atmospheric pressure, demonstrates superior performance with a heat-transfer temperature difference of 7.95 °C and a maximum efficiency of 1.86. The use of an ejector may enhance efficiency depending on its ejection ratio, confirming the energy-saving advantages of the proposed method.

3.5. Irons Steel Industry

The energy consumed by the iron and steel industry accounts for 10–15% of the globe's energy expenditure, and its CO₂ emissions account for about 7% of all anthropogenic CO₂ emissions [111]. Thus, waste heat recovery in the iron and steel industry is very important to enhance energy efficiency and reduce CO₂ emissions due to the significant production of heat at high (>400 °C), medium, and low (<100 °C) temperatures [112]. Specific findings suggest heat recovery offers low payback periods (<2 years) under various energy price scenarios, with potential energy consumption reductions up to 79 MJ/t steel and heat pumps among the most interesting technological solutions to achieve this objective. Some solutions have been proposed in recent years to integrate heat pumps in iron and steel production processes, as exemplified in Figure 41 [113].

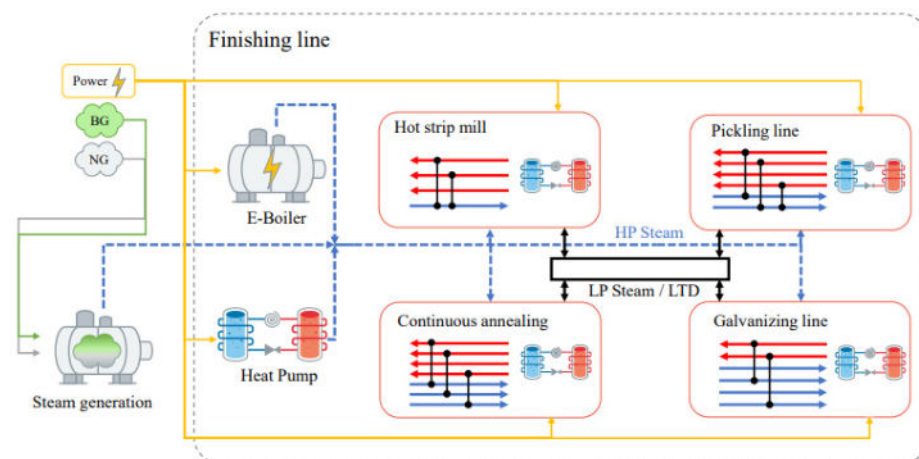


Figure 41. Schematic representation of the optimization model for the energy system in the finishing line [113].

Alshehhi et al. [114] focus on recovering waste heat from electric arc furnace (EAF) exhaust gasses in the steel industry to enhance production efficiency and sustainability. Simulations in Aspen Plus[®] (<https://www.aspentech.com/en/products/engineering/aspen-plus>, accessed on 23 September 2024) and STAR-CCM+ (<https://plm.sw.siemens.com/en-US/simcenter/fluids-thermal-simulation/star-ccm/>, accessed on 23 September 2024) assessed waste heat recovery (WHR) via thermal energy storage (TES) using high-temperature concrete and Therminol VP-1 fluid. An Organic Rankine Cycle (ORC) with cyclopentane maximized energy extraction. WHR could potentially offset 11.9% to 13.4% of EAF energy consumption, reducing CO₂ emissions. Hoettecke et al. [115] discuss resilience in the energy-intensive metal industry, focusing on integrated supply systems using heat pumps, electrolyzers, and combined heat-and-power units. Heat pumps reduce groundwater use by 18% and meet over 70% of space heating needs with waste heat, enhancing system resilience against future environmental and regulatory challenges. Beck et al. [116] explore emission reduction and energy efficiency in the steel processing industry by replacing natural gas-fired steam with heat recovery and heat pumps. Pinch analysis identifies opportunities for direct heat recovery and heat pump integration across four facilities, with surplus heat transfer between plants also considered. Economic optimization

models suggest substituting 20–80% of steam through direct recovery, up to 100% with heat pumps, and fully utilizing an inter-plant low-temperature distribution (LTD) system. Payback periods range from 1 to 4 years depending on technical configurations and energy costs. A future scenario favors integrating a combined direct heat recovery, heat pump, and LTD system, potentially yielding significant savings over 10 years despite integration challenges and uncertainties. Brough and Jouhara [117] explore aluminum's growing industrial use and its production process, emphasizing energy efficiency and environmental impact. Heat pumps are highlighted for their role in recovering waste heat, which is crucial in reducing energy consumption and emissions. Various types of heat pumps, including air, water, and ground source, are discussed, showcasing their application beyond residential settings into industrial contexts like aluminum production. Case studies, such as at Alcoa Deschambault Quebec, illustrate potential CO₂eq. savings and economic benefits through efficient heat recovery for space heating.

3.6. Textile Industry

The textile industry contributes approximately 2% of global greenhouse gas emissions, with a significant opportunity for decarbonization via the electrification of process heating. To have an idea of the importance of heating in textile production processes, Hasanbeigi and Zubeiri [118] report that in China, Japan, and Taiwan industries heating represents over half of total energy demand and around 25–30% of thermal energy is lost during steam generation and distribution. They estimate that around one-third of the total fuel used in the textile industry in these three economies can be spared through electrification. Thus, there is significant room to reduce CO₂ emissions by electrifying the heating processes. Heat pumps are among the possible technological heating solutions for electrification and can be integrated in some of the most important processes. Akarslan et al. [119] investigate wool drying in a heat-pump-assisted dryer using fuzzy logic methods. Variables such as air velocity (0.8–1.5 m/s), loading ratio (0.5–2.5), and temperature (40–90 °C) were analyzed. The fuzzy logic model assessed the impact of these parameters on drying rates. Results showed increased drying rates with higher air velocity, temperature, and longer drying times, while higher loading ratios decreased drying velocity. The study confirmed the effectiveness of fuzzy logic in optimizing drying conditions, providing valuable reference data for future research. Park et al. [120] designed a heat pump clothing care system for fabric care tasks like sterilization and wrinkle release with minimal fabric damage. The study experimentally investigated the system's performance under various conditions. Optimal steam injection and stay times were found to be 5 min each, improving wrinkle release by 225% and increasing energy consumption by 125%. The drying performance was optimized by adjusting steam injection time, compressor speed, and fan speed. The best compressor frequency was 65 Hz, saving 26.6% energy compared to 75 Hz. The study provides design guidelines to reduce energy consumption while maintaining effective performance.

The current dyeing process in the textile industry consumes significant energy for heating fresh water and cooling wastewater due to the lack of a heat recovery system. Kim et al. [121] propose an optimal heat exchanger network design integrating a heat pump to maximize wastewater heat recovery efficiency. The model recovers high- and low-temperature wastewater through a heat exchanger and heat pump, respectively. Pinch analysis was used to retrofit the heat exchanger network, reducing operating costs. Simulation results showed quantitative reductions in hot and cold utility consumption. A techno-economic analysis (TEA) confirmed the model's viability, showing a 43.2% reduction in total annualized cost (TAC) and a payback period (PBP) of up to 0.65 years.

Textile dyeing discharges wastewater with significant thermal energy, requiring efficient heat recovery. Kim et al. [122] propose an optimal wastewater heat recovery (WWHR) system using a two-step approach: defining feasible WWHR methods and integrating a heat pump and heat exchanger. Pinch analysis was applied to maximize waste-heat recovery efficiency. The system reduced total annualized cost (TAC) by 28.6% and had a payback period of 4.3 years. The energy consumption was cut by 73.65%.

3.7. Wood Industry

Wood drying is a crucial process that increases the quality of wood products. Heat pumps can help in increasing the efficiency of traditional drying processes, producing high quality dried wood more quickly at a lower cost. Some papers in the last 5 years have proposed solutions to integrate heat pumps in drying wood processes. Thomasson et al. [123] explore hybrid solar-assisted heat pump drying for biomass in Nordic conditions. Solar thermal collectors have been combined with an air-source heat pump to enhance drying performance and cost-effectiveness, particularly under variable electricity pricing. A scheme of the solution is shown in Figure 42. Experimental results show a significant improvement in drying rate ($33.0 \text{ kg/h} \pm 5.4 \text{ kg/h}$) compared to pure solar drying ($9.0 \text{ kg/h} \pm 3.2 \text{ kg/h}$), with a slight increase in specific electricity consumption ($0.26 \text{ kWh}_{\text{el}}/\text{kg}$ vs. $0.18 \text{ kWh}_{\text{el}}/\text{kg}$). Economic analysis indicates a simple payback time of 7.5 years for commercial-scale deployment without subsidies.

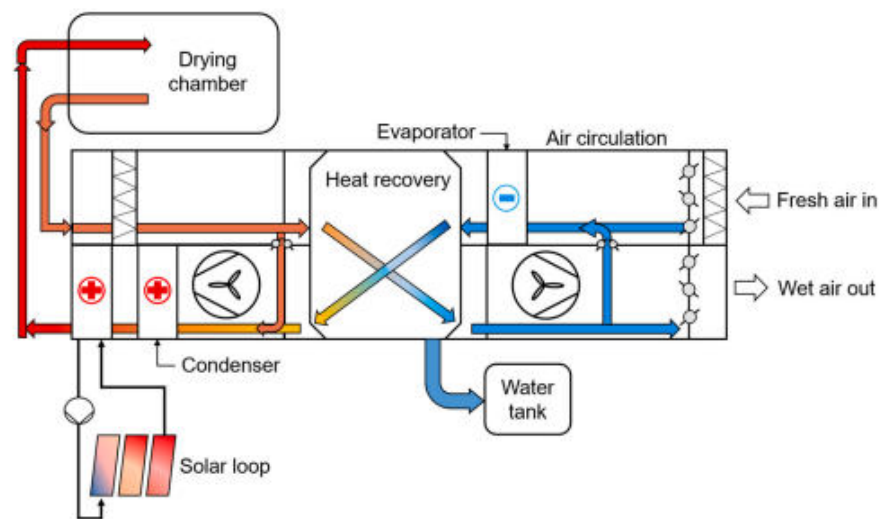


Figure 42. Flowsheet of the hybrid drying system used in the study [123].

Escalona et al. [124] focus on developing an energy autonomous wood drying system for slow-drying hardwoods like Patagonian oak in Chile, integrating a heat pump with a hybrid non-conventional renewable energy (NCRE) plant. Figure 43 reports a diagram of the drying chamber. Simulation results show oak moisture content can decrease from 102% to 12% in 30 days, with a specific moisture extraction rate (SMER) of 2.2 kg water/kWh . The hybrid plant, including photovoltaic panels, a wind turbine, and batteries, meets 97% of the dryer's electric demand in summer and 70% in winter. Additional auxiliary units cover remaining power needs.

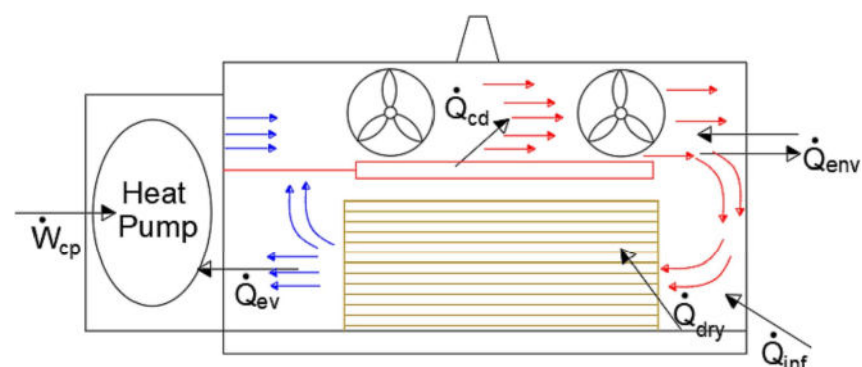


Figure 43. Diagram of the energy balance of the drying chamber [124].

Khouya [125] proposes a hybrid solar dryer (see Figure 44) for wood stacks integrating a heat pump and concentrated photovoltaic thermal (CPV/T) technology using air for cooling pump and solar cells. The mathematical model showed that compared to heat pump drying alone, the combined system reduced drying time by up to 18%, enhancing overall efficiency. CPV/T system efficiency ranged from 34% to 52%, with significant improvements noted with higher optical factors and concentration ratios.

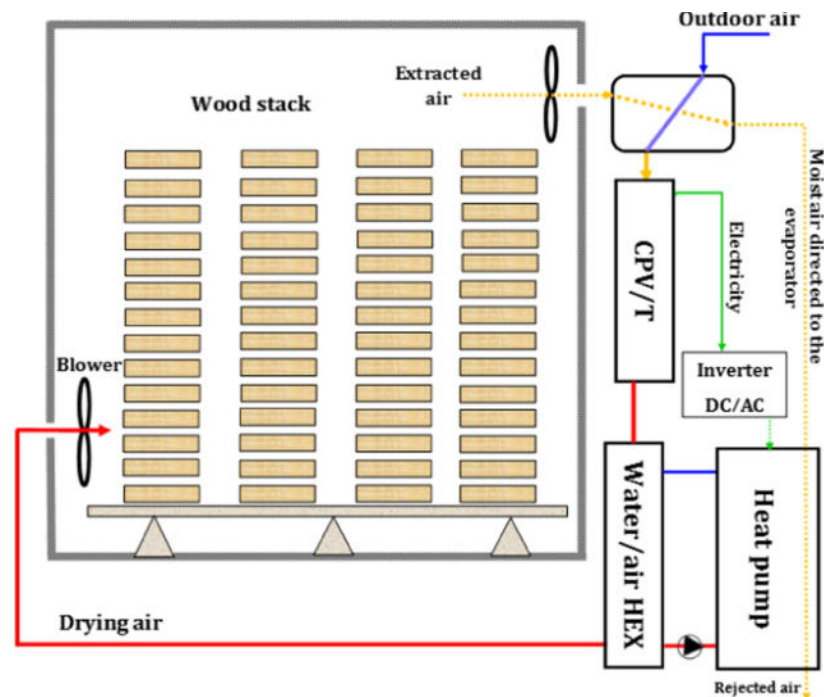


Figure 44. Block diagram of the proposed dryer [125].

Khouya [126] proposed a hybrid wood drying system using a water/air heat pump powered by a concentrated photovoltaic thermal system. The system reduces energy consumption significantly, with an electrical energy consumption ratio of 29 to 52 kWh.m⁻³ and a coefficient of performance (COP) ranging from 3.91 to 7.2. Lowering the heat pump set temperature from 75 °C to 65 °C improved COP by 17%. Combining heat pump and photovoltaic thermal systems reduced energy consumption ratio by up to 86%. Kumar et al. [127] explored optimizing wood-based biofuel quality using solar drying and heat pump techniques. In Chile, a model for drying Patagonian Oak lumber using a heat pump and a hybrid renewable energy plant was developed, showing significant moisture reduction and energy efficiency. The heat pump consumed 585 kWh per m³ of dried oak, with the hybrid plant meeting up to 97% of summer and 70% of winter power demands. Solar drying solutions, including kilns and heat pumps, offer high-quality feedstock for woody biomass boilers. The study highlights solar drying classifications, modeling approaches, and the importance of hybrid systems for efficient fuel drying and storage, aiming at sustainable development and improved boiler performance.

3.8. Drying

Drying is a very important process in several industrial sectors, such as food, chemicals, paper and pulp, textiles, and wood. Great attention is presently paid to the application of heat pumps to this process, since they are very attractive, compared to other technologies, for their excellent efficiency, specific high drying quality and environmental friendliness [128]. Several papers have been recently published regarding innovative solutions for the integration of heat pumps in the drying processes utilized in various industrial sectors. For this reason, a paragraph is fully dedicated to analyzing the recent literature on this specific process. Zhang et al. [128] investigate four drying modes to be applied in cold

regions: heat pump drying (HPD), dehumidification with increased air enthalpy (DEHPD), solar-assisted heat pump drying (SAHPD), and a combination of SAHPD and DEHPD. The schemes of the four systems are reported in Figure 45. Experiments in Shangri-La, China, showed DEHPD increased chamber temperatures by 25% and recovered 78.25% of wasted heat. SAHPD maintained heating capacity with a slight reduction of 3.27%. The combined mode improved heat utilization by 86.60%, reduced drying time by 31.10%, and decreased energy consumption by 37.99%, proving to be the optimal mode for stable drying performance.

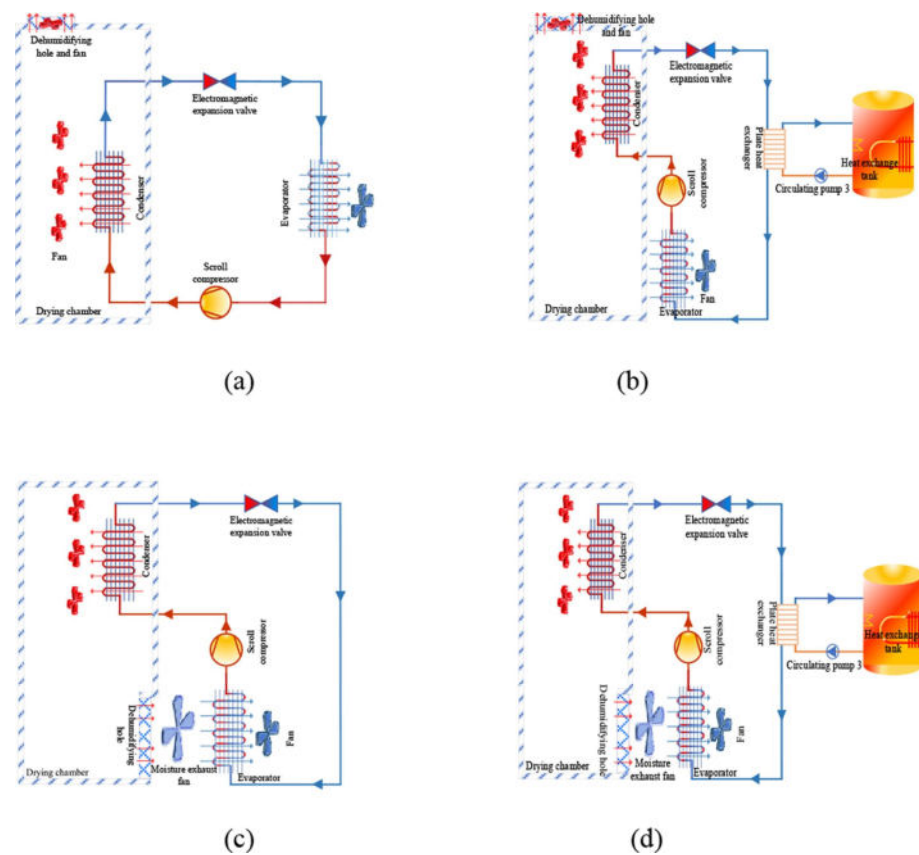


Figure 45. Schematic diagram of different energy supply modes; (a) HPD; (b) SAHPD; (c) DEHPD; (d) SAHPD&DEHPD [128].

Yu et al. [129] experimentally investigate a solar-assisted ejector-enhanced heat pump dryer (SE-HPD) using R134A refrigerant and compare it with a conventional heat pump dryer (CHPD). The scheme of SE-HPD system is shown in Figure 46. SE-HPD demonstrated superior dynamic drying characteristics, achieving a 54.3% improvement in moisture extraction rate (MER) and a 28.7% increase in exergy efficiency compared to CHPD under the same conditions. Higher solar radiation intensity significantly enhanced SE-HPD's performance, increasing MER by up to 66.1%.

Xu et al. [130] explore thermal digestion and vacuum-assisted heat pump drying for efficient kitchen waste management. A novel cascade heat recovery system is proposed, addressing dynamic load challenges in batch processing. The scheme of the system is shown in Figure 47. Experimentally, schemes with high volumetric heating capacity (VHC) outperformed high COP schemes, reducing energy consumption by 4% and drying time by 29%. Filling rate significantly influences energy efficiency, with a 11.5% decrease in consumption observed from 62.5% to 93.8% filling. Liu et al. [131] investigate metal–organic framework (MOF) desiccants in heat pump–desiccant wheel systems for low-grade heat source regeneration. The MOF system consumes only 42.77% of energy compared to electrically heated systems, achieving a dehumidification energy factor of 2.07, higher than

silica gel systems. Utilizing condensation heat boosts energy efficiency, with a coefficient reaching 2.07, 2.66 times more effective than silica gel systems.

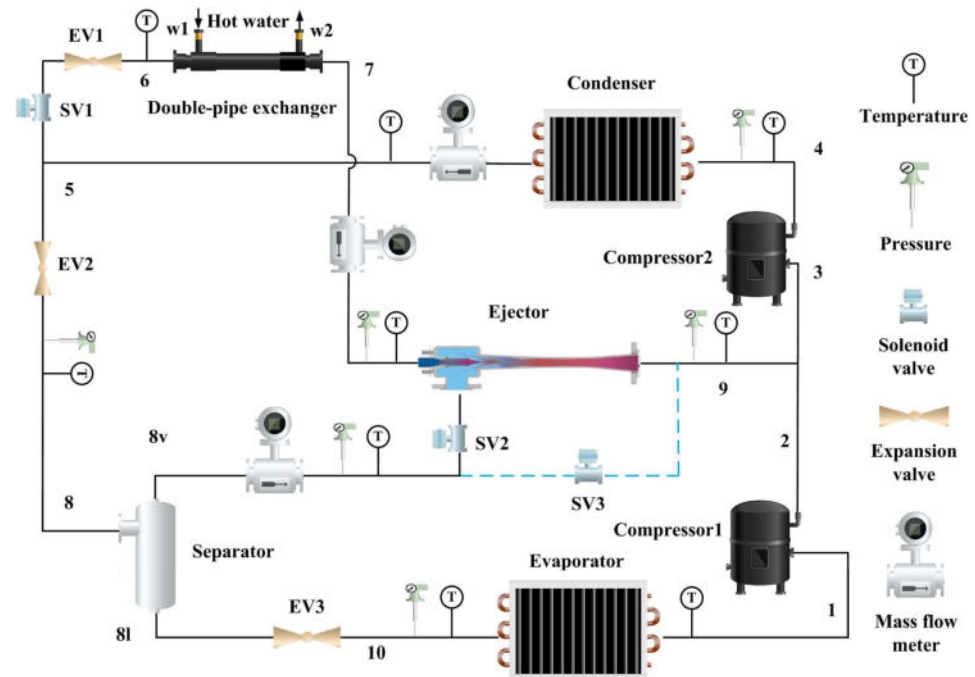


Figure 46. Schematic diagram of heat pump experimental system of SE-HPD [129].

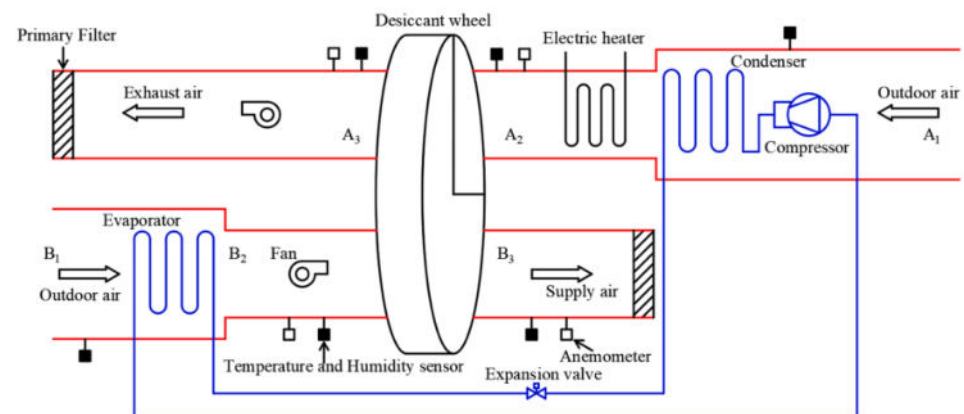


Figure 47. Schematic of the system configuration [131].

Fix et al. [132] introduce the MemDry system, combining water vapor-selective membranes with heat pumps for industrial drying. Energy savings of 30–40% compared to traditional drying methods are evaluated by modelization, with potential temperature reductions of 10–20 °C. The system design enhances heat pump COPs by up to 2x through exhaust air condensation. Results show drying efficiency ranges from 3 to 10 under ideal conditions and 0.8–3 under practical scenarios. Le Anh Duca et al. [133] investigate radio-assisted (RF) heat pump drying of carrots, focusing on heat and mass transfer dynamics. RF power levels of 0, 0.5, and 1.5 kW were tested alongside conventional HP drying. Results showed enhanced drying and heating rates with increasing RF power. Drying times decreased to 335 min at 1.5 kW from 480 min with HP drying. Material temperature reached drying air temperature in 25–30 min at higher RF powers compared to 310 min with HP drying. Schlosser et al. [134] explore the economic viability of heat pumps for milk spray drying, focusing on achieving high temperatures economically. Using the Grand Composite Curve and Modified Energy Transfer Diagram, they analyze market-available and

prototype heat pump concepts. Results show potential for reaching drying temperatures up to 210 °C, with break-even electricity-to-reference-fuel price ratios ranging from 1.20 for Stirling heat pumps to 1.56 for simulated transcritical cascade cycles. Market-available heat pumps achieve 127.3 °C, covering 60.3% of heat demand with a ratio of 1.41. Yahya et al. [135] evaluate a hybrid solar-assisted heat pump dryer (HS-AHPD) for paddy drying, using R22 as the working fluid. Key metrics include an average drying rate of 8.34 kg/s, specific moisture extraction rate (SMER) of 0.44 kg/kWh, and specific energy consumption (SEC) of 4.69 kWh/kg. Thermal efficiency reaches 29.1%, with drying section exergy efficiency at 18.4%. Jing et al. [136] introduce the modified booster-assisted ejector heat pump (MBEHP) cycle for heat pump dryer applications, enhancing performance with dual condensers. By integrating a low-temperature condenser into the basic booster-assisted ejector heat pump (BEHP) cycle, the MBEHP achieves dual-pressure condensation, improving cycle efficiency. The schemes of the two cycles are shown in Figure 48. Evaluations using thermodynamic principles reveal that with R134a, the heating coefficient of performance COP_{hw} and COP_h of MBEHP increase by 50.34% and 16.97% compared to BEHP. MBEHP outperforms BEHP across all conditions, notably under severe ones like high condensing and low evaporating temperatures. It reduces total exergy destruction by 12.70%, highlighting the ejector's optimization potential. R1234ze(Z) emerges as the optimal refrigerant, offering 42.49% higher Q_c and 12.79% higher COP_{hw} than R134a in MBEHP, enhancing practical feasibility and performance.

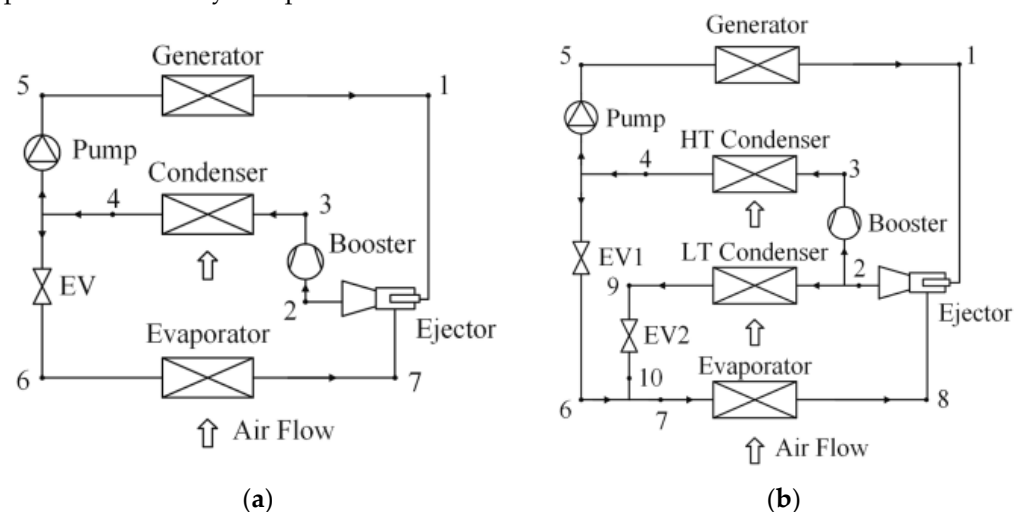


Figure 48. The schematic diagram of (a) BEHP cycle and (b) MBEHP [136].

Yao et al. [137] propose a solar vacuum tube collector coupled heat pump drying (HPD) system with three operational modes tailored to varying climatic conditions. The system achieves drying temperatures exceeding 50 °C in solar drying (SD) mode. In HPD mode, it operates with an average heating power of 11.88 kW, COP of 2.26, and thermal efficiency of 39.3%. Transitioning to solar-assisted heat pump drying (SAHPD) mode enhances COP by 44.2% compared to HPD. Yu and Yu [138] introduce a solar-assisted ejector-enhanced vapor injection cycle with a subcooler (SE-SVIC) for heat pump dryer (HPD) applications, emphasizing enhanced heat absorption in the evaporator via ejector pressure lift. SE-SVIC outperforms basic subcooler vapor injection cycle (SVIC) and ejector-enhanced SVIC (E-SVIC) with COP_h improvements of 23.8% and 19.0%, respectively. Solar energy input significantly enhances SE-SVIC's heating capacity, aligning with solar collector parameters like radiation intensity and area. A layout of the SE-SVIC and its P-h diagram are shown in Figure 49.

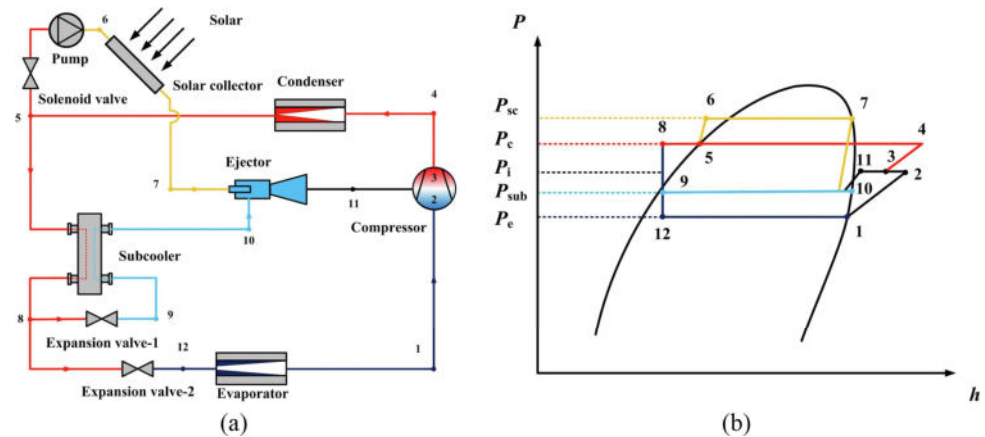


Figure 49. (a) cycle layout and (b) P-h diagram of SE-SVIC [138].

Loemba et al. [139] evaluate diverse types of recently developed heat pump dryers, emphasizing performance metrics, food quality impacts, and economic and environmental considerations often overlooked in existing reviews. Results indicate high coefficients of performance (COP) ranging from 1.94 to 5.338 and specific moisture extraction rates from 0.156 to 9.25 kg/kWh, reducing energy consumption by up to 80%. Techno-economic analysis reveals short payback periods (1.6 to 3.6 years) for most models. Zhang et al. [140] employ response surface methodology to optimize variable-temperature drying of shiitake mushrooms, focusing on quality, energy efficiency, and production efficacy. A mode-switchable heat pump system runs four drying stages (35 °C, 45 °C, 55 °C, and 65 °C), revealing drying time at 55 °C crucial for rehydration ratio and at 35 °C for heat pump COP. Optimal drying times are identified (2.4 h, 3.3 h, 5.6 h, and 2.6 h, respectively), achieving a comprehensive score of 0.837, 49% higher than constant-temperature drying at 65 °C. Yahya et al. [141] investigate a solar-biomass hybrid heat pump batch-type horizontal fluidized bed dryer (FBD) for paddy drying (a scheme is reported in Figure 50), comparing two modes: FBD with heat recovery (FBD-WHR) and without (FBD-NHR). Both modes reduced paddy moisture content effectively, achieving higher drying rates and specific moisture extraction rates (SMER) in FBD-WHR (0.24 kg/kWh) compared to FBD-NHR (0.19 kg/kWh). Specific energy consumption (SEC), thermal energy consumption (STEC), and electrical energy consumption (SEEC) were lower in FBD-WHR (7.43 kWh/kg, 4.22 kWh/kg, 3.21 kWh/kg) than in FBD-NHR (8.85 kWh/kg, 5.81 kWh/kg, 3.04 kWh/kg). The FBD-WHR mode reduced thermal energy consumption by approximately 46.7% compared to FBD-NHR, suggesting potential enhancements such as recirculating exhaust systems and economic analysis for broader applicability in agricultural drying systems.

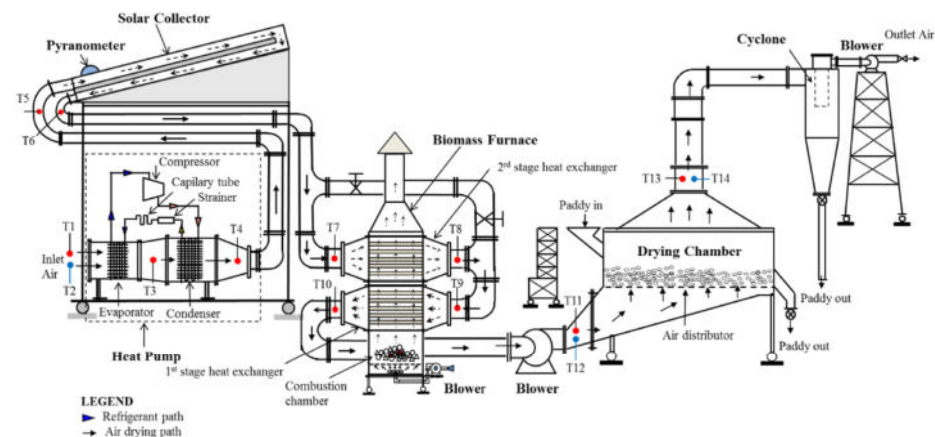


Figure 50. Schematic of the solar-biomass hybrid heat pump batch-type horizontal fluidized bed dryer using the multi-stage heat exchanger [141].

Yan et al. [142] developed a closed-loop heat pump drying system with an auxiliary condenser to address energy inefficiencies, complex structures, and low drying temperatures in industrial metal part drying. Experimental investigations varied compressor speed, air volume, cooling water inlet temperature (5–30 °C), and flow rate (30.6–50.1 kg/h). Results indicated drying temperature increased with higher inlet temperatures and lower flow rates, reaching 70.02 °C at 20 °C and 34.3 kg/h, suitable for industrial needs. System COP peaked at 5.64 at 20 °C inlet temperature, while cooling water flow rate minimally impacted COP. At 20 °C inlet temperature and 34.3 kg/h flow rate, maximum (MER) and specific (SMER) moisture extraction rate were 3.8 kg/h and 1.68 kg/kW/h, respectively, highlighting strong dehumidification capability. Hamid et al. [143] investigate the performance of a closed-loop heat pump dryer using R-134a with moist sodium polyacrylate (Orbeez). Figure 51 reports the scheme of the system. Experiments on 6–8 kg loads show higher coefficient of performance (5.2–5.8) and heat transfer rates (0.56–0.64 kW). Similarly, these loads yield peak moisture extraction rates (~0.66–0.75 kg/h), specific moisture extraction rates (~2.15–2.27 kg/kWh), and weight reduction (~91%). Drying air temperature and velocity enhance water removal.

Carbon dioxide heat pump-driven liquid desiccant dehumidification leverages CO₂'s eco-friendly heating capabilities, enhancing regeneration efficiency for greener and efficient air conditioning [144].

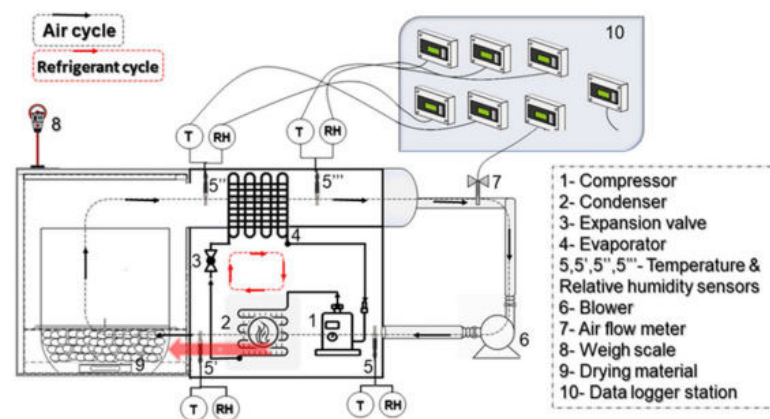


Figure 51. Schematic diagram of the heat pump dryer [141,145].

Cui et al. [144] compare refrigerants and heat pump system configurations (see Figure 52), developing and validating mathematical models. Results demonstrate up to 51.67% lower power consumption and 106.89% improved dehumidification performance compared to condensing methods. CO₂ systems outperform R134a at high dehumidification demands, with up to 18.84% reduced total power consumption and 23.21% enhanced seasonal performance. Challenges include CO₂ pump limitations in self-circulating desiccant systems, warranting future optimization for efficiency and practical applications.

Su et al. [145] propose an absorption-based enclosed heat pump drying (HPD) system that combines liquid desiccant dehumidification and mechanical vapor recompression for total waste heat recovery. A scheme of the proposed system is shown in Figure 53. Thermodynamic modeling shows an energy utilization ratio of 4.54 and a specific moisture extraction rate (SMER) of 4.25 kg/kWh, which are 18.7% and 18.5% higher than traditional HPD systems. Economic analysis reveals a 5.05% increase in annual investment and maintenance costs but a 19.94% reduction in annual operation costs. The payback period is approximately 18.5 months with a 20-year project life cycle, indicating profitability.

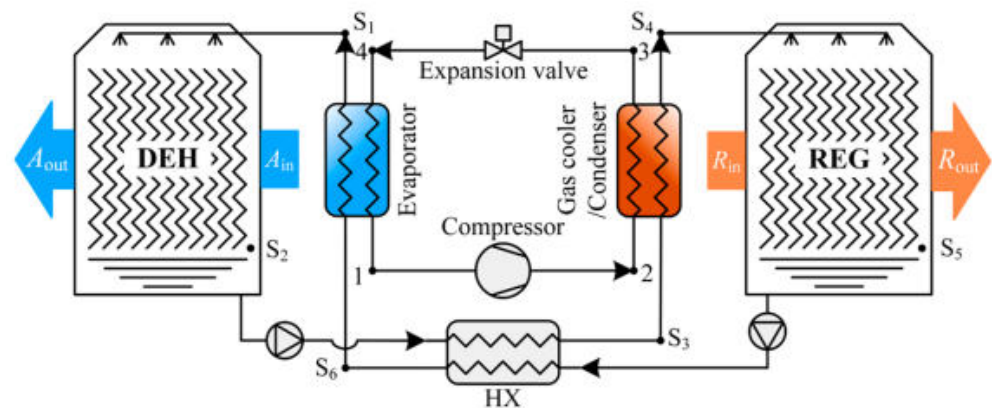


Figure 52. Typical heat pump driven liquid desiccant dehumidification system [144].

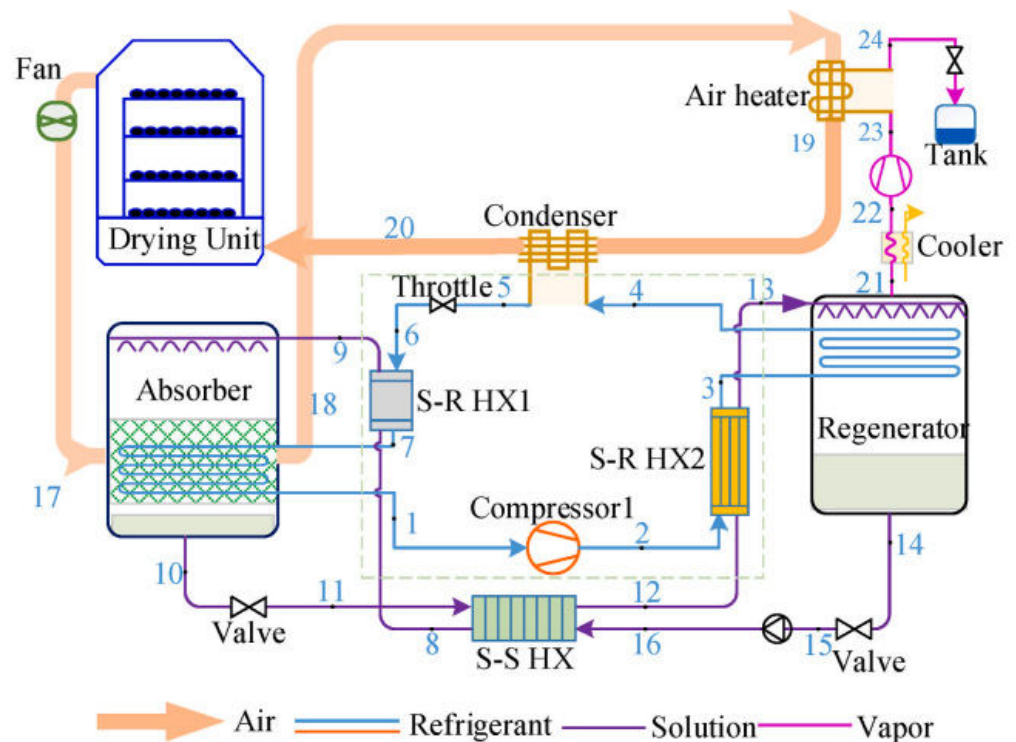


Figure 53. Schematic of the proposed absorption-based enclosed HPD system [145].

Heat pump drying technology is promising for sludge drying due to its clean, low-carbon, and efficient features. Zheng et al. [146] performed a field experiment in an electroplating factory revealing that 20% of the condensed water in the sludge heat pump dryer (SHPD) came from the air precooling dehumidifier (APCD). Increasing supply air temperature and circulating fan frequency decreased sludge moisture content, but had mixed effects on energy efficiency and drying performance. Higher fan frequency improved the specific moisture extraction rate (SMER) from 1.98 kgw/kWh to 2.07 kgw/kWh. Extending sludge residence time reduced drying efficiency, suggesting thinner sludge layers improve performance. Lower supply air temperature, increased fan frequency, and shorter residence time enhance dryer efficiency and reduce energy consumption. A scheme of the analyzed system is shown in Figure 54.

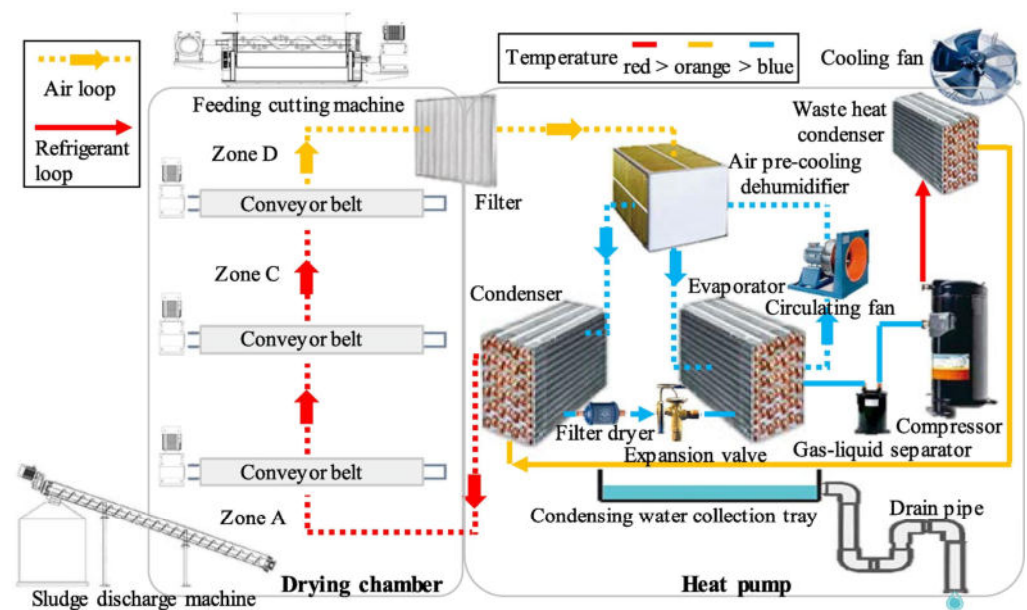


Figure 54. Schematic diagram of the sludge heat pump dryer [146].

Chen et al. [147] examine desiccant wheel-assisted high temperature heat pump (HTHP) technology for heating dryer inlet air up to $150\text{ }^{\circ}\text{C}$ using recovered exhaust heat. Thermodynamic models and a one-dimensional finite difference model assessed the HTHP components and dehumidification process. The desiccant wheel-assisted HTHP requires a smaller evaporator (50–60% less) and performs similarly to HTHP with a heat recuperator. It shows marginal improvements in COP, exergy efficiency, and drying capacity, which become significant with high humidity incoming air. Cheng et al. [148] evaluate vapor compression heat pump dryers HPDs, used in food and industrial drying, for energy efficiency and operational robustness in various applications, using a conveyor seaweed drying case study. Three systems are compared (see Figure 55): basic HPD (HPDbasic), HPD with air bypass (HPDbypass), and HPD with air bypass and subcooler (HPDsubcooler). HPDbasic is unsuitable for seaweed drying due to high air flow requirements. HPDbypass and HPDsubcooler show better performance, with HPDsubcooler achieving a moisture extraction rate (MER) of 35.8 kg/h and specific moisture extraction rate (SMER) of 2.58 kg/kWh .

Kushwah et al. [149] explore drying fresh banana slices at temperatures of 35° , 40° , and $45\text{ }^{\circ}\text{C}$ using a novel heat pump-assisted drying system (HPADS) in a closed loop. Higher drying temperatures reduce drying time linearly, and thicker slices require more time to dry. The system's specific moisture removal ratio is 0.230 kg/kWh , and its coefficient of performance is 3.168 at $45\text{ }^{\circ}\text{C}$. HPADS is recommended for small farmers and cottage industries, offering a reliable method for drying high-moisture agricultural products. Jokiel et al. [150] investigate using a CO_2 heat pump for heating and cooling in a drying cabinet at $50\text{--}70\text{ }^{\circ}\text{C}$ with various moist air bypass ratios. A dynamic heat pump-assisted dryer model was developed and validated experimentally. Results show that a closed-loop heat pump-assisted drying process can reduce energy demand by up to 84% compared to open-loop systems, with a specific moisture extraction rate (SMER) up to four times higher. However, drying time increases by up to 69%.

Storing solar energy in an underground Thermal Energy Storage (TES) tank for use by a heat pump in drying systems enhances the effective use of solar and ground heat sources. Ismael and Yumrutaş [151] model a wheat-drying system with a heat pump and underground TES, charged by solar energy, to evaluate long-term performance. A scheme of the system is reported in Figure 56. Key components include a wheat dryer, TES tank, solar collectors, and a heat pump. Results of the simulation show performance parameters stabilize from the fifth year, with COP, system COPs, and SMER reaching

4.43, 4.3, and 6.05, respectively. The system primarily relies on solar energy (76.6%) with minimal compressor (22.7%) and fan power (0.7%) inputs. Optimal installation region and system size are critical for efficiency, with recommendations for further optimization and thermo-economic analysis.

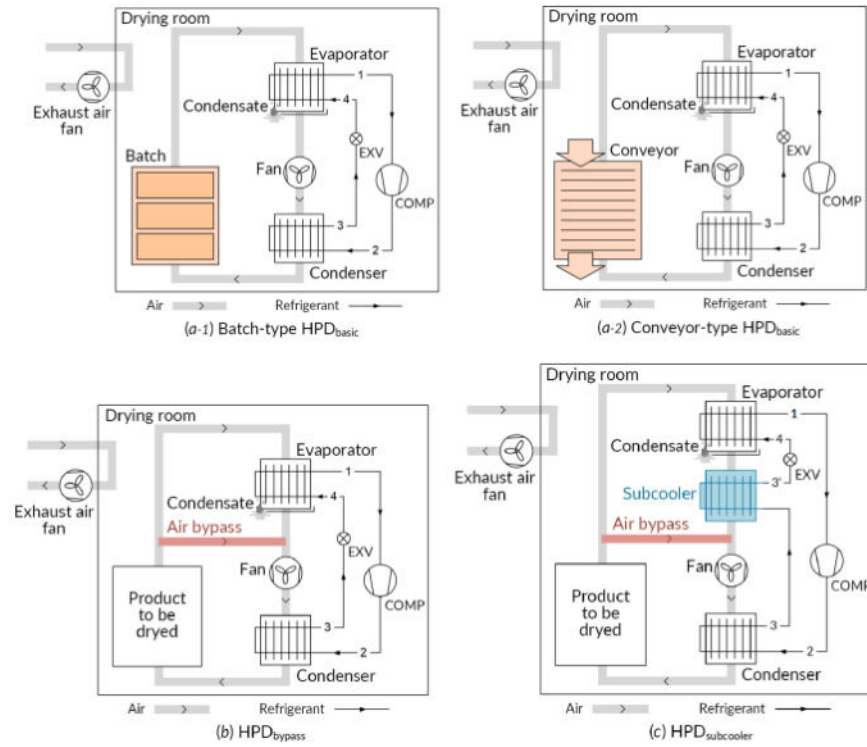


Figure 55. Various heat pump dryer (HPD) configurations [148].

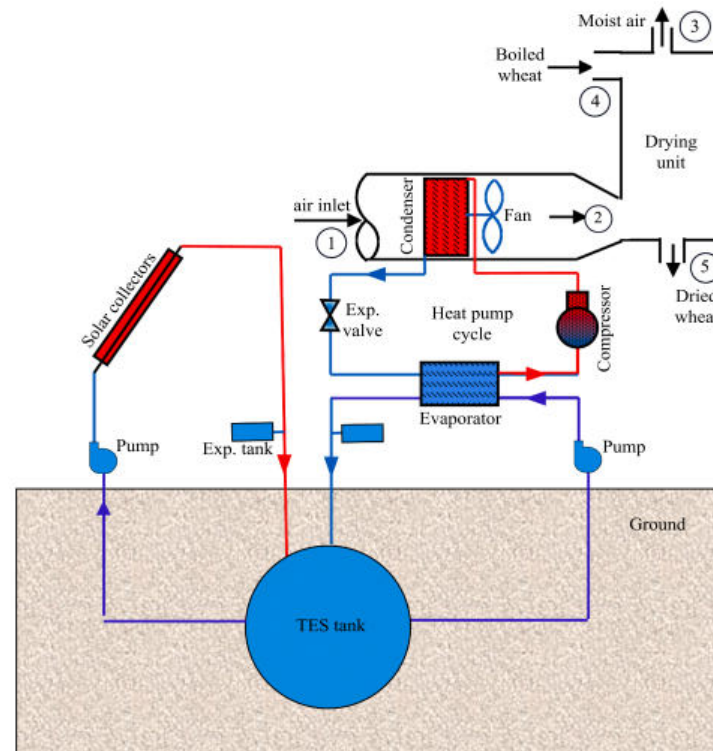


Figure 56. Schematic diagram of the drying system with underground TES tank [151].

4. New Refrigerants for Industrial Heat Pumps

The choice of refrigerant also plays a fundamental role due to its impact on the thermodynamic cycle performance and on the environment, with the need to phase out refrigerants with high global warming potential (GWP) [152]. The 4th generation of refrigerants, characterized by very low GWP, is given by natural fluids (CO₂, ammonia, hydrocarbons) and synthetic hydrofluoroolefins (HFOs). However, since it is difficult for pure compounds to meet all the requirements for a given application, an important opportunity to make the proper selection of the working fluid is given by multicomponent mixtures, which allow for optimization of the performance and the environmental and safety characteristics. At the moment, a great research effort is underway to identify the fluids, pure or mixtures, that will replace the current refrigerants (mainly HFCs) characterized by high GWP, in particular for application in high-temperature heat pumps, as attested by the numerous articles published in the last 5 years. Andersen et al. [153] focus on optimizing High-Temperature Heat Pumps (HTHPs) by evaluating 16 working fluids across 10 heat pump configurations under diverse high-temperature conditions (0 °C to 100 °C, up to 150 K temperature lifts). Results show that configurations using isobutane, isopentane, hexane, and R-718 in one-stage or cascade cycles with suction line heat exchangers consistently achieved high Lorenz efficiency across 95% of conditions. Including ammonia and CO₂ extended this performance to 98%, particularly beneficial at higher sink temperature ranges. Natural refrigerants like R-600, R-600a, R-601a, and hexane showed negligible efficiency gains over HFOs, emphasizing their potential in sustainable HTHP applications despite higher volumetric heating capacities. Spale et al. [154] address the challenge of finding suitable working fluids for industrial High-Temperature Heat Pumps (HTHPs) operating at 200 °C, where single-component options are limited by technical constraints. Utilizing Python code with REFPROP and Cantera libraries, over 460,000 mixtures of hydrocarbons and H(C)FOs were evaluated for their suitability in a vapor-compression cycle. A binary blend of cyclopentane and R1336mzz(Z) ([0.68, 0.32]) emerged as the optimal candidate based on thermodynamic and technical criteria, despite all mixtures being classified as flammable. Abedini et al. [155] investigate HTHPs to optimize, among a set of 1346 binary zeotropic mixtures, the selection of the working fluids for applications up to 200 °C. This study evaluates the binary mixtures for three industrial processes: latent/latent, latent/sensible, and sensible/sensible heat sources and sinks. An optimization framework was developed to maximize the coefficient of performance (COP). Results show that binary mixtures generally outperform pure fluids, especially in processes with varying temperature glides. However, many top-performing mixtures are highly flammable hydrocarbons. Water/ammonia, a mildly flammable mixture, showed potential but also presented technical challenges. Adding an internal heat exchanger (IHX) generally increased COPs but also system complexity and cost, with water/ammonia performing better without an IHX. Zini et al. [156] explore the potential of heat pumps across diverse industrial sectors, particularly emphasizing applications in sectors such as pulp and paper, food and beverage, and chemicals, where temperatures above 200 °C are crucial. Analysis reveals that natural fluids like water and alcohols perform well across a wide temperature range, while synthetic options face regulatory challenges due to their environmental impact. The study underscores the complexity of fluid selection and highlights the optimal performance of ammonia at low temperatures, alcohols at medium temperatures, and water at ultra-high temperatures (see Figure 57).

Vering et al. [157] focus on enhancing refrigerant selection for residential heat pumps, crucial for overall system efficiency and sustainability. A guided seven-phase decision process integrating stakeholder perspectives, using prescriptive decision theory and the PROMETHEE method, is proposed. Hydrocarbons and their blends emerge as sustainable choices, though their flammability necessitates robust safety measures. The process underscores the need for stakeholder involvement to navigate complex selection criteria and boundary conditions effectively. Hosseinnia et al. [158] propose a novel high-temperature cascade heat pump system with water (R718) in the high stage and six low-GWP refrigerants (R1234ze(Z), R1233zd(E), R1336mzz(Z), R600, R600a, R601) in the low stage. The

system uses liquid water injection during high-stage compression to manage high discharge temperatures. R718 + R600 was identified as the optimal pair, achieving a COP \times VHC of 2895.1 kJ m⁻³. The system offers superior performance and environmental benefits compared to current multi-compressor HTHPs. Navarro-Esbrí and Mota-Babiloni [159] assess a HTHP using the climate-friendly refrigerant R-1336mzz(Z), a low-GWP alternative to R-245fa. Experiments were conducted with production temperatures between 100 and 160 °C, and waste heat temperatures between 80 and 118 °C. Results showed a volumetric heating capacity of 9.2–12.3 kW and a coefficient of performance (COP) of 1.9–4.4. The system demonstrated superior environmental performance compared to natural gas boilers. Jiang et al. [160] evaluate an advanced HTHP using low-GWP refrigerant R1233zd(E) under a 50 °C temperature lift. The unit features a high-efficiency centrifugal compressor and enhanced heat exchangers. Experimental tests achieved a heating capacity of 381 kW and a COP of 3.67 at 50 °C source and 100 °C output, the highest efficiency reported for similar conditions. Arpagaus et al. [161] explore R1336mzz(E) as a promising refrigerant for electrically driven HTHP. Demonstrated in a 10 kW capacity lab setup, R1336mzz(E) exhibits high volumetric heating capacity, A1 safety class, and low GWP. Experimental tests cover a heat sink outlet range of 70 °C to 130 °C and a heat source between 30 °C and 80 °C, showing comparable COPs with other tested refrigerants (± 0.4 COP) but significantly higher heating capacity, e.g., 117% and 18% more than R1336mzz(Z) and R245fa at W60/W110 reference conditions. Sulaiman et al. [162] investigate HTHP using eco-friendly refrigerants to recover industrial waste heat effectively. R1233zd(E), R1336mzz(Z), and R601 are evaluated against R245fa, showing up to 8.32%, 11.68%, and 19.61% higher COP, respectively, and enhanced exergetic efficiency. The study employs a single-stage cycle with an internal heat exchanger, emphasizing environmental benefits and operational constraints. Environmental analysis indicates a 20% to 30% lower total environmental impact when using low GWP refrigerants compared to R245fa. Mateu-Royo et al. [163] evaluated HCFO-1224yd(Z) as a low-GWP substitute for HFC-245fa in HTHPs using theoretical and semi-empirical methods. Despite an 8.9% lower heating capacity compared to HFC-245fa, HCFO-1224yd(Z) benefits from higher suction density, reducing compressor power consumption by 11.3% and achieving up to 4.5% higher COP at 140 °C high-temperature reservoir. Environmental analysis shows HCFO-1224yd(Z) can cut equivalent CO₂ emissions by up to 90%, depending on national energy profiles. Zhang and Xu [164] analyzed R1234ze(Z) as a promising low-GWP refrigerant for moderately high temperature heat pump (MHTHP) applications in industry. Theoretical analysis revealed superior thermodynamic properties of R1234ze(Z) compared to R114, R134a, R227ea, R236fa, and R245fa. Experimental tests in a vapor compression system showed R1234ze(Z) achieved a COP of 3.55 with a 45 K temperature lift at a condensation temperature of 85 °C, surpassing R245fa by 40%. Mateu-Royo et al. [165] evaluated HFO-1234ze(E) and R-515B as low GWP replacements for HFC-134a in heat pump applications, focusing on energy performance and carbon footprint. Despite a 25% lower heating capacity compared to HFC-134a due to different thermophysical properties, HFO-1234ze(E) and R-515B show less than 2% difference in heating capacity between them. Both refrigerants achieve similar COP to HFC-134a under proposed conditions, with lower discharge temperatures benefiting from IHX effectiveness. For moderately high temperatures, both reach up to 90 °C, making them viable alternatives to conventional heating. IHX usage is recommended for enhancing system COP and slight capacity increase. Environmental analysis reveals up to 18% and 15% CO₂ emission reductions for HFO-1234ze(E) and R-515B compared to HFC-134a in low-temperature heating, and up to 78% reduction compared to natural gas boilers in moderately high temperature applications. R-515B holds an advantage as a non-flammable refrigerant (A1) over HFO-1234ze(E), emphasizing safety in installation. Again, Mota-Babiloni et al. [166] explored replacing HFC-134a with low GWP alternatives HFO-1234ze(E) and R-515B in heat pump water heaters (HPWH) and moderately high temperature heat pumps (MHTHP). Although HFC-134a shows higher heating capacity, HFO-1234ze(E) and R-515B have 25% lower compressor power consumption, resulting in comparable or slightly higher COPs. These alternatives also

significantly lower carbon emissions by up to 28% and have a 20 K lower discharge temperature, extending the operational range. R-515B, being non-flammable, offers safer operation while maintaining energetic and environmental benefits. Koundinya and Seshadri [167] explored a comprehensive 4E analysis of fourteen refrigerants, emphasizing low-GWP alternatives post-Montreal Protocol. Through TOPSIS methodology, R407C, R1270, R290, R152a, and R1234ze(E) emerged as optimal choices across varying condenser temperatures from 45 to 95 °C, tailored to current emission factors in India. R455A is proposed as an alternative to R407C due to its impending phase-out. Malavika et al. [168] used Engineering Equation Solver (EES) to evaluate refrigerants suitable for HTHPs, such as R1233zd(E) and R1336mzz(Z), based on their properties like maximum temperature and COP. A case study on a dairy plant demonstrated potential energy savings up to 46%, affirming heat pumps as viable alternatives to conventional industrial heating systems and recommending R1233zd(E) as a refrigerant. Wu et al. [169] focus on HTHPs with outputs above 100 °C for industrial heat recovery. Six refrigerants including R718, R600, R601, R1234ze(Z), R1336mzz(Z), and R245fa were simulated in a refrigeration cycle, with R718 demonstrating superior system performance and Carnot efficiency. Experimental validation confirmed R718's advantages over R1336mzz(Z), R600, and R245fa in terms of safety, performance, and environmental impact, despite requiring a compressor with higher compression ratio and volume flow rate.

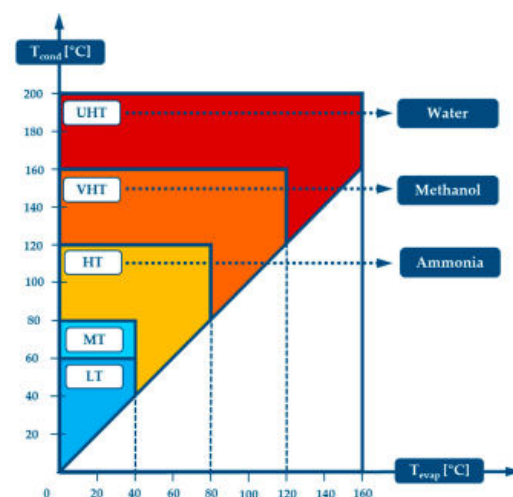


Figure 57. Guidelines for fluid selection at different T_{cond} and T_{evap} [156].

As refer multicomponent mixtures, Dávila et al. [170] investigate the viability of using a CO_2 /acetone mixture as a working fluid in a compressor-resorption heat pump for industrial energy recovery. Experimental validation focuses on the desorption process, confirming its applicability through a series of conducted tests. Key findings include heat transfer coefficients ranging from 0.10 to 0.52 $\text{kW} \times \text{m}^{-2} \times \text{K}^{-1}$, influenced significantly by test pressure and heating water temperature at the desorber inlet. Results indicate favourable heat transfer characteristics, but lower thermal conductivity compared to ammonia-based mixtures. Wang et al. [171] investigate again the use of the low-GWP refrigerant HP-1 in HTHPs, showing its advantages in performance and environmental impact over HFC-245fa. Three types of injection pressures were identified, optimizing system performance and safety. HP-1 improved the coefficient of performance (COP) by 2.1–5.2%, heating capacity by 10.8%, and reduced carbon emissions by 15.4–39.1%. Gómez-Hernández et al. [172] explore the potential of CO_2 /acetone zeotropic mixtures as refrigerants in HTHPs for industrial heating above 150 °C. The mixtures exhibit significant thermodynamic advantages, offering temperature glides below 50 K, with CO_2 /acetone (0.05/0.95) showing optimal performance, achieving a COP of 5.63 at 200 °C outlet sink temperature and 70 K temperature difference. Ganesan and Eikevik [29] model a HTHP employing a two-stage cascade refrigeration system with CO_2 /butane and CO_2 /pentane

mixtures. The MATLAB-based model explores heating applications from 115 °C onwards using source temperatures of 10–50 °C. Results highlight up to 181 °C heat sink temperatures, achievable with 20% CO₂ composition, and an enhancement of COP by 20% compared to pure fluids. Optimal CO₂ concentrations for temperature lift are identified, emphasizing suitability for both residential and industrial heating in cold climates. Hu et al. [173] propose the use of R1234ze(E)/R1336mzz(E) binary refrigerant to address temperature mismatch in heat pump processes. Through theoretical analysis and Epsilon simulations, optimal mass proportions (0.3/0.7) are determined for maximizing temperature glide (21.52 °C) and thermal performance. Significant improvements are observed in COP (up to 67.25%) for steam and hot water heat pumps compared to pure R1336mzz(E), highlighting the potential to replace multi-stage evaporator or condenser schemes. This research underscores the role of binary refrigerants in enhancing heat pump efficiency under varying heat source conditions, laying the groundwork for future applications in industrial settings. Fernández-Moreno et al. [174] explore HTHPs using binary and ternary refrigerant mixtures optimized for low global warming potential (GWP) and high operational temperatures. Key parameters considered include COP, volumetric heating capacity, flammability, and glide matching. No single mixture optimally meets the criteria, necessitating trade-offs, particularly concerning flammability, which significantly impacts COP. Promising mixtures based on R-1233zd(E) and R-1336mzz(Z) are identified, meeting environmental restrictions. However, flammable components often enhance performance but require blending with non-flammable refrigerants. Amongst others, the research highlights R-601/1234ze(Z) (0.74/0.26) as potentially offering the highest COP as drop-in replacement for R245fa, albeit with flammability concerns. Dai et al. [175] proposed using CO₂/low-global warming potential (GWP) fluid mixtures in heat pump dryers, comparing them to traditional boiler drying systems. A life-cycle assessment model evaluates energy consumption and emissions. CO₂/R32 mixtures significantly enhance the coefficient of performance (COP) and reduce discharge pressure, achieving a COP of 4.29. Yıldırım [176] evaluated R450A as a potential replacement for R134a in low and medium-temperature heat pump systems through energy, exergy, environmental, and enviro-economic analyses. The analysis was made for two heat source temperatures (10 °C and 20 °C) and six heat sink temperatures (from 30 °C to 55 °C). Despite R450A's lower mass flow rate due to lower density in the suction line compared to R134a, it exhibits comparable COP values due to lower compressor energy consumption. Exergy analysis highlights compressor-related exergy destruction across operating conditions, with minimal destruction occurring in the expansion valve at low heat sink temperatures and in the evaporator at high temperatures. Environmental analysis shows R450A has slightly higher results than R134a, while enviro-economic analysis indicates comparable performance.

5. Conclusions

This review of the international literature published in the last 5 years on industrial heat pumps has highlighted a very important effort on the part of the research community to identify efficient and cost-effective solutions aimed at recovering waste heat and requalifying heat at high temperatures in industrial processes. Electrification of heat delivery through heat pumps is mandatory to reduce energy consumption and greenhouse gas emissions, substituting the generally applied gas boilers or optimizing the present industrial processes. Many solutions have been proposed to design new cycle configurations for HTHPs in such a way as to extend the range of sink temperatures from the present 100 °C up to 200 °C. Cascade and transcritical HTHPs are the most studied and the most promising technologies to obtain these objectives, but hybrid absorption-compression heat pumps and many specific HP configurations (e.g., dual-temperature condensation and dual-temperature evaporation (Ej-DCDE) heat pump systems, vapor-injected high-temperature heat pump (LEHP) integrating a liquid-separation condenser and an ejector, ammonia-based hybrid chemisorption-compression high-temperature heat pump, etc.) have also been proposed. This offers a variety of solutions to tailor the system to the specific

needs of each application. A wide variety of literature has also been produced regarding innovative heat pump systems for the most important industrial processes of different industrial sectors. Distillation, drying, and desalination are the most studied processes for the integration of heat pumps, but specific solutions have been proposed for all the main industrial processes. Finally, many papers studied alternative refrigerants to identify the most efficient solution in connection to the various applications and cycle configurations. The most studied pure compounds are CO₂, ammonia, water, R600, and R601, while, amongst synthetic HFOs, the fluids considered are R1234ze(Z), R1336mzz(Z), R1233zd(E), and R1224ze(Z). Many works regard multicomponent mixtures as a suitable solution to tailor the properties of the refrigerant to the specific needs of each application. Many kinds of mixtures have been explored from a thermodynamic point of view, identifying several interesting solutions. However, the adoption of a refrigerant by the industry requires satisfying many other conditions (e.g., compatibility with lubricants, safety, costs, etc.). In conclusion, much progress has been realized in the last five years regarding the identification of innovative heat pumps for industrial applications, but further research work is certainly required to refine these solutions and define the concrete systems to be applied.

Author Contributions: Conceptualization, S.B. and L.F.; methodology, S.B.; validation, G.L., D.M. and L.V.; investigation, G.L., D.M. and L.V.; writing—original draft preparation, S.B.; writing—review and editing, L.F.; supervision, L.F.; project administration, L.F. All authors have read and agreed to the published version of the manuscript.

Funding: This research received no external funding.

Data Availability Statement: No new data were created or analyzed in this study. Data sharing is not applicable to this article.

Acknowledgments: During the preparation of this work the authors used ChatGTP3.5 in order to synthesize methodology and results of each cited paper. However, all the texts elaborated by the AI were carefully revised, compared with the originals and adapted to the needs of the paper. The authors take full responsibility for the content of the publication.

Conflicts of Interest: The authors declare no conflicts of interest.

References

1. United Nations. *United Nations Framework Convention on Climate Change (UNFCCC) Agreement*; United Nations: New York, NY, 1992.
2. United Nations Framework Convention on Climate Change. Kyoto Protocol to the United Nations Framework Convention on Climate Change. 1998. Available online: <https://unfccc.int/resource/docs/convkp/kpeng.pdf> (accessed on 18 June 2024).
3. United Nations Framework Convention on Climate Change. Paris Agreement. 2015. Available online: https://unfccc.int/sites/default/files/english_paris_agreement.pdf (accessed on 18 June 2024).
4. Ritchie, H.; Roser, M. Energy. Our World in Data. 2022. Available online: <https://ourworldindata.org/energy> (accessed on 18 June 2024).
5. Greenhouse IEA. Gas Emissions from Energy. IEA. 2021. Available online: <https://www.iea.org/reports/greenhouse-gas-emissions-from-energy-overview> (accessed on 18 June 2024).
6. Kosmadakis, G. Estimating the potential of industrial (high-temperature) heat pumps for exploiting waste heat in EU industries. *Appl. Therm. Eng.* **2019**, *156*, 287–298. [[CrossRef](#)]
7. Ononogbo, C.; Nwosu, E.C.; Chukwuezie, O.C.; Nwakuba, N.R.; Chukwu, M.M.; Nwaji, G.N.; Anyanwu, E.E. Opportunities of waste heat recovery from various sources: Review of technologies and implementation. *Helyon* **2023**, *9*, e13590. [[CrossRef](#)]
8. Hamida, K.; Sajjadb, U.; Ahrensa, M.U.; Rena, S.; Ganesana, P.; Tolstorebrova, I.; Arshadc, A.; Saidd, Z.; Hafnera, A.; Wange, C.-C.; et al. Potential evaluation of integrated high temperature heat pumps: A review of recent advances. *Appl. Therm. Eng.* **2023**, *230 Pt A*, 120720. [[CrossRef](#)]
9. Golmohamadi, H. Demand-Side Flexibility in Power Systems: A Survey of Residential, Industrial, Commercial, and Agricultural Sectors. *Sustainability* **2022**, *14*, 7916. [[CrossRef](#)]
10. Maruf, M.N.I.; Morales-España, G.; Sijm, J.; Heliöstö, N.; Kiviluoma, J. Classification, potential role, and modeling of power-to-heat and thermal energy storage in energy systems: A review. *Sustain. Energy Technol. Assess.* **2022**, *53 Pt B*, 102553. [[CrossRef](#)]
11. Nandhini, R.; Sivaprakash, B.; Rajamohan, N. Waste heat recovery at low temperature from heat pumps, power cycles and integrated systems—Review on system performance and environmental perspectives. *Sustain. Energy Technol. Assess.* **2022**, *52 Pt B*, 102214. [[CrossRef](#)]

12. Leonzio, G.; Fennell, P.S.; Shah, N. Air-source heat pumps for water heating at a high temperature: State of the art. *Sustain. Energy Technol. Assess.* **2022**, *54*, 102866. [[CrossRef](#)]
13. Wang, Y.; Wang, J.; He, W. Development of efficient, flexible and affordable heat pumps for supporting heat and power decarbonization in the UK and beyond: Review and perspectives. *Renew. Sustain. Energy Rev.* **2022**, *154*, 111747. [[CrossRef](#)]
14. Carmona-Martínez, A.A.; Fresneda-Cruz, A.; Rueda, A.; Birgi, O.; Khawaja, C.; Janssen, R.; Davidis, B.; Reumerman, P.; Vis, M.; Karampinis, E.; et al. Renewable Power and Heat for the Decarbonisation of Energy-Intensive Industries. *Processes* **2023**, *11*, 18. [[CrossRef](#)]
15. Rajabloo, T.; De Ceunincka, W.; Van Wortswinkel, L.; Rezakazemie, M.; Aminabhavi, T. Environmental management of industrial decarbonization with focus on chemical sectors: A review. *J. Environ. Manag.* **2022**, *302*, 114055. [[CrossRef](#)]
16. Wu, D.; Jiang, J.; Hu, B.; Wang, R.Z. Experimental investigation on the performance of a very high temperature heat pump with water refrigerant. *Energy* **2020**, *190*, 116427. [[CrossRef](#)]
17. Arpagaus, C.; Blessa, F.; Uhlmann, M.; Schiffmann, J.; Bertsch, S.S. High temperature heat pumps: Market overview, state of the art, research status, refrigerants, and application potentials. *Energy* **2018**, *152*, 985–1010. [[CrossRef](#)]
18. Adamson, K.M.; Walmsley, T.G.; Carson, J.K.; Chen, Q.; Schlosser, F.; Kong, L.; Cleland, D.J. High-temperature and transcritical heat pump cycles and advancements: A review. *Renew. Sustain. Energy Rev.* **2022**, *167*, 112798. [[CrossRef](#)]
19. Tveit, T.M.; Khan, U.; Zevenhoven, R. Environmental impact of high temperature industrial heat pumps from a global warming potential (GWP) perspective. In *ECEEE Industrial Summer Study Proceedings*; European Council for an Energy Efficient Economy (ECEEE): Hyères, France, 2020; pp. 223–232.
20. Jiang, J.; Hu, B.; Wang, R.Z.; Deng, N.; Cao, F.; Wang, C.C. A review and perspective on industry high-temperature heat pumps. *Renew. Sustain. Energy Rev.* **2022**, *161*, 112106. [[CrossRef](#)]
21. Mateu-Royo, C.; Arpagaus, C.; Mota-Babiloni, A.; Navarro-Esbrí, J.; Bertsch, S.S. Advanced high temperature heat pump configurations using low GWP refrigerants for industrial waste heat recovery: A comprehensive study. *Energy Convers. Manag.* **2021**, *229*, 113752. [[CrossRef](#)]
22. Hu, X.; Shi, C.; Liu, Y.; Fu, X.; Ma, T.; Jin, M. Advanced Exergy and Exergoeconomic Analysis of Cascade High-Temperature Heat Pump System for Recovery of Low-Temperature Waste Heat. *Energies* **2024**, *17*, 1027. [[CrossRef](#)]
23. Dong, Y.; Wang, R. When and how to use cascade high temperature heat pump—Its multi-criteria evaluation. *Energy Convers. Manag.* **2024**, *309*, 118435. [[CrossRef](#)]
24. Schlemminger, C.; Bantle, M.; Jenssen, S.; Dallai, M. Industrial high temperature heat pump for simultaneous production of ice-water and process-heat. In *Proceedings of the 15th IIR-Gustav Lorentzen Conference on Natural Refrigerants (GL2022)*, Trondheim, Norway, 13–15 June 2022.
25. Dai, B.; Liu, X.; Liu, S.; Wang, D.; Meng, C.; Wang, Q.; Song, Y.; Zou, T. Life cycle performance evaluation of cascade-heating high temperature heat pump system for waste heat utilization: Energy consumption, emissions and financial analyses. *Energy* **2022**, *261*, 125314. [[CrossRef](#)]
26. Dong, S.; Meng, X.; Hu, X.; Sun, Z.; Wang, H.; Luo, Y. Investigation of cascade high temperature heat pump optimal design theory based on experiment supporting multi-objective optimization. *Energy Convers. Manag.* **2022**, *267*, 115873. [[CrossRef](#)]
27. Wu, Z.; Wang, X.; Sha, L.; Li, X.; Yang, X.; Ma, X.; Zhang, Y. Performance analysis and multi-objective optimization of the high-temperature cascade heat pump system. *Energy* **2021**, *223*, 120097. [[CrossRef](#)]
28. Ganesan, P.; Eikevik, T.M.; Hamid, K.; Wang, R.; Yan, H. Thermodynamic analysis of cascade high-temperature heat pump using new natural zeotropic refrigerant mixtures: R744/R600 and R744/R601. *Int. J. Refrig.* **2023**, *154*, 215–230. [[CrossRef](#)]
29. Ganesan, P.; Eikevik, T.M. New zeotropic CO₂-based refrigerant mixtures for cascade high-temperature heat pump to reach heat sink temperature up to 180° C. *Energy Convers. Manag.* **2023**, *20*, 100407. [[CrossRef](#)]
30. Navarro-Esbrí, J.; Fernández-Moreno, A.; Mota-Babiloni, A. Modelling and evaluation of a high-temperature heat pump two-stage cascade with refrigerant mixtures as a fossil fuel boiler alternative for industry decarbonization. *Energy* **2022**, *254*, 124308. [[CrossRef](#)]
31. Chen, J.; Chen, Q.; Qin, X.; Wang, D. Energy, exergy, economic and environmental analyses and optimization of a novel vapor injection autocascade heat pump for high-temperature water heating. *Energy Convers. Manag.* **2022**, *267*, 115909. [[CrossRef](#)]
32. Kezier, D.; Cheng, J.H.; Li, X.Y.; Cao, X.; Zhang, C.L. A semi-cascade heat pump system for different temperature lifts. *Appl. Therm. Eng.* **2024**, *236*, 121767. [[CrossRef](#)]
33. Chen, J.; Wang, D.; Zhang, G.; Peng, X.; Qin, X.; Wang, G. 4E analyses of a novel solar-assisted vapor injection autocascade high-temperature heat pump based on genetic algorithm. *Energy Convers. Manag.* **2024**, *299*, 117863. [[CrossRef](#)]
34. Zhao, A.; Pecnik, R.; Peeters, J.W. Thermodynamic analysis and heat exchanger calculations of transcritical high-temperature heat pumps. *Energy Convers. Manag.* **2024**, *303*, 118172. [[CrossRef](#)]
35. Yang, Y.; Wang, Y.; Xu, Z.; Xie, B.; Hu, Y.; Yu, J.; Chen, Y.; Zang, T.; Lu, Z.; Gong, Y. Performance Comparison of High-Temperature Heat Pumps with Different Vapor Refrigerant Injection Techniques. *Processes* **2024**, *12*, 566. [[CrossRef](#)]
36. Kong, L.; Walmsley, T.G.; Hoang, D.K.; Schlosser, F.; Chen, Q.; Carson, J.K.; Cleland, D.J. Transcritical-transcritical cascade CO₂ heat pump cycles for high-temperature heating: A numerical evaluation. *Appl. Therm. Eng.* **2024**, *238*, 122005. [[CrossRef](#)]
37. Udriou, C.M.; Navarro-Esbrí, J.; Giménez-Prades, P.; Mota-Babiloni, A. Towards sustainable process heating at 250 °C: Modeling and optimization of an R1336mzz (Z) transcritical High-Temperature heat pump. *Appl. Therm. Eng.* **2024**, *242*, 122521. [[CrossRef](#)]

38. Vieren, E.; Demeester, T.; Beyne, W.; Arteconi, A.; De Paepe, M.; Lecompte, S. The thermodynamic potential of high-temperature transcritical heat pump cycles for industrial processes with large temperature glides. *Appl. Therm. Eng.* **2023**, *234*, 121197. [[CrossRef](#)]
39. Dai, B.; Liu, C.; Liu, S.; Wang, D.; Wang, Q.; Zou, T.; Zhou, X. Life cycle techno-enviro-economic assessment of dual-temperature evaporation transcritical CO₂ high-temperature heat pump systems for industrial waste heat recovery. *Appl. Therm. Eng.* **2023**, *219*, 119570. [[CrossRef](#)]
40. You, J.; Zhang, X.; Gao, J.; Wang, R.; Xu, Z. Entransy based heat exchange irreversibility analysis for a hybrid absorption-compression heat pump cycle. *Energy* **2024**, *289*, 129990. [[CrossRef](#)]
41. Dai, B.; Wang, Q.; Liu, S.; Wang, D.; Yu, L.; Li, X.; Wang, Y. Novel configuration of dual-temperature condensation and dual-temperature evaporation high-temperature heat pump system: Carbon footprint, energy consumption, and financial assessment. *Energy Convers. Manag.* **2023**, *292*, 117360. [[CrossRef](#)]
42. Huang, Y.; Chen, J.; Chen, Y.; Luo, X.; Liang, Y.; He, J.; Yang, Z. Performance explorations of a novel high temperature heat pump with multi-adjusted compositions of zeotropic mixture. *Appl. Therm. Eng.* **2023**, *235*, 121409. [[CrossRef](#)]
43. Wang, H.; Ponciroli, R.; Vilim, R.B. *Assessments of Advanced Reactor Heat Supply to High Temperature Industrial Unit Operations: Heat Engines and Heat Pumps*; No. ANL/NSE-23/91; Argonne National Laboratory (ANL): Argonne, IL, USA, 2024.
44. Pettinari, M.; Frate, G.F.; Tran, A.P.; Oehler, J.; Stathopoulos, P.; Kyprianidis, K.; Ferrari, L. Impact of the Regulation Strategy on the Transient Behavior of a Brayton Heat Pump. *Energies* **2024**, *17*, 1020. [[CrossRef](#)]
45. Briola, S.; Barberis, S.; Renzi, M.; Gabbriellini, R. Theoretical investigation of a novel high-temperature heat pump exploiting low-temperature waste heat and using two-phase machines with zero electric consumption. *Appl. Therm. Eng.* **2023**, *235*, 121322. [[CrossRef](#)]
46. Xie, X.; Jin, S.; Gao, P.; Wu, W.; Yang, Q.; Wang, L. Ammonia-based hybrid chemisorption-compression heat pump for high-temperature heating. *Appl. Therm. Eng.* **2023**, *232*, 121081. [[CrossRef](#)]
47. Kim, S.T.; Hegner, R.; Özüylasi, G.; Stathopoulos, P.; Nicke, E. Performance analysis of multistage high-temperature heat pump cycle. *Energy Sci. Eng.* **2023**, *11*, 3500–3511. [[CrossRef](#)]
48. Marinelli, S.; Lolli, F.; Butturi, M.A.; Rimini, B.; Gamberini, R. Environmental performance analysis of a dual-source heat pump system. *Energy Build.* **2020**, *223*, 110180. [[CrossRef](#)]
49. Zhang, C.; Wu, J.; Gao, J.; Huang, X. Experimental study of a novel double-effect evaporation concentration system for high temperature heat pump. *Desalination* **2020**, *491*, 114495. [[CrossRef](#)]
50. Talaba, O.; Dima, D.; Buiuc, V.; Ionita, C.; Stefanescu, M.F.; Serban, A.; Dobrovicescu, A. CO₂ high temperature heat pump—A promising solution. In *IOP Conference Series: Materials Science and Engineering*; IOP Publishing: Bristol, UK, 2020; Volume 997, p. 012157.
51. Stefanou, M.A.R. Design and Development of a High Temperature Heat Pump (HTHP) for Industrial Applications. Ph.D. Thesis, Ulster University, Belfast, Northern Ireland, 2023.
52. Gao, J.T.; Xu, Z.Y.; Wang, R.Z. An air-source hybrid absorption-compression heat pump with large temperature lift. *Appl. Energy* **2021**, *291*, 116810. [[CrossRef](#)]
53. Organisation for Economic Co-Operation and Development. *Saving Costs in Chemicals Management: How the OECD Ensures Benefits to Society*; Organisation for Economic Co-Operation and Development: Paris, France, 2019.
54. Saygin, D.; Gielen, D. Zero-emission pathway for the global chemical and petrochemical sector. *Energies* **2021**, *14*, 3772. [[CrossRef](#)]
55. Marina, A.; Spoelstra, S.; Zondag, H.; Wemmers, A. An estimation of the European industrial heat pump market potential. *Renew. Sustain. Energy Rev.* **2021**, *139*, 110545. [[CrossRef](#)]
56. Kiss, A.A.; Smith, R. Rethinking energy use in distillation processes for a more sustainable chemical industry. *Energy* **2020**, *203*, 117788. [[CrossRef](#)]
57. Wu, T.; Wang, C.; Liu, J.; Zhuang, Y.; Du, J. Design and 4E analysis of heat pump-assisted extractive distillation processes with preconcentration for recovering ethyl-acetate and ethanol from wastewater. *Chem. Eng. Res. Des.* **2024**, *201*, 510–522. [[CrossRef](#)]
58. Wang, H.; Yu, P.; Chen, L.; Chen, L.; Sun, B. Simulation and modification of an Ethane-Ethylene separation Unit using vapor recompression heat Pump: Energy, Exergy, and economic analyses. *Appl. Therm. Eng.* **2024**, *239*, 121993. [[CrossRef](#)]
59. Li, X.; Ye, Q.; Li, J.; Liu, Y.; Yan, L.; Jian, X.; Zhang, J. Investigation on energy-efficient heterogeneous pressure-swing azeotropic distillation for recovery of cyclohexane and tert-butanol from industrial effluent. *Sep. Purif. Technol.* **2023**, *306*, 122705. [[CrossRef](#)]
60. Vieren, E.; Demeester, T.; Beyne, W.; Magni, C.; Abedini, H.; Arpagaus, C.; Bertsch, S.; Arteconi, A.; De Paepe, M.; Lecompte, S. The Potential of Vapor Compression Heat Pumps Supplying Process Heat between 100 and 200 °C in the Chemical Industry. *Energies* **2023**, *16*, 6473. [[CrossRef](#)]
61. Li, Y.; Ding, Y.; Cao, M. Optimization of energy-saving distillation system of absorption heat pump based on intermediate heat exchange. *Appl. Therm. Eng.* **2022**, *213*, 118721. [[CrossRef](#)]
62. Xu, Y.; Li, J.; Ye, Q.; Li, Y. Design and optimization for the separation of tetrahydrofuran/isopropanol/water using heat pump assisted heat-integrated extractive distillation. *Sep. Purif. Technol.* **2021**, *277*, 119498. [[CrossRef](#)]
63. Xu, Y.; Li, J.; Ye, Q.; Li, Y. Energy efficient extractive distillation process assisted with heat pump and heat integration to separate acetonitrile/1,4-dioxane/water. *Process Saf. Environ.* **2021**, *156*, 144–159. [[CrossRef](#)]

64. Zhu, Z.; Qi, H.; Shen, Y.; Qiu, X.; Zhang, H.; Qi, J.; Yang, J.; Wang, L.; Wang, Y.; Ma, Y.; et al. Energy-saving investigation of organic material recovery from wastewater via thermal coupling extractive distillation combined with heat pump based on thermoeconomic and environmental analysis. *Process Saf. Environ. Prot.* **2021**, *146*, 441–450. [[CrossRef](#)]
65. Wang, N.; Ye, Q.; Chen, L.; Zhang, H.; Zhong, J. Improving the economy and energy efficiency of separating water/acetonitrile/isopropanol mixture via triple-column pressure-swing distillation with heat-pump technology. *Energy* **2021**, *215*, 119126. [[CrossRef](#)]
66. Janković, T.; Straathof, A.J.; Kiss, A.A. Thermally self-sufficient heat pump-assisted azeotropic dividing-wall column for biofuels recovery from isopropanol-butanol-ethanol fermentation. *Chem. Eng. Process. Intensif.* **2024**, *197*, 109689. [[CrossRef](#)]
67. Zhai, J.; Chen, X.; Xie, H.; Sun, X.; Hu, M.; Dang, M.; Zhao, P.; Liu, Y. Energy-saving heat pump-assisted extractive-azeotropic dividing wall column with heat exchanger network for separating acetonitrile and water: A techno-economic and inherent safety investigation. *Process Saf. Environ. Prot.* **2023**, *173*, 178–190. [[CrossRef](#)]
68. Zhai, J.; Chen, X.; Xie, H.; Sun, X.; Zhao, P.; Liu, Y. Improving the economic saving, environmental sustainability, and energy efficiency of separating acetone/n-heptane mixture via heat pump-assisted extractive dividing wall column with heat exchanger network. *Chem. Eng. Process. Intensif.* **2023**, *187*, 109354. [[CrossRef](#)]
69. Yang, D.; Wan, D.; Yun, Y.; Yang, S. Energy-saving distillation process for mixed trichlorobenzene based on ORC coupled MVR heat pump technology. *Energy* **2023**, *262*, 125565. [[CrossRef](#)]
70. Wang, C.; Zhuang, Y.; Liu, L.; Zhang, L.; Du, J. Heat pump assisted extractive distillation sequences with intermediate-boiling entrainer. *Appl. Therm. Eng.* **2021**, *186*, 116511. [[CrossRef](#)]
71. Zhai, J.; Chen, X.; Sun, X.; Xie, H. Economically and thermodynamically efficient pressure-swing distillation with heat integration and heat pump techniques. *Appl. Therm. Eng.* **2023**, *218*, 119389. [[CrossRef](#)]
72. Ulyev, L.M.; Kanishev, M.V.; Chibisov, R.E.; Vasilyev, M.A. Heat integration of an industrial unit for the ethylbenzene production. *Energies* **2021**, *14*, 3839. [[CrossRef](#)]
73. Boldyryev, S.; Ilchenko, M.; Krajačić, G. Improving the Economic Efficiency of Heat Pump Integration into Distillation Columns of Process Plants Applying Different Pressures of Evaporators and Condensers. *Energies* **2024**, *17*, 951. [[CrossRef](#)]
74. Wu, Z.; Xu, G.; Zhang, W.; Xue, X.; Chen, H. Thermodynamic and economic analysis of a new methanol steam reforming system integrated with CO₂ heat pump and cryogenic separation system. *Energy* **2023**, *283*, 128501. [[CrossRef](#)]
75. de Raad, B.; van Lieshout, M.; Stougie, L.; Ramirez, A. Improving plant-level heat pump performance through process modifications. *Appl. Energy* **2024**, *358*, 122667. [[CrossRef](#)]
76. Angappan, G.; Pandiaraj, S.; Alrubaie, A.J.; Muthusamy, S.; Said, Z.; Panchal, H.; Katekar, V.P.; Shoeibi, S.; Kabeel, A.E. Investigation on solar still with integration of solar cooker to enhance productivity: Experimental, exergy, and economic analysis. *J. Water Process Eng.* **2023**, *51*, 103470. [[CrossRef](#)]
77. Moustafa, E.B.; Hammad, A.H.; Elsheikh, A.H. A new optimized artificial neural network model to predict thermal efficiency and water yield of tubular solar still. *Case Stud. Therm. Eng.* **2022**, *30*, 101750. [[CrossRef](#)]
78. Sharshir, S.W.; Joseph, A.; Elsayad, M.M.; Tareemi, A.A.; Kandeal, A.W.; Elkadeem, M.R. A review of recent advances in alkaline electrolyzer for green hydrogen production: Performance improvement and applications. *Int. J. Hydrogen Energy* **2023**, *49*, 458–488. [[CrossRef](#)]
79. Liu, H.; Joseph, A.; Elsayad, M.M.; Elshernoby, B.; Awad, F.; Elsharkawy, M.; Kandeal, A.W.; Hussein, A.A.; An, M.; Sharshir, S.W. Recent advances in heat pump-coupled desalination systems: A systematic review. *Desalination* **2022**, *543*, 116081. [[CrossRef](#)]
80. Tareemi, A.A.; Joseph, A.; Elsayad, M.M.; Abdullah, A.S.; Sharshir, S.W.; Jang, S.H. Thermoenviroeconomic assessment of upgraded solar desalination with heat pump, various active and passive modifications. *Process Saf. Environ. Prot.* **2024**, *184*, 411–427. [[CrossRef](#)]
81. Hai, T.; Chauhan, B.S.; Aksoy, M.; Mahariq, I.; Al-Kouz, W.; Muhammad, T.; ELmonser, H.; Nhang, H. Enhancing the proficiency of heat pump-driven humidification-dehumidification desalination systems using eco-environmentally friendly organic mixtures. *Process Saf. Environ. Prot.* **2024**, *183*, 1117–1134. [[CrossRef](#)]
82. Petersen, N.H.; Arras, M.; Wirsum, M.; Ma, L. Integration of large-scale heat pumps to assist sustainable water desalination and district cooling. *Energy* **2024**, *289*, 129733. [[CrossRef](#)]
83. Shahzad, M.K.; Ding, Y.; Zhang, H.; Dong, Y.; Jamil, S.R.; Adnan, M. Performance analysis of a novel combined open absorption heat pump and FlashME seawater desalination system for flue gas heat and water recovery. *Energy Convers. Manag.* **2024**, *301*, 117996. [[CrossRef](#)]
84. Shahzad, M.K.; Ding, Y.; Zhang, H.; Dong, Y.; Jamil, S.R.; Gillani, S.S.J. Energy efficiency analysis of novel combined open absorption multifunctional heat pump and FlashME desalination system with a compressed air dryer. *Desalination* **2024**, *582*, 117662. [[CrossRef](#)]
85. Chen, L.; Liu, X.; Ye, K.; Xie, M.; Lan, W. Thermodynamic and economic analysis of an integration system of multi-effect desalination (MED) with ice storage based on a heat pump. *Energy* **2023**, *283*, 129064. [[CrossRef](#)]
86. Zhou, S.; Zhang, K.; Yang, W.; Zhu, X.; Shen, S. Evaluation of a heat pump coupled two-stage humidification-dehumidification desalination system with waste heat recovery. *Energy Convers. Manag.* **2023**, *278*, 116694. [[CrossRef](#)]
87. Ghiasirad, H.; Baris, T.G.; Javanfam, F.; Kalkhoran, H.R.; Skorek-Osikowska, A. Indirect integration of a thermal-mechanical heat pump with a humidification-dehumidification desalination unit. *Appl. Therm. Eng.* **2023**, *230*, 120852. [[CrossRef](#)]

88. Khalifa, A.; Mezghani, A.; Alawami, H. Analysis of integrated membrane distillation-heat pump system for water desalination. *Desalination* **2021**, *510*, 115087. [[CrossRef](#)]
89. Sovacool, B.K.; Bazilian, M.; Griffiths, S.; Kim, J.; Foley, A.; Rooney, D. Decarbonizing the food and beverages industry: A critical and systematic review of developments, sociotechnical systems and policy options. *Renew. Sustain. Energy Rev.* **2021**, *143*, 110856. [[CrossRef](#)]
90. Dano, T. Experimental Investigation of a High Temperature Heat Pump for Food Processing Applications. Ph.D. Thesis, Norwegian University of Science and Technology, Trondheim, Norway, 2023.
91. Zuberi, M.J.S.; Hasanbeigi, A.; Morrow, W. Bottom-up assessment of industrial heat pump applications in US Food manufacturing. *Energy Convers. Manag.* **2022**, *272*, 116349. [[CrossRef](#)]
92. Loemba, A.B.T.; Kichonge, B.; Kivevele, T. Thermal Performance and Technoeconomic Analysis of Solar-Assisted Heat Pump Dryer Integrated with Energy Storage Materials for Drying Cavendish Banana (*Musa acuminata*). *J. Food Process. Preserv.* **2024**, *2024*, 7496826. [[CrossRef](#)]
93. Bhadbhade, N.; Ong, B.H.; Olsen, D.G.; Wellig, B.; Patel, M.K. Assessment of CO₂ abatement potential of heat pumps using pinch analysis for the Swiss chocolate industry. *J. Clean. Prod.* **2024**, *455*, 142323. [[CrossRef](#)]
94. Moritani, S.; Nanjo, H.; Itou, A.; Win Win, P.; Elbasit, M.A.A. Heating and cooling methods for the subirrigation of strawberry plants using air and geothermal heat pumps. *Environ. Dev. Sustain.* **2024**, *26*, 7235–7253. [[CrossRef](#)]
95. Knorr, L.; Schlosser, F.; Meschede, H. Assessment of energy efficiency and flexibility measures in electrified process heat generation based on simulations in the animal feed industry. *J. Sustain. Dev. Energy Water Environ. Syst.* **2023**, *11*, 1–16. [[CrossRef](#)]
96. Klinac, E.; Carson, J.K.; Hoang, D.; Chen, Q.; Cleland, D.J.; Walmsley, T.G. Multi-level process integration of heat pumps in meat processing. *Energies* **2023**, *16*, 3424. [[CrossRef](#)]
97. Foslie, S.S.; Knudsen, B.R.; Korpås, M. Integrated design and operational optimization of energy systems in dairies. *Energy* **2023**, *281*, 128242. [[CrossRef](#)]
98. Martyanov, A.; Zimina, Y.; Antipin, D. Application of heat pumps in the food industry: Purification plant. In *E3S Web of Conferences*; EDP Sciences: Les Ulis, France, 2023; Volume 419, p. 01025.
99. Hermanucz, P.; Geczi, G.; Barotfi, I. Energy efficient solution in the brewing process using a dual-source heat pump. *Therm. Sci.* **2022**, *26 Pt A*, 2311–2319. [[CrossRef](#)]
100. Ahrens, M.U.; Foslie, S.S.; Moen, O.M.; Bantle, M.; Eikevik, T.M. Integrated high temperature heat pumps and thermal storage tanks for combined heating and cooling in the industry. *Appl. Therm. Eng.* **2021**, *189*, 116731. [[CrossRef](#)]
101. Payá, J.; Cazorla-Marín, A.; Arpagaus, C.; Corrales Ciganda, J.L.; Hassan, A.H. Low-Pressure Steam Generation with Concentrating Solar Energy and Different Heat Upgrade Technologies: Potential in the European Industry. *Sustainability* **2024**, *16*, 1733. [[CrossRef](#)]
102. Ma, X.; Du, Y.; Lei, B.; Wu, Y. Energy, exergy, economic, and environmental analysis of a high-temperature heat pump steam system. *Int. J. Refrig.* **2024**, *160*, 423–436. [[CrossRef](#)]
103. Feng, C.; Guo, C.; Chen, J.; Tan, S.; Jiang, Y. Thermodynamic analysis of a dual-pressure evaporation high-temperature heat pump with low GWP zeotropic mixtures for steam generation. *Energy* **2024**, *294*, 130964. [[CrossRef](#)]
104. Klute, S.; Budt, M.; van Beek, M.; Doetsch, C. Steam generating heat pumps—Overview, classification, economics, and basic modeling principles. *Energy Convers. Manag.* **2024**, *299*, 117882. [[CrossRef](#)]
105. Kosmadakis, G.; Meramveliotakis, G.; Bakalis, P.; Neofytou, P. Waste heat upgrading with high-temperature heat pumps for assisting steam generation in ships: Performance, cost and emissions benefits. *Appl. Therm. Eng.* **2024**, *236*, 121890. [[CrossRef](#)]
106. Koundinya, S.; Jothilingam, J.; Seshadri, S. Low-pressure steam generating heat pump—A design and field implementation case study. *Therm. Sci. Eng. Prog.* **2023**, *45*, 102140. [[CrossRef](#)]
107. Zeilerbauer, L.; Hubmann, F.; Puschnigg, S.; Lindorfer, J. Life cycle assessment and shadow cost of steam produced by an industrial-sized high-temperature heat pump. *Sustain. Prod. Consum.* **2023**, *40*, 48–62. [[CrossRef](#)]
108. Liu, C.; Han, W.; Xue, X. Experimental investigation of a high-temperature heat pump for industrial steam production. *Appl. Energy* **2022**, *312*, 118719. [[CrossRef](#)]
109. Zhao, Z.; Gao, S.; Tian, Y.; Zhang, H. Study on performance of high temperature heat pump system integrated with flash tank for waste heat recovery employed in steam production. *Int. J. Energy Res.* **2021**, *45*, 20318–20330. [[CrossRef](#)]
110. Yan, H.; Wang, R.; Du, S.; Hu, B.; Xu, Z. Analysis and perspective on heat pump for industrial steam generation. *Adv. Energy Sustain. Res.* **2021**, *2*, 2000108. [[CrossRef](#)]
111. Chen, L.; Yang, B.; Shen, X.; Xie, Z.; Sun, F. Thermodynamic optimization opportunities for the recovery and utilization of residual energy and heat in China's iron and steel industry: A case study. *Appl. Therm. Eng.* **2015**, *86*, 151–160. [[CrossRef](#)]
112. Inayat, A. Current progress of process integration for waste heat recovery in steel and iron industries. *Fuel* **2023**, *338*, 127237. [[CrossRef](#)]
113. Beck, A.; Unterluggauer, J.; Helminger, F.; Solís-Gallego, I. Decarbonisation Pathways for the Finishing Line in a Steel Plant and Their Implications for Heat Recovery Measures. *Energies* **2023**, *16*, 852. [[CrossRef](#)]
114. Alshehhi, I.; Alnahdi, W.; Ali, M.; Bouabid, A.; Slepchenko, A. Assessment of waste heat recovery in the steel industry. *J. Sustain. Dev. Energy Water Environ. Syst.* **2023**, *11*, 1100440. [[CrossRef](#)]
115. Hoettecke, L.; Thiem, S.; Schäfer, J.; Niessen, S. Resilience optimization of multi-modal energy supply systems: Case study in German metal industry. *Comput. Chem. Eng.* **2022**, *162*, 107824. [[CrossRef](#)]

116. Beck, A.; Unterluggauer, J.; Knöttner, S.; Niño, C.G.; Angel, J.G.; Arias, M.L.; Solis, I. Optimized waste heat utilization in the steel industry with industrial heat pumps and low-temperature distribution system. In Proceedings of the 12. Internationale Energiewirtschaftstagung an der TU Wien (IEWT 2021), Wien, Austria, 7–10 September 2021.
117. Brough, D.; Jouhara, H. The aluminium industry: A review on state-of-the-art technologies, environmental impacts and possibilities for waste heat recovery. *Int. J. Thermofluids* **2020**, *1–2*, 100007. [[CrossRef](#)]
118. Hasanbeigi, A.; Zuberi, J. *Electrification of Heating in the Textile Industry. A Techno-Economic Analysis for China, Japan, and Taiwan Report*; Global Efficiency Intelligence: San Francisco, CA, USA, 2022.
119. Akarslan, K.F.; Elbir, A.; Sahin, M.E. Wool drying process in heat-pump-assisted dryer by fuzzy logic modelling. *Therm. Sci.* **2022**, *27 Pt B*, 3043–3050. [[CrossRef](#)]
120. Park, S.; Lee, D.; Kim, Y. Experimental evaluation of the performance characteristics of a heat pump clothing care system under various operating conditions. *Int. J. Therm. Sci.* **2023**, *192*, 108433. [[CrossRef](#)]
121. Kim, Y.; Lim, J.; Cho, H.; Lee, J.; Moon, I.; Kim, J. Novel Design of Optimum Heat Exchanger Networks for Textile Dyeing Process to Maximize Wastewater Heat Recovery Efficiency. *Comput. Aided Chem. Eng.* **2022**, *49*, 1093–1098.
122. Kim, Y.; Lim, J.; Shim, J.Y.; Lee, H.; Cho, H.; Kim, J. Optimizing wastewater heat recovery systems in textile dyeing processes using pinch analysis. *Appl. Therm. Eng.* **2022**, *214*, 118880. [[CrossRef](#)]
123. Thomasson, T.; Raitila, J.; Tsupari, E. Experimental and techno-economic analysis of solar-assisted heat pump drying of biomass. *Energy Rep.* **2024**, *11*, 316–326. [[CrossRef](#)]
124. Escalona, A.; Cuevas, C.; Salazar, L.; Hernandez, V. Modelling of heat pump drying system powered by a hybrid PV-wind-battery plant for slow-drying hardwoods. *Energy Sustain. Dev.* **2023**, *76*, 101282. [[CrossRef](#)]
125. Khouya, A. Energy analysis of a combined solar wood drying system. *Sol. Energy* **2022**, *231*, 270–282. [[CrossRef](#)]
126. Khouya, A. Performance assessment of a heat pump and a concentrated photovoltaic thermal system during the wood drying process. *Appl. Therm. Eng.* **2020**, *180*, 115923. [[CrossRef](#)]
127. Kumar, B.; Raj, A.K.; Szepesi, G.; Szamosi, Z. A conspectus review on solar drying of wood: Regional and technical contrivances. *J. Therm. Anal. Calorim.* **2023**, *148*, 9237–9261. [[CrossRef](#)]
128. Zhang, Z.; Li, M.; Wang, Y.; Li, G.; Xing, T.; Yao, M.; Hassanien, R.H.E. Study on the performance of heat pump drying system under the synergistic effect of humidity enthalpy enhancement and solar heat storage under low temperature working conditions. *Appl. Therm. Eng.* **2024**, *244*, 122626. [[CrossRef](#)]
129. Yu, M.; Zou, L.; Yu, J. Experimental investigation on the drying characteristics in a solar assisted ejector enhanced heat pump dryer system. *Sol. Energy* **2024**, *267*, 112265. [[CrossRef](#)]
130. Xu, C.; Ma, H.; Wang, S. Thermal digestion characteristics of kitchen waste based on high temperature heat pump combined with vacuum drying. *Appl. Therm. Eng.* **2024**, *244*, 122703. [[CrossRef](#)]
131. Liu, Z.; Gong, H.; Cheng, C.; Qie, Z. Experimental evaluation of metal–organic framework desiccant wheel combined with heat pump. *Appl. Therm. Eng.* **2024**, *236*, 121542. [[CrossRef](#)]
132. Fix, A.; Braun, J.E.; Warsinger, D.M. High Efficiency Heat Pump Industrial Drying with Water Vapor-Selective Membranes. In Proceedings of the 14th IEA Heat Pump Conference, Chicago, IL, USA, 15–18 May 2023.
133. Le Anh Duca, P.V.K.; Tanb, N.T.; Sonb, D.T.; Van Nguyenc, N.; Nguyend, N.X. Heat and mass transfer in drying of carrot by radio frequency assisted heat pump drying. *Front. Heat Mass Transf.* **2023**, *20*, 25.
134. Schlosser, F.; Zysk, S.; Walmsley, T.G.; Kong, L.; Zühlsdorf, B.; Meschede, H. Break-even of high-temperature heat pump integration for milk spray drying. *Energy Convers. Manag.* **2023**, *291*, 117304. [[CrossRef](#)]
135. Yahya, M.; Fahmi, H.; Hasibuan, R.; Fudholi, A. Development of hybrid solar-assisted heat pump dryer for drying paddy. *Case Stud. Therm. Eng.* **2023**, *45*, 102936. [[CrossRef](#)]
136. Jing, S.; Chen, Q.; Zhou, Y.; Yu, J. Thermodynamic analysis of a modified booster-assisted ejector heat pump cycle with dual condensers. *Appl. Therm. Eng.* **2023**, *235*, 121351. [[CrossRef](#)]
137. Yao, M.; Li, M.; Wang, Y.; Li, G.; Zhang, Y.; Gao, M.; Deng, Z.; Xing, T.; Zhang, Z.; Zhang, W. Analysis on characteristics and operation mode of direct solar collector coupled heat pump drying system. *Renew. Energy* **2023**, *206*, 223–238. [[CrossRef](#)]
138. Yu, M.; Yu, J. Thermodynamic analyses of a solar assisted ejector enhanced vapor injection cycle with subcooler for heat pump dryer application. *Sol. Energy* **2022**, *232*, 376–387. [[CrossRef](#)]
139. Loemba, A.B.; Kichonge, B.; Kivevele, T. Comprehensive assessment of heat pump dryers for drying agricultural products. *Energy Sci. Eng.* **2023**, *11*, 2985–3014. [[CrossRef](#)]
140. Zhang, L.Z.; Jiang, L.; Xu, Z.C.; Zhang, X.J.; Fan, Y.B.; Adnoui, M.; Zhang, C.B. Optimization of a variable-temperature heat pump drying process of shiitake mushrooms using response surface methodology. *Renew. Energy* **2022**, *198*, 1267–1278. [[CrossRef](#)]
141. Yahya, M.; Rachman, A.; Hasibuan, R. Performance analysis of solar-biomass hybrid heat pump batch-type horizontal fluidized bed dryer using multi-stage heat exchanger for paddy drying. *Energy* **2022**, *254*, 124294. [[CrossRef](#)]
142. Yan, R.E.N.; Wang, P.D.; Wu, W.D.; Hao, W.A.N.G.; Yang, Y.Y.; Yang, Q.G. Study on the effects of auxiliary condenser operation parameters on the performance of closed loop heat pump drying system. *Int. J. Refrig.* **2022**, *136*, 17–26.
143. Hamid, K.; Sajjad, U.; Yang, K.S.; Wu, S.K.; Wang, C.C. Assessment of an energy efficient closed loop heat pump dryer for high moisture contents materials: An experimental investigation and AI based modelling. *Energy* **2022**, *238*, 121819. [[CrossRef](#)]
144. Cui, Q.; Qu, H.; Sun, B.; Gao, E.; Zhang, X. Operating characteristics and performance evaluation of carbon dioxide heat pump driven liquid desiccant dehumidification systems: A comparative study. *Energy Convers. Manag.* **2022**, *254*, 115298. [[CrossRef](#)]

145. Su, W.; Ma, D.; Lu, Z.; Jiang, W.; Wang, F.; Xiaosong, Z. A novel absorption-based enclosed heat pump dryer with combining liquid desiccant dehumidification and mechanical vapor recompression: Case study and performance evaluation. *Case Stud. Therm. Eng.* **2022**, *35*, 102091. [[CrossRef](#)]
146. Zheng, Q.; Cao, L.; Ni, L.; Huang, G. Operating characteristics of sludge heat pump dryer and influencing factors of performance: A field experiment in an electroplating factory. *Appl. Therm. Eng.* **2022**, *212*, 118602. [[CrossRef](#)]
147. Chen, Q.; Cleland, D.J.; Carson, J.K.; Walmsley, T.G. Integration of desiccant wheels and high-temperature heat pumps with milk spray dryers. *Appl. Therm. Eng.* **2022**, *216*, 119083. [[CrossRef](#)]
148. Cheng, J.H.; Yu, W.; Cao, X.; Shao, L.L.; Zhang, C.L. Evaluation of heat pump dryers from the perspective of energy efficiency and operational robustness. *Appl. Therm. Eng.* **2022**, *215*, 118995. [[CrossRef](#)]
149. Kushwah, A.; Kumar, A.; Gaur, M.K. Drying kinetics, performance, and quality assessment for banana slices using heat pump-assisted drying system (HPADS). *J. Food Process Eng.* **2022**, *45*, e13964. [[CrossRef](#)]
150. Jokiel, M.; Bantle, M.; Kopp, C.; Verpe, E.H. Modelica-based modelling of heat pump-assisted apple drying for varied drying temperatures and bypass ratios. *Therm. Sci. Eng. Prog.* **2020**, *19*, 100575. [[CrossRef](#)]
151. Ismael, H.H.; Yumrutaş, R. Investigation of a solar assisted heat pump wheat drying system with underground thermal energy storage tank. *Sol. Energy* **2020**, *199*, 538–551. [[CrossRef](#)]
152. Regulation (EU) 2024/573 of the European Parliament and of the Council of 7 February 2024 on Fluorinated Greenhouse Gases, Amending Directive (EU) 2019/1937 and Repealing Regulation (EU) No 517/2014. OJ L, 2024/573. 20 February 2024. Available online: <http://data.europa.eu/eli/reg/2024/573/oj> (accessed on 18 June 2024).
153. Andersen, M.P.; Zühlsdorf, B.; Markussen, W.B.; Jensen, J.K.; Elmegaard, B. Selection of Working Fluids and Heat Pump Cycles at High Temperatures: Creating a Concise Technology Portfolio. *Appl. Energy* **2024**, *376*, 124312. [[CrossRef](#)]
154. Spale, J.; Hoess, A.J.; Bell, I.H.; Ziviani, D. Exploratory Study on Low-GWP Working Fluid Mixtures for Industrial High Temperature Heat Pump with 200 C Supply Temperature. *Energy* **2024**, *308*, 132677. [[CrossRef](#)]
155. Abedini, H.; Vieren, E.; Demeester, T.; Beyne, W.; Lecompte, S.; Quoilin, S.; Arteconi, A. A comprehensive analysis of binary mixtures as working fluid in high temperature heat pumps. *Energy Convers. Manag.* **2023**, *277*, 116652. [[CrossRef](#)]
156. Zini, A.; Socci, L.; Vaccaro, G.; Rochetti, A.; Talluri, L. Working Fluid Selection for High-Temperature Heat Pumps: A Comprehensive Evaluation. *Energies* **2024**, *17*, 1556. [[CrossRef](#)]
157. Vering, C.; Kroppa, H.; Venzik, V.; Streblov, R.; Müller, D. Towards an integral decision-making process applied to the refrigerant selection in heat pumps. *Renew. Energy* **2022**, *192*, 815–827. [[CrossRef](#)]
158. Hosseinnia, S.M.; Amiri, L.; Nesreddine, H.; Monney, D.; Poncet, S. Thermodynamic analysis of high temperature cascade heat pump with R718 (high stage) and six different low-GWP refrigerants (low stage). *Case Stud. Therm. Eng.* **2024**, *53*, 103812. [[CrossRef](#)]
159. Navarro-Esbri, J.; Mota-Babiloni, A. Experimental analysis of a high temperature heat pump prototype with low global warming potential refrigerant R-1336mzz (Z) for heating production above 155 °C. *Int. J. Thermofluids* **2023**, *17*, 100304. [[CrossRef](#)]
160. Jiang, J.; Hu, B.; Wang, R.Z.; Ge, T.; Liu, H.; Zhang, Z.; Zhou, Y. Experiments of advanced centrifugal heat pump with supply temperature up to 100 °C using low-GWP refrigerant R1233zd (E). *Energy* **2023**, *263*, 126033. [[CrossRef](#)]
161. Arpagaus, C.; Paranjape, S.; Brendel, L.; Simoni, L.D.; Kontomaris, K.; Bertsch, S.S. Experimental Investigation of R1336mzz (E) in a High-temperature Heat Pump. In Proceedings of the 19th International Refrigeration and Air Conditioning Conference at Purdue, West Lafayette, IN, USA, 10–14 July 2022.
162. Sulaiman, A.Y.; Cotter, D.F.; Le, K.X.; Huang, M.J.; Hewitt, N.J. Thermodynamic analysis of subcritical High-Temperature heat pump using low GWP Refrigerants: A theoretical evaluation. *Energy Convers. Manag.* **2022**, *268*, 116034. [[CrossRef](#)]
163. Mateu-Royo, C.; Mota-Babiloni, A.; Navarro-Esbri, J. Semi-empirical and environmental assessment of the low GWP refrigerant HCFO-1224yd (Z) to replace HFC-245fa in high temperature heat pumps. *Int. J. Refrig.* **2021**, *127*, 120–127. [[CrossRef](#)]
164. Zhang, X.; Xu, H. Experimental performance of moderately high temperature heat pump with working fluid R1234ze (Z). *J. Therm. Anal. Calorim.* **2021**, *144*, 1535–1545. [[CrossRef](#)]
165. Mateu-Royo, C.; Mota-Babiloni, A.; Navarro-Esbri, J.; Barragán-Cervera, Á. Comparative analysis of HFO-1234ze (E) and R-515B as low GWP alternatives to HFC-134a in moderately high temperature heat pumps. *Int. J. Refrig.* **2021**, *124*, 197–206. [[CrossRef](#)]
166. Mota-Babiloni, A.; Mateu-Royo, C.; Navarro-Esbri, J.; Barragán-Cervera, Á. Experimental comparison of HFO-1234ze (E) and R-515B to replace HFC-134a in heat pump water heaters and moderately high temperature heat pumps. *Appl. Therm. Eng.* **2021**, *196*, 117256. [[CrossRef](#)]
167. Koundinya, S.; Seshadri, S. Energy, exergy, environmental, and economic (4E) analysis and selection of best refrigerant using TOPSIS method for industrial heat pumps. *Therm. Sci. Eng. Progress* **2022**, *36*, 101491. [[CrossRef](#)]
168. Malavika, S.; Chiranjeevi, C.; Sekhar, Y.R.; Srinivas, T.; Natarajan, M.; Myo, W.P.P.; Singh, A. Performance optimization of a heat pump for high temperature application. *Mater. Today Proc.* **2021**, *46*, 5278–5285. [[CrossRef](#)]
169. Wu, D.; Hu, B.; Wang, R.Z.; Fan, H.; Wang, R. The performance comparison of high temperature heat pump among R718 and other refrigerants. *Renew. Energy* **2020**, *154*, 715–722. [[CrossRef](#)]
170. Dávila, P.; Bourouis, M.; Nicolalde, J.F.; Martínez-Gómez, J. CO₂/acetone mixture desorption process in a plate heat exchanger for compression/resorption heat pumps. *Appl. Therm. Eng.* **2024**, *244*, 122704. [[CrossRef](#)]

171. Wang, Y.; Nan, X.; Ouyang, H.; Guo, Z.; Hu, B.; Wang, R.Z. Analysis and optimization of injection characteristics and comprehensive performance of low GWP refrigerant HP-1 in high temperature heat pump systems. *Energy Build.* **2024**, *303*, 113799. [[CrossRef](#)]
172. Gómez-Hernández, J.; Grimes, R.O.N.A.N.; Briongos, J.V.; Marugán-Cruz, C.; Santana, D. Carbon dioxide and acetone mixtures as refrigerants for industry heat pumps to supply temperature in the range 150–220 °C. *Energy* **2023**, *269*, 126821. [[CrossRef](#)]
173. Hu, H.; Wang, T.; Jiang, Y.; Bi, C.; Zhang, B.; Fan, S.; Li, J.; An, S.; Bai, X.; Guo, C. Thermodynamic performance of heat pump with R1234ze (E)/R1336mzz (E) binary refrigerant. *Appl. Therm. Eng.* **2023**, *230*, 120795. [[CrossRef](#)]
174. Fernández-Moreno, A.; Mota-Babiloni, A.; Giménez-Prades, P.; Navarro-Esbrí, J. Optimal refrigerant mixture in single-stage high-temperature heat pumps based on a multiparameter evaluation. *Sustain. Energy Technol. Assess.* **2022**, *52*, 101989. [[CrossRef](#)]
175. Dai, B.; Zhao, P.; Liu, S.; Su, M.; Zhong, D.; Qian, J.; Hu, X.; Hao, Y. Assessment of heat pump with carbon dioxide/low-global warming potential working fluid mixture for drying process: Energy and emissions saving potential. *Energy Convers. Manag.* **2020**, *222*, 113225. [[CrossRef](#)]
176. Yıldırım, R. Evaluation of the use R450A as an alternative to R134A in low and medium temperature heat pump systems: 4-E (Energy, Exergy, Environmental and Enviro-Economic) analysis. *J. Adv. Res. Nat. Appl. Sci.* **2021**, *7*, 556–569.

Disclaimer/Publisher's Note: The statements, opinions and data contained in all publications are solely those of the individual author(s) and contributor(s) and not of MDPI and/or the editor(s). MDPI and/or the editor(s) disclaim responsibility for any injury to people or property resulting from any ideas, methods, instructions or products referred to in the content.